

JAK-STAT SIGNALING  
IN LIVER DISEASE AND REPAIR  
*a Way of living*

**Inauguraldissertation**

zur  
Erlangung der Würde eines Doktors der Philosophie  
vorgelegt der  
Philosophisch-Naturwissenschaftlichen Fakultät  
der Universität Basel

von

**Simone Tjitske Dorothea Stutvoet**  
aus Apeldoorn, die Niederlande

**Basel, 2005**

Genehmigt von der Philosophisch-Naturwissenschaftlichen Fakultät

auf Antrag von

Prof. Dr. phil. H.P.Hauri  
Prof. Dr. med. M.H.Heim  
Prof. Dr. med. U.A. Meyer

Basel, den 28. September 2004

Prof. Dr. M. Tanner  
Dekan der Philosophisch-  
Naturwissenschaftlichen Fakultät

*Such knowledge is a wonder greater than my powers;  
it is so high that I may not come near it.*

Ps.139:6

# Contents

Abbreviations	7	
Abstract of this thesis	9	
Chapter 1	General Introduction	11
1.1	Jak-STAT signaling	12
1.1.1	Ligands and their receptors	12
1.1.2	Janus kinases (Jaks)	14
1.1.3	STATs: structure and functional domain	14
1.2	Mechanisms and regulation of Jak-STAT signaling	17
1.2.1	IFN signaling	17
1.2.2	IL-6 signaling	20
1.2.3	Nucleocytoplasmic transport	21
1.2.4	STAT DNA binding and transcriptional activation	22
1.2.5	Negative regulation	23
1.2.6	Specificity and diversity in signaling	24
1.3	Biological functions of STAT proteins	25
1.3.1	Impact of STATs in disease	28
1.4	Hepatitis C virus (HCV)	29
1.4.1	Genomic organization of HCV and functions of viral proteins	29
1.4.2	HCV polyprotein processing and replication	31
1.4.3	Models to study HCV escape of immune response	32
1.5	Liver cell regeneration	33
1.5.1	Liver	33
1.5.2	Regulation of liver regeneration	33
1.6	Aim of this thesis	35
Chapter 2	Expression of Hepatitis C virus proteins inhibits Interferon-alpha signaling in the liver of transgenic mice	37
Chapter 3	Expression of Hepatitis C virus structural proteins inhibits Interferon-alpha induced signaling through the Jak-STAT pathway	55

Chapter 4	A fusionprotein between wild type murine STAT3 and the modified ligand-binding domain of the estrogen receptor can mimic activated STAT3 in the presence of 4-hydroxytamoxifen	73
Chapter 5	Generation of <i>in vivo</i> conditional gain-of-function models to study the role of STAT3 and STAT5a signaling in liver	93
Chapter 6	Outlook on the use of the conditional <i>albm</i> STAT3 <sup>wt</sup> -ER and <i>albm</i> STAT5a <sup>R618K</sup> -rER gain-of-function mice models	113
	References	118
	Acknowledgments	134
	Curriculum vitÆ	138



## Abbreviations

4-HT	4-hydroxytamoxifen	LIF	leukemia inhibitory factor
aa	amino acids	LPS	lipopolysaccharide
AFP	alpha-fetoprotein	MAPK	mitogen-activated protein kinase
Alb	albumin promoter	MEF	mouse embryonic fibroblasts
ALT	alanine aminotransferase	MHC	major histocompatibility complex
BAC	bacterial artificial chromosome	Na <sub>3</sub> VO <sub>4</sub>	sodium orthovanadate
Cdc	cell-division-cycle (gene)	NFκB	nuclear factor κB
Cdk	cyclin-dependent kinase	NP-40	nonidet P40
CTL	cytotoxic T lymphocytes	NS	non-structural
DMEM	Dulbecco's minimum essential medium	NTR	non-translated region
EDTA	ethylene-diamine-tetraacetic acid	OAS	2'-5'-oligoadenylate synthetase
EGF	epidermal growth factor	ORF	open reading frame
EGTA	ethylene glycol tetraacetic acid	PAC	P1-derived artificial chromosome
eIF2α	eukaryotic translation initiation factor-2 alpha	PBS	phosphate-buffered saline
EMSA	electrophoretic mobility shift assay	PCK-1	phosphoenolpyruvate carboxykinase-1
ER	estrogen receptor	PCR	polymerase chain reaction
Frtd	FLPe recombinase target	PFGE	pulsed-field gel electrophoresis
G6PC	glucose 6-phosphatase	Pfu	plaque-forming units
GAS	gamma interferon activated sequence	PH	partial hepatectomy
GH	growth hormone	PIAS	protein inhibitor of activated STAT
gp-130	glycoprotein 130	PKR	double-stranded RNA-activated protein kinase
GTP	guanosine triphosphate	PMSF	phenylmethylsulfonyl fluoride
HCC	hepatocellular carcinoma	PP2Ac	protein phosphatase 2A catalytic subunit
HCV	hepatitis C virus	PRMT1	protein arginine methyltransferase
HGF	hepatocyte growth factor	PTK	protein tyrosine kinase
His	histidine	PTP	protein tyrosine phosphatase
HR	homologous region	rER	rat estrogen receptor
ICE	interleukin-1β converting enzyme	RT	room temperature
IFN	interferon	RT-PCR	reverse-transcriptase PCR
IFNAR	interferon alpha receptor	SAP	serum amyloid P
IFNGR	interferon gamma receptor	SDS-PAGE	sodium dodecyl sulfate polyacrylamide-gel electrophoresis
Ig	immunoglobulin	Ser	serine
IH	immunohistochemistry	SH2	src-homology 2
IL-6	interleukin-6	SHP1	SH2-containing tyrosine phosphatase 1
IL-6R	interleukin-6 receptor	SIF	serum inducible factor
IP	immunoprecipitation	SOCS	suppressor of cytokine signaling
IRES	internal ribosomal entry site	STAT	signal transducer and activator of transcription
IRF	interferon regulatory factor	SUMO	small ubiquitin-related modifier
ISG	interferon-stimulated gene	TAD	transcriptional activation domain
ISGF3	interferon-stimulated gene factor 3	TC-PTP	T-cell protein tyrosine phosphatase
ISRE	interferon-stimulated response element	TGF	transforming growth factor
Jak	Janus kinase	TNF	tumor necrosis factor
KO	knock-out	Tyr	tyrosine
LBD	ligand binding domain	VEGF	vascular endothelial growth factor
LCMV	lymphocytic choriomeningitis virus	VSV	vesicular stomatitis virus





## Abstract of this thesis

Signaling through the Jak-STAT pathway is initiated when an extracellular signaling protein binds to its corresponding transmembrane receptor. This leads to activation of the Jaks. The Jaks mediate phosphorylation at the specific receptor tyrosine residues, which then serve as docking sites for the STATs. Once recruited to the receptors, the STATs become phosphorylated by the Jaks. Activated STATs will dimerize, translocate to the nucleus and target gene promoters. STAT proteins display a wide range of functions in many biological aspects. Consequently they are involved in or mediating pathological processes.

This thesis describes and discusses our research, performed to understand in more detail the role of Jak-STAT signaling in liver pathophysiology.

Hepatitis C virus (HCV) is a major cause of chronic liver disease. It is believed that HCV proteins interfere with interferon alpha induced Jak-STAT signaling in order to escape the interferons induced antiviral state. We therefore analyzed interferon alpha induced Jak-STAT signaling in the presence of HCV viral proteins in *in vivo* and *in vitro* models to gain more insight in this interference, as well as to identify the viral protein(s) responsible for this interference. In *chapter 2* we show inhibition of Jak-STAT signaling in transgenic mice that express HCV proteins in their liver cells. The inhibition occurred in the nucleus and blocked binding of STATs to the promoters of interferon stimulated genes. This inhibition of interferon induced signaling resulted in an enhanced susceptibility of the HCV transgenic mice to LCMV infection and the development of severe hepatitis. The results described in *chapter 3*, show that the combined HCV structural proteins and the core protein alone partly inhibit interferon alpha induced Jak-STAT signaling, using a panel of tetracycline-regulated cell lines inducibly expressing individual HCV proteins or in different combinations. In cells expressing HCV nonstructural proteins, interferon alpha induced Jak-STAT signaling was not impaired.

The last chapters of this thesis describe the generation of conditional active gain-of-function models to study STAT signaling independent of natural ligands. Fusion proteins were constructed between STAT1, STAT3 or STAT5a and the modified ligand binding domain of the estrogen receptor (ER) and subsequently expressed in mouse embryonic fibroblasts. In addition several mutants of the fusion proteins were generated. The fusion protein between wild-type STAT3 and the ER (mSTAT3<sup>wt</sup>-ER) was shown to bind DNA and mimic STAT3 signaling upon activation by 4-hydroxytamoxifen (synthetic steroid ligand) only (*chapter 4*). mSTAT3<sup>wt</sup>-ER and mSTAT5a<sup>R618K</sup>-rER (SH-2 domain mutant) fusion protein constructs were used to generate liver-specific conditional active gain-of-function mouse models.

*Chapter 5* describes the multistep cloning approach to prepare the constructs for injection and the analysis of the transgenic mice designated *alb*STAT3<sup>wt</sup>-ER and *alb*STAT5<sup>R618K</sup>-rER. The transgenic mice were designed to express the fusion proteins under control of the albumin promoter allowing liver-specific expression. Transgenic founders have been identified, as well as a transgenic F1 offspring. The transgenic mice appeared to be healthy and show a normal phenotype. Further characterization has to be completed. In *chapter 6* possibilities for future use of the in *chapter 5* described transgenic mice are discussed. The mice could be used to study STAT3 and STAT5a signaling in processes as liver cell regeneration, cellular transformation, bacterial infection, gluconeogenesis and cell survival.



Chapter 1



**General Introduction**

---

## 1.1 Jak-STAT signaling

The Janus kinase (Jak)-signal transducer and activator of transcription (STAT) pathway is an intracellular signal transduction pathway that transmits information received from extracellular signaling proteins (cytokines, growth factors and hormones) through transmembrane receptors to target gene promoters in the nucleus<sup>1</sup>. Binding of the ligand to its corresponding receptor leads to conformational changes in the cytoplasmic part of the receptor, allowing homo- or heterodimerization of the receptor subunits and initiating signaling through tyrosine phosphorylation of the receptor associated members of the Jak family of protein tyrosine kinases. The activated Jaks mediate phosphorylation at the specific receptor tyrosine residues, which will then serve as docking sites for the STATs. STAT proteins comprise a family of transcription factors latent in the cytoplasm that consists of seven different members in mammals; i.e. STAT1, 2, 3, 4, 5a, 5b and 6. The STATs bind to the receptors' docking sites through their src-homology 2 (SH2) domain and are phosphorylated by the Jaks at single tyrosine residues. STATs dimerize by reciprocal phosphotyrosine-SH2 domain interactions and translocate to the nucleus. Activated STATs initiate transcription by binding as dimers to response elements in the promoters of target genes. Different ligands specifically activate different members of the Jak and STAT families. The Jak-STAT pathway is modulated by a range of regulatory proteins, which contribute to the specificity and diversity of cellular responses<sup>2-6</sup>.

### 1.1.1 Ligands and their receptors

The extracellular signaling proteins that signal through the Jak-STAT pathway bind members of various receptor families: single transmembrane receptors with an intrinsic protein tyrosine kinase domain (PTK receptors), single transmembrane receptors without kinase domain (non-PTK receptors) and seven transmembrane receptors (G-protein coupled receptors).

#### *PTK receptors*

To this group of receptors belong receptors for epidermal growth factor (EGF), platelet derived growth factor (PDGF), colony stimulating factor 1 (CSF-1), hepatocyte growth factor (HGF), basic fibroblast growth factor (bFGF), c-Kit and insulin. These receptors may activate STATs indirectly through Jak kinases or directly, as was described for STAT1 activation in vitro by PDGF or EGF receptor<sup>7, 8</sup>. STAT1 can bind directly to tyrosine residues on the EGF-R and CSF-1-R, STAT3 to EGF-R and HGF-R, and STAT5 to PDGF-R and insulin-R. Additionally STAT1, 3, 5 and/or 6 can be activated through these receptors<sup>5, 9</sup>.

#### *Non-PTK receptors*

This group of receptors lacks an intrinsic protein kinase tyrosine domain, but they signal through associated Jaks. They are also referred to as cytokine receptors, and divided into four subtypes (class I-IV) based on similarities in their extracellular binding domains. Class I cytokine receptors include the following four families; i.e. gp130 family, IL-2 family, IL-3/ IL-5/GM-CSF family (gp140 family) and growth hormone (GH) family. All of the receptors belonging to class I contain four conserved cysteine residues, extracellular a tryptophan-serine-X-tryptophan-serine (WSXWS) motive and variable

intracellular domains. Class II cytokine receptors only contains the interferon (IFN) family. Receptors within one family share two or more subunits that are brought together upon ligand binding <sup>5, 10, 11</sup>.

*gp130 family.* Receptors for interleukins-6 (IL-6) and IL-11, oncostatinM, LIF, cardiotrophin-1, G-CSF, IL-12, IL-23, leptin and ciliary neurotrophic factor (CNTF) all signal through a common  $\beta$ -chain called gp130. The IL-6 receptor (IL-6R) complex consists of a non-signal-transducing ligand binding IgG-like  $\alpha$ -chain and two gp130 chains <sup>12</sup>. The LIF receptor is composed out of a signal transducing LIFR $\beta$  chain and a gp130. The CNTF receptor  $\alpha$  chain associates with gp130 and the LIF $\beta$  chain. The IL-11 receptor  $\alpha$  chain requires gp130 for high affinity binding and signal transduction. The receptors associate with either Jak1, Jak2 or Tyk2 and activate STAT3 using the motif YXXQ as STAT3 docking site.

*IL-2 receptor family.* IL-2 and IL-15 signal both through the IL-2 receptor, which consists of a non transducing  $\alpha$  chain (IL-2R $\alpha$ ) and two signal transducing chains, IL-2R $\beta$  or IL-2R $\gamma$ . The receptor for IL-4, IL-7 and IL-9 consists of individual  $\alpha$  chains, and share the IL-2R $\gamma$  chain. The IL-4R $\alpha$  chain can also combine with the IL-13R $\alpha$  chain to form a functional high affinity receptor for both IL-4 and IL-13. The IL-2R $\gamma$  chain associates with Jak3, and IL-2R $\beta$ , IL-7R $\alpha$  and IL-9R $\alpha$  chains with Jak1. IL-4R $\alpha$  and IL-13R $\alpha$  bind Jak1, Jak3 or Tyk2. They mainly activate STAT5 and STAT6.

*gp140 family.* Receptors for IL-3, -5 and GM-CSF have individual  $\alpha$  chains and share the gp140 component, which associates with Jak2. They all signal through STAT5.

*GH family.* Receptors for GH, prolactin, erythropoietin (EPO) and thrombopoietin (TPO) form homodimers after ligand binding and do not share any receptor components. All members of the GH receptor family associate with Jak2 and bind to or activate STAT5 <sup>9</sup>.

*IFN family.* The receptors contain four cysteine residues, but lack extracellular domains and bind IFN  $\alpha, \beta, \omega$ , limitin, IFN $\gamma$  and IL-10 <sup>5, 13</sup>. Type I interferons; i.e. IFN $\alpha/\beta/\omega$  and limitin signal through an interferon alpha receptor (IFNAR) complex, which consists of two subunits IFNAR-1 and IFNAR-2. Human IFNAR-1 is a 557-aa glycoprotein with a 21-aa transmembrane segment and a 100-aa cytoplasmic domain. IFNAR-2 exists in three forms; IFNAR-2a (short form), IFNAR-2b (soluble form) and IFNAR-2c (long form). IFNAR-2c is composed of 515 aa and acts as a functional receptor for IFN $\alpha/\beta$  signaling. The tyrosine kinases Tyk2 and Jak1 are associated with IFNAR-1 and IFNAR-2 respectively <sup>14, 15</sup>. IFNAR-2 can bind additionally STAT2 through tyrosine residues Y466 and Y481 on the receptor <sup>16</sup>. Type II IFN, IFN $\gamma$  binds to IFN $\gamma$  receptor complex IFNGR, containing a chain 1 ( $\alpha$ ) and 2 ( $\beta$ ). IFNGR-1 and -2 bind Jak1 and Jak2 respectively <sup>17</sup>. Type I IFNs activate mainly STAT1, 2 and 3, type II IFN STAT1 <sup>18</sup>.

#### *G-protein coupled receptors*

These receptors span the cell membrane seven times and they activate GTP-binding proteins. Only angiotensin has been shown to signal through the Jak-STAT pathway. Angiotensin II receptor (AT1) associates with Jak2 and activates STAT1 and STAT2 <sup>19</sup>.

---

### 1.1.2 Janus kinases (Jaks)

Jaks are a family of cytoplasmic receptor associated protein tyrosine kinases required for cytokine signaling. In mammals the family consists of four members; Jak1, Jak2, Jak3 and Tyk2, which are activated by cytokine induced receptor dimerization. Once they are activated they cause the phosphorylation of tyrosine residues on the receptor cytoplasmic tails to provide docking sites for the recruitment of STATs recognizing these phosphotyrosines via their src-homology-2 (SH-2) domains, and thus mediating signaling of the activated STATs<sup>13</sup>. Jak1, Jak2 and Tyk2 are expressed ubiquitously, whereas the expression of Jak3 is only expressed by myeloid and lymphoid cells<sup>20</sup>. The Jaks contain seven regions of homology, JH1-JH7. JH1 encodes for a kinase and is located at the C-terminal. The catalytic activity of JH1 is stimulated by phosphorylation of two tyrosine residues (Y1038/Y1039 in Jak1, Y1007/Y1008 in Jak2, Y980/Y981 in Jak3, and Y1054/Y1055 in Tyk2) in the domain. JH2 represents a pseudokinase domain; it has no catalytic function, however a Jak2 mutant lacking the domain was able to mediate GH signaling<sup>21</sup>. A single glutamic acid to lysine substitution in the JH2 domain resulted in hyperphosphorylated and hyperactivated STAT when overexpressed in cells<sup>22</sup>. The other Jak homology domains (JH7-JH3) are located at the N-terminal end and thought to be involved in receptor association and in determining the specificity of the Jak-receptor binding. The Jaks have clear functions in vivo as has been shown by knockout studies in mice<sup>23</sup>.

The *Jak1* knockout mouse exhibited an early post-natal lethal phenotype, probably caused by a neurological defect due to loss of LIF function, which express itself in the inability to suckle<sup>24</sup>. Decreased responses to IL-7 resulted in impaired lymphopoiesis. Also responses to IFNs and IL-10 were diminished. *Jak2* null mice die at embryonic day 12.5 caused by failure of erythropoiesis and immunological impairments<sup>13</sup>. Mice lacking *Jak3* suffer from defects in B-cell maturation (IL-7 mediated) and T-cell negative selection because of loss of gamma receptor chain ( $\gamma$ C) (in IL-2R, IL-4R, IL-7R, IL-9R, IL-15R and IL21R) signaling. Also humans suffering from SCID were found to have mutations in the *Jak3* gene<sup>9</sup>. *Tyk2* deficient mice were shown to be more susceptible to pathogens caused by defective responses to IL-12 and in less degree to IFN type I<sup>25</sup>.

### 1.1.3 STATs: structure and functional domains

The STAT genes have been identified in three chromosomal clusters. The genes encoding STATs 1 and 4 map to a region of mouse chromosome 1 (equivalent to human chromosome 2, q12-q33), STATs 3, 5a and 5b map to a region of mouse chromosome 11 (human chromosome 12, q13-14.1), STATs 2 and 6 map to a region of mouse chromosome 10 (human chromosome 17, q11.1-q22). STATs 1, 3, 4, 5a and 5b are between 750 and 795 aa long, whereas STATs 2 and 6 are approximately 850 aa long<sup>26, 27</sup>. Despite functional differences of the individual STAT proteins, crystallography studies (an example of the crystal structure of activated STAT1 bound to DNA is shown in Figure 2) and protein sequence comparisons of STAT1, STAT3 and STAT4 display common STAT structural domains (an overview is depicted in Figure 1)<sup>28, 29</sup>.



**Figure 1. Domain structure of STAT proteins.** Defined structural and functional regions of the STAT proteins: N, N-terminal domain; C-C, coiled-coil domain; DNA, DNA binding domain; LD, linker domain; SH2, SH2 domain with the arginine (R) conserved in all STATs depicted; P, phosphorylated tail segment with the tyrosine (Y) on which all STATs are activated; T, transactivation domain with the serine (S) on which STAT1, 3, 4 and 5a/b can be phosphorylated. Colors of the domains do correspond to the domain colors in the three-dimensional STAT picture (Figure 4).

The *N-terminal domain* is highly conserved and is required for the dimer-dimer interactions to form tetramers or oligomers of STATs. It has been shown for STAT1, 4 and 5 that they are able to form tetrameric complexes on tandemly linked GAS (gamma interferon activated sequence) motifs. The tetramerization of STATs contributes to the stabilization of the STAT-DNA binding and allows STAT proteins to bind with higher affinity, and therefore increases the transcriptional activity. The formation of this complex is thought to be mediated through protein-protein interactions involving tryptophan 37 (W37). Studies have demonstrated that a STAT1 W37F mutant was still able to form a dimer, however lost the ability to form tetrameric complexes on tandem sites on DNA, which resulted in loss of transcriptional activity<sup>30-32</sup>. Furthermore, STAT1 mutations of phenylalanine (F) 77 and leucine (L) 78 were shown to interfere with dimer formation<sup>33</sup>. The N-domain in STAT1 also enhances transcription by interaction with histone transacetylases (CBP/p300 proteins)<sup>34</sup>.

Arginine (R) 31 in the N-terminal domain of STAT1 is required for dephosphorylation of tyrosine 701 of STAT1. Methylation of R31 has shown to prevent STAT1 from binding to PIAS1. PIAS1 binding prevent STAT1 from binding DNA<sup>35</sup>. The deletion of the STAT1 N-terminal domain resulted in a mutant STAT1 protein which was constitutively phosphorylated on Tyr-701<sup>36</sup>. STAT3 proteins lacking the N-terminal domain did show that the domain is not required for Y705 phosphorylation of STAT3 stimulated by IL-6<sup>37</sup>. The N-terminal domain is also involved in nuclear translocation. Activated STAT1 molecules lacking the entire N-terminal domain were not able to translocate to the nucleus<sup>38</sup>.

The *coiled-coil domain* is located between residues 136 and 315 and consists of four  $\alpha$ -helices<sup>28</sup>. The coiled-coil domain of STAT1 (in particular lysine (K) 161) for example interacts with IRF9/p48, which makes part of the interferon stimulated gene factor 3 complex<sup>39</sup>. This domain of STAT3 interacts with transcription factor c-jun<sup>40</sup> and STAT5a and 5b with the silencing mediator of retinoic acid and thyroid hormone receptors (SMRT)<sup>41</sup>. Single mutations of STAT3' aspartic acid (D) residue 170 or, to a lesser extent K177 diminishes receptor binding and tyrosine phosphorylation, and consequently dimer formation, nuclear translocation and transcriptional activation. Further mutation experiments with STAT3 showed that all four

coiled-coil domain helices are required for recruitment of STAT3 to the IL-6 receptor and for Y705 phosphorylation<sup>37</sup>. Furthermore, mutation studies of coiled-coil domain of STAT3 have revealed that only residues R214/R215 in the domain (but not R152/K153/R154, K161/K163, K177/K180, R197/R199 and K244/R245/R246) have influence on nuclear import<sup>42</sup>.

The *DNA-binding domain* (approx. aa 320-480) is structurally similar to the immunoglobulin-like DNA-binding domain and shows similarities to the DNA-binding domains of NF $\kappa$ B and p53<sup>29</sup>. The domain determines the DNA binding specificity. The analysis of the crystal structure of phosphorylated STAT1 bound to DNA (Figure 2) suggested that there are few direct contacts between the DNA-binding domain of the DNA bases, i.e. K336, E421 and N460 are essential for the binding of the DNA bases, whereas R378, K410, E411, K413, T427 and T459 make contacts with phosphate backbone of DNA<sup>29</sup>. The activated STAT3 dimer requires residues K340 and N466 for the binding to the bases in the response elements, aa M331, H332, V343, Q344, R382, R417, I431, V432, S465, I467 and Q469 make contacts to the DNA sugar-phosphate backbone<sup>28</sup>.

The domain is also important for nuclear translocation of the STAT dimers<sup>42</sup>.

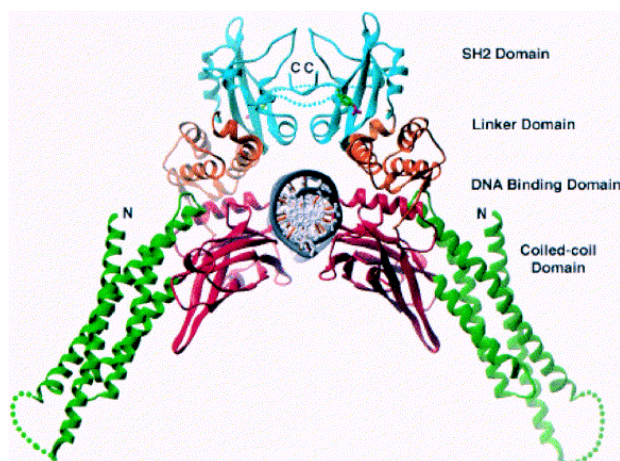


**Figure 2. Crystal structure of tyrosine phosphorylated STAT1 dimer bound to DNA.** Ribbon presentation of the STAT1 core dimer (aa 136-710) on DNA. The coiled-coil domain is shown in green, the DNA-binding domain in red, the linker domain in orange and the SH2 domain is shown in blue. The phosphorylated tail segment is colored purple and the DNA backbone in grey. 'N' and 'C' indicate the location of the lacking N- and C-termini in this STAT1 dimer. Reprint from a publication by Chen et al.<sup>29</sup>.

The  $\alpha$ -helical linker domain (approx. aa 485-575) separates the DNA domain from the SH2 domain<sup>29</sup>. For STAT1 it was reported that its linker domain may play a role in transcriptional responses. Mutations (W539A, K544A and E545A, but not F506A and R512A) resulted in the lack of ability to induce transcriptional responses to IFN $\gamma$ , but not to IFN $\alpha$ , although STAT1 phosphorylation, dimerization, nuclear translocation and DNA binding were normal in response to IFN $\gamma$ <sup>43</sup>. Additional analyses of this STAT1 (K544A/E545A) mutant have suggested that the primary defect in this mutant is its abnormal DNA binding kinetics (it binds and dissociates from DNA more rapidly than wild type STAT1 protein) and inability to accumulate on DNA



response elements, rather than a defective co-activator recruitment mechanism<sup>44</sup>.

The *SH2* (*src* homology domain 2) domain is located between aa 575 and 680. It is required for the recruitment of STATs to phosphorylated receptors and for the reciprocal SH2-phosphotyrosine interactions between monomeric STATs to form dimers<sup>45</sup>. The binding of the STATs to the receptors occurs through the interaction of the conserved arginine in the SH2 domain (R602 for STAT1, R609 for STAT3 and R618 for STAT5) with the phosphorylated tyrosine residues located in the intracellular domains of the receptors. This interaction is highly specific and determines the STAT binding to the different cytokine receptors<sup>28, 46</sup>. This conserved arginine residue is also essential for the recognition of the single phosphate group of the phosphotyrosine to initiate dimerization of the STAT proteins required for STAT transcriptional activity<sup>47</sup>. Additional contacts between A641 and V642 in the SH2 domain and L706 C-terminal of the phosphotyrosine are essential in the dimer formation in STAT1. For STAT3 are these N641, M642 in the SH2 domain and F706<sup>29</sup>.

The *phosphorylated tail segment* harbours the tyrosine residue (Y701 for STAT1, Y690 for STAT2, Y705 for STAT3, Y693 for STAT4, Y694 for STAT5 and Y641 for STAT6), which phosphorylation is essential for STAT dimerization through SH2 domain binding and DNA binding activity<sup>48</sup>. The four to five aa C-terminal of the phosphorylated tyrosine (for STAT1 Y<sub>701</sub>IKTEL, for STAT3 Y<sub>705</sub>LKTKF and for STAT5a Y<sub>694</sub>VKPQI) make the contacts with other aa of the SH2 domain and are therefore essential in dimerization<sup>28, 29, 49</sup>.

The *transcriptional activation domain (TAD)* at the C-terminal region between approximately aa 700 and 851, is involved in the communication with transcriptional complexes. A conserved serine in STAT1 (S727), 3 (S727), 4 (S722) and 5 (S726/731) can be phosphorylated and regulates STAT transcription. Several studies showed an reduced transcriptional activity when this serine is replaced by alanine<sup>50-52</sup>. Alternative splicing at the 3'end of the gene transcripts generates shorter isoforms of STAT1, 3, 4, 5a and 5b. The isoforms lack the functional transcriptional activation domain, but are still able to bind to the response elements of target genes. When the isoforms are overexpressed, they can act as dominant negative regulators of transcription, by competing with full length STATs for the DNA binding sites<sup>53</sup>.

## 1.2 Mechanisms and regulation of Jak-STAT signaling

### 1.2.1 IFN signaling

Type I interferons are produced by leukocytes and fibroblasts upon virus infection and type II IFN is produced by activated Thelper (Th)<sub>1</sub>-cells and natural killer (NK) cells<sup>54, 55</sup>. IFN $\alpha/\beta$  (type I) gene transcription in virus infected cells is an important early event in the host response to infections. IFN $\alpha/\beta$  is produced by virus-infected cells within hours and plays an important role in preventing virus spread. Production of IFN-gamma on the other hand needs activation of the immune system<sup>56</sup>. The induction of transcription of IFN $\alpha/\beta$  genes is mediated through the binding of interferon regulatory factors (IRF) to virus-inducible enhancers in their promoter

regions<sup>17</sup>. IRF3 and IRF7 are the key regulators of the induction of IFN $\alpha/\beta$  genes. IRF3 is phosphorylated and translocated to the nucleus upon viral infection. It associates with the co-activator p300/CBP, and activates IFN $\beta$  and IFN $\alpha$ 1 genes. IFN $\alpha$  and  $\beta$  are produced, bind to their receptors, signal through the Jak-STAT pathway and activate a number of target genes, collectively called interferon stimulated genes (ISGs). One of them is IRF7. In the presence of viral infection IRF7 is also phosphorylated, translocates to the nucleus, forms a dimer with IRF3 and transcriptionally stimulates additional IFN $\alpha$  genes<sup>57, 58</sup>.

Signals of both types IFN are transmitted through the Jak-STAT pathway, as illustrated in Figure 3. Binding of the IFNs to their receptors links the two components of the receptors and results in the activation of Jak1 and Tyk2 for IFN $\alpha/\beta$ , and Jak1 and Jak2 for IFN $\gamma$ . The two kinases (Jak1/Tyk2 and Jak1/Jak2) transactivate each other by transphosphorylation. The activated kinases then phosphorylate tyrosine residues on the receptors: Y440 on IFNGR-1 and Y466 on IFNAR-2, which are then able to bind STAT1 and STAT2 respectively through their SH2 domains on these sites. As a result STAT1 is phosphorylated by the Jaks on its tyrosine 701, STAT2 on Y690 and STAT3, which is also activated by IFN $\alpha/\beta$ , on Y705.

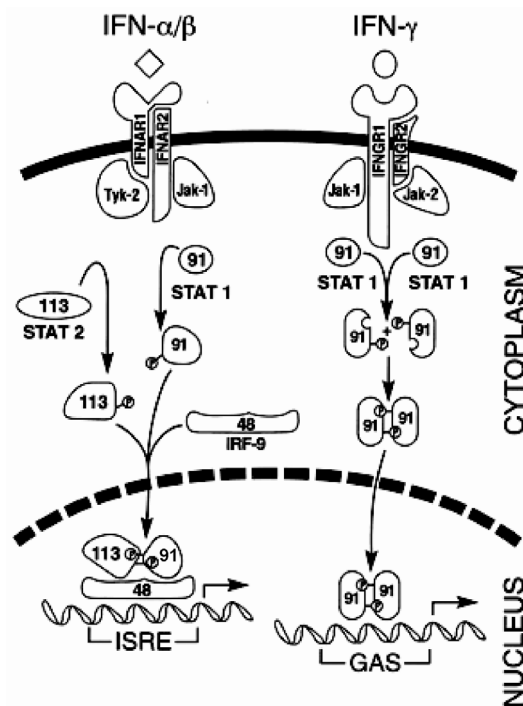


**Figure 3. Schematic overview of IFN $\alpha/\beta$  and  $\gamma$  induced signal transduction through the Jak-STAT pathway.** The Jak1 and Tyk2 kinases are activated by IFN $\alpha/\beta$ , which leads to phosphorylation, dimerization and nuclear translocation of STATs. IFN type I activates two classes of STAT complexes. STAT1 (p91) and STAT2 (p113) heterodimer combine with IRF9 (p48) to form ISGF3, which activate transcription of ISGs through ISRE and STAT1 and STAT3 homodimers, which bind to GAS elements. Upon IFN $\gamma$  binding are STAT1 homodimers formed, which induces transcription by binding to GAS element<sup>60</sup>.

Through reciprocal phosphotyrosine-SH2 domain interactions STAT1 forms homodimers (IFN $\alpha/\beta/\gamma$ ), STAT3 forms homodimers and heterodimers with STAT1 (IFN $\alpha/\beta$ ) and additionally upon IFN $\alpha/\beta$  signaling STAT1 and STAT2 are able to form a heterotrimeric complex with IRF-9 (p48), designed interferon stimulated gene factor 3 (ISGF3). The STAT dimers will translocate to the nucleus and to the specific response elements (STAT1 and 3 homo and heterodimers to GAS elements, and ISGF3 to ISRE) in promoters of target genes and stimulate transcription <sup>59</sup>.

IFNs have antiproliferative, immunomodulatory and antiviral activity. Mice lacking IFNAR1 have increased susceptibility to vesicular stomatitis virus (VSV), Semliki Forest virus (SFV), vaccinia virus or lymphocytic choriomeningitis (LCMV). In contrast mice deficient for IFNGR1 were able to overcome a VSV and SFV infection, died from vaccinia virus infection and were increased susceptible, however less than the IFNAR KO mice, to LCMV. Furthermore IFNAR KO mice were resistant against the pathogen *Listeria monocytogenes*, whereas the IFNGR deficient mice were highly susceptible. This points out that IFN type I and II have partially overlapping but distinct antiviral effects <sup>61, 62</sup>. Differences in the induction of target genes by IFN type I and II are responsible for the differences in antiviral effects. Especially the use of oligonucleotide arrays to study the differential expression of mRNA in response to IFNs have identified many new and confirmed known interferon-stimulated genes and provided insights into the mechanisms of IFN action <sup>63, 64</sup>. IFN $\alpha/\beta$  induced genes (i.e. ISG) include ISG-56K, MxA, 6-16, IRF1, 2'-5'-oligoadenylate synthetase (OAS), double stranded RNA activated protein kinase (PKR), eIF-2 $\alpha$ , MHC-class I, IL-12, IL-15, ICE and IFN $\alpha/\beta$ . Antiviral activity requires induction of OAS, PKR and Mx proteins <sup>65, 15</sup>. Direct antiviral effects of IFN $\gamma$  are mediated through its upregulation of PKR, OAS and dsRNA specific adenosine deaminase (dsRAD) <sup>55</sup>. IFN $\gamma$  has direct antibacterial activity through the activation of monocytes, lymphocytes, neutrophils and macrophages by the enhancement of expression of chemokines, inducible nitric oxide synthase (iNOS) and natural resistance-associated macrophage protein1 (NRAMP1) <sup>55, 65</sup>.

IFNs are also modulators of the immune system and do influence cell growth and differentiation. IFN $\alpha/\beta$  suppress the antigen-specific- or mitogen-induced proliferation of T helper cells and cytotoxic T cells on one hand, while at the other hand they induce IL-15 production in macrophages, which enhances T-cell growth and proliferation of NK-cells. IFN $\alpha/\beta$  also induce expression of MHC class I, thereby stimulating antigen presentation <sup>15, 61</sup>.

IFN $\gamma$  is a strong inducer of both MHC class I and II molecules. <sup>55</sup> IFN $\gamma$  can also regulate the isotypes of immunoglobulins secreted during humoral immune responses <sup>63</sup> and induces cell death of T-cells <sup>54</sup>.

IFN signaling is also involved in apoptosis and in the regulation of cell cycle. IFN induced growth inhibiting and proapoptotic genes included IRF1, tumor necrosis factor-related apoptosis-inducing ligand (TRAIL), XIAP-associated factor 1 (XAF1), galectin 9, a cyclin E binding protein, amphiphysin 1, MyD88, and several ubiquitin pathway genes <sup>15, 55, 64</sup>.

### 1.2.2 IL-6 signaling

IL-6 is a cytokine that exhibits a wide range of biological effects. It is induced by proinflammatory stimuli like IL-1 and TNF $\alpha$ , which are expressed at most inflammatory sites.<sup>11</sup> TNF $\alpha$  activation leads to activation of NF $\kappa$ B, which is the transcription factor for the induction of IL-6 gene expression. In liver, TNF $\alpha$  activates IL-6 expression mainly in Kupffer cells, but also in endothelial cells and hepatic stellate cells, resulting in Jak-STAT/ SHP2/MAPK activation in hepatocytes<sup>66-68</sup>.

Signaling through the Jak-STAT pathway is illustrated in Figure 4. IL-6 binds specifically to the IL-6R  $\alpha$ -chain, which allows recruitment of the two signaling gp130 receptor subunits. The receptor subunit gp130 is ubiquitously expressed, but the number of cells responding to IL-6 is limited because of the restricted availability of the  $\alpha$ -chain. The soluble form of IL-6R $\alpha$  (sIL-6R $\alpha$ ) can as well be used to initiate IL-6 signaling when bound to IL-6. In addition to sIL-6R $\alpha$ , also soluble gp130 (sgp130) is present in serum. Soluble gp130 is probably translated from an alternative spliced mRNA and can neutralize IL-6/sIL-6R $\alpha$  complexes, thereby acting as an antagonist. IL-6 alone is not able to interact or cause homodimerization of gp130<sup>12, 69-71</sup>.

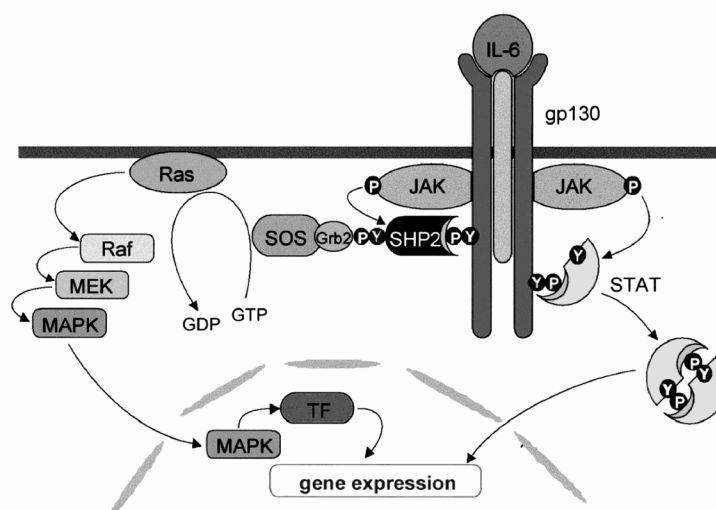


**Figure 4. Schematic diagram of IL-6 induced signaling.** IL-6 activates the Jak-STAT pathway and the MAPK cascade. IL-6 binding to the IL-6 receptor causes aggregation of the three receptor chains and consequently activation of Jak1, Jak2 or Tyk2. The receptor chain gp130 is phosphorylated on four tyrosine residues (Y767, Y814, Y905 and Y915) to allow binding of STAT3. Activated STAT3 forms homodimers, which are binding to GAS-like response elements. Through activation of SHP2 is IL-6 also coupled to MAPK signaling (TF, transcription factor)<sup>70</sup>.

As result of the receptor-IL-6 binding, gp130 associated kinases Jak1, Jak2 and Tyk2 become phosphorylated and will in return phosphorylate six tyrosine residues on the cytoplasmic tail of the gp130 receptor chains. Four of these tyrosine residues serve as docking sites for the SH2 domains of STAT3 (Y767, Y814, Y905 and Y915) and of STAT1 (Y905 and Y915)<sup>70</sup>, which will subsequent be phosphorylated on their single tyrosine residues (Y705,

respectively Y701). The phosphorylated STAT1 and 3 will form homo and heterodimers and translocate to the nucleus to bind to GAS-like response elements.

Activation of the IL-6R complex does not only lead to signaling through the Jak-STAT pathway, but also to activation of the SHP2/MAPK signaling pathway. One of the six tyrosine residues (Y759) on gp130 cytoplasmic tail, is bound by SHP2 (SH2 domain containing tyrosine phosphatase). Upon Jak-SHP2 interaction, SHP2 will be phosphorylated by Jak1 on its tyrosine residues 304 and 327. Subsequently Grb2 (growth-factor-receptor-bound protein), which is linked to SOS (son of Sevenless), can bind to the pY304 of SHP2. Recruitment of SOS to the receptor complex at the membrane allows Ras activation. This leads to signaling through the Ras-Raf-MAPK cascade <sup>12, 70</sup>. Activated MAPK activates the transcription factors NF (nuclear factor)-IL6, and CAAT/enhancer binding protein (C/EBP)  $\beta$  and  $\delta$ , which bind to the promoters of acute phase proteins to induce transcription <sup>11, 72</sup>. Through association of SHP2 with Gab1 (a scaffolding adaptor protein) ERK2 is activated. This interaction links IL-6 signaling to the activation of the PI3K/Akt pathway which mediates anti-apoptotic effects and cell growth <sup>12, 70</sup>.

SHP2 not only links IL-6R complex activation to the MAPK pathway, it also has an inhibitory role. Through its activation and association with Y759 on the receptor, it counteracts receptor and STAT activation by tyrosine dephosphorylation of receptor kinase sites, resulting in inhibition of IL-6 induced gene expression. Furthermore, IL-6 signaling is negatively regulated by SHP1, which can dephosphorylate Jak2 and Tyk2, and by SOCS3, which competes with SHP2 for binding of Y759 on the IL-6R complex and inhibits Jak activity <sup>71, 73, 74</sup>.

IL-6 acts on various cells. In addition to its important role in inflammation, IL-6 induces differentiation and development of haematopoietic cells, osteoclasts, neural cells and hepatocytes. It also acts as growth factor for renal cell carcinoma and Kaposi's sarcoma, and promotes growth of haematopoietic stem cells <sup>67</sup>.

IL-6 deficient mice develop normally, probably because other members of the gp-130 cytokine family do compensate for the lack of IL-6. However they fail to control efficiently infection with vaccinia virus or *Listeria monocytogenes* and have an impaired T-cell dependent antibody response against vesicular stomatitis virus. Most important, the inflammatory acute-phase response after minor tissue damage or infection with bacterial lipopolysaccharide (LPS), was severely impaired <sup>75, 76</sup>. Furthermore do they show a decreased IL-10 production and increased IL-12 production in macrophages.

IL-6 target genes involved in anti-inflammatory responses include IL-1R antagonist, soluble TNF $\alpha$ -R, IL-10, acute phase proteins, glucocorticoids, tissue inhibitor of metalloproteinase-1 (TIMP-1) and SOCS3 <sup>66, 77</sup>.

### 1.2.3 Nucleocytoplasmic transport

In unstimulated cells STATs predominantly localize to the cytoplasm, and upon stimulation rapidly translocate to the nucleus and induce gene expression. Nuclear translocation is mediated by the nuclear pore complex (NPC).

Active *nuclear import* is directed by a nuclear localization signal (NLS), which is recognized and bound by members of the importin family. Importin- $\alpha$ 5

---

recognizes the NLS and functions as an adaptor for the binding of importin- $\beta$ . Importin- $\beta$  interacts with the NPC and mediates the transport of the STAT dimer into the nucleus. Hydrolysis of GTP by Ran, a Ras-like small GTPase, provides the energy that is required to translocate the STATs through the central gated channel of the NPC. NLS elements include a short stretch arginine and lysine residues. Mutagenesis studies of possible NLS motifs have indicated that K410-R418 in STAT1 and R409-K415 in STAT2 are required for IFN-induced nuclear import <sup>78</sup>. Also a single mutation in STAT1 leucine 407 (L407A), or double mutations in lysines 410 and 413 (K410A/K413A), were shown to block nuclear import due to abolishment of the importin- $\alpha$ 5 binding to these mutated STAT1 molecules. The L407 mutant can still bind DNA, whereas the K410A/K413A mutant can not <sup>79</sup>. Mutations of R414/417 in STAT3, corresponding to K410/413 in STAT1, also caused loss of nuclear import ability of STAT3 <sup>42</sup>.

*Nuclear export* is specified by nuclear export signal (NES) elements. Three nuclear export signal (NES) elements have been described for STAT3; i.e. aa306-318, aa404-414 and aa524-535, and for STAT1; aa302-314, aa399-410 and aa534-533<sup>80, 81</sup>. The NES element is recognized by an exportin CRM1 (chromosome region maintenance 1), which is bound as well to Ran-GTP in the nucleus. The CRM1-STAT-Ran/GTP complex is exported through the NPC and dissociates in the cytoplasm after the hydrolysis of Ran-GTP <sup>13, 81</sup>.

#### **1.2.4 STAT DNA binding and transcriptional activation**

Activated STATs can bind to two classes of DNA response elements in promoters of target genes. The STAT dimers, STAT1, 3, 4, 5 and 6 homodimers and STAT1 and 3 heterodimer bind to variations of GAS (gamma activated sequence)-like motifs, palindromic response elements TTCNNNGAA, except for STAT6 which prefers TTCNNNNGAA <sup>82</sup>. GAS-like elements have been identified in promoters of many different genes, like for cFos, M67, Fc $\gamma$ R1, IRF1 and  $\beta$ -casein. The other class of response elements where STATs bind to are interferon stimulated response elements (ISRE); i.e. AGTTTNNNTTCC. ISRE elements are bound by ISGF3 (interferon stimulated gene factor 3); i.e. the complex of STAT1 and STAT2 together with IRF9/p48 (interferon regulatory factor 9) <sup>83</sup>. These elements can be found in ISG like ISG54, ISG15, 6-16 and OAS <sup>4</sup>.

Once the activated STAT dimer binds to its target promoter, the transcription rate from this promoter is increased. The STATs have the ability through their TAD to recruit nuclear co-activators that mediate chromatin modifications and communication with the promoter. The TAD of STAT1 can directly interact with the CREB-binding protein (CBP)/p300 family of transcriptional coactivators to contribute to transcriptional activation. Recently was shown that both tyrosine-phosphorylated STAT1 $\alpha$  (full-length wild-type protein) and STAT1 $\beta$  (lacking the TAD) stimulate *in vitro* transcription on a naked DNA template. Using a system with purified proteins and naked DNA, it was shown that STAT1 $\alpha$ - and STAT1 $\beta$ -dependent transcription is stimulated by the TRAP/Mediator co-activator complex. Although both STAT1 $\alpha$  and STAT1 $\beta$  bind to known STAT sites within *in vitro* assembled chromatin templates, only STAT1 $\alpha$ , and not STAT1 $\beta$ , in cooperation with p300 and acetyl-CoA, stimulated *in vitro* transcription from chromatin. After IFN $\gamma$  treatment, it was shown that cells recruit STAT1 $\alpha$  or - $\beta$

to the chromosomal interferon-1 gene, but only STAT1 $\alpha$ -containing cells recruit p300 and stimulate transcription. The results indicate that the recruitment of p300 to the chromatin is required to make TRAP/Mediator effective in stimulating transcription<sup>34, 84</sup>.

Furthermore, transcriptional activity can be positively regulated by phosphorylation of the conserved serine residue in the TAD. Serine phosphorylation is independent of tyrosine phosphorylation<sup>85</sup> and is not required for DNA binding of the activated STATs<sup>86</sup>. It has been described that an activated JAK2 is the kinase responsible for serine phosphorylation<sup>85</sup>; other candidates include p38, ERK and JNK<sup>83</sup>. Expression of a dominant-negative p38 led to defective STAT1 serine 727 phosphorylation and diminished IFN $\gamma$  mediated protection against viral killing<sup>87</sup>. In contrast Zhu et al. showed that ERK, JNK and p38 do not exhibit kinase activity under IFN $\gamma$  stimulation<sup>85</sup>.

### 1.2.5 Negative regulation

Inactivation or inhibition of Jak-STAT activation is important in the regulation of their biological signaling effects. As result of actions of negative regulators at several points in the signaling pathway, the duration of STAT activation is temporary. After STATs are phosphorylated, dimerized, translocated to the nucleus and have induced transcription, they are exported back to the cytoplasm in dephosphorylated state.

Factors involved in negative regulation are members of the SOCS (suppressors of cytokine signaling) family, of the PIAS (protein inhibitor of activated STATs) family, PTPs (protein tyrosine phosphatases) and enzymes that mediate modifications of STATs proteins, like ubiquitination and SUMOylation<sup>13, 23</sup>. At the receptor level the pathway is negatively regulated through receptor internalization to endocytic vesicles<sup>88</sup>.

#### *SOCS*

They comprise a family of eight members who share a similar structure, with a central SH2 domain, a region of homology called the SOCS box at the C-terminal and a kinase inhibitory region located at the N-terminal. Members are CIS-1 (cytokine-inducible SH2 containing protein) and SOCS1-7<sup>89</sup>. SOCS are target genes of the STATs and do thus generate a negative feedback loop. They inhibit STAT signaling by binding to the phosphorylated tyrosine residues on the receptors to physically block binding of STATs, by binding of Jaks or to the receptors to inhibit Jak kinase activity or by interacting with the elongin BC complex and cullin 2 to induce ubiquitination of the Jaks<sup>6, 89</sup>. Ubiquitination of the Jaks prepares them for proteasomal degradation<sup>5</sup>. The essential negative regulatory function of SOCS1 was revealed by the fatal, immune-mediated inflammatory disease which is present in SOCS 1 deficient mice<sup>23</sup>.

#### *PIAS*

This family contains five members, PIAS1, PIAS3, PIAS $\gamma$ , PIAS $\alpha$  and PIAS $\beta$ . PIAS1, PIAS3 and PIAS $\alpha$  can specifically interact with STAT1, STAT3 and STAT4, respectively. PIAS-STAT interaction is cytokine dependent. PIAS family members have a central Zn-binding RING-finger domain, a well conserved domain at the N-terminus and a less-well conserved C-terminal

---

domain. PIAS bind to phosphorylated STAT dimers and prevent them from binding DNA <sup>90</sup>. Inhibition of R31 methylation of STAT1 proteins, by methylthioadenosine (MTA), a methyl-transferase inhibitor promotes PIAS1 binding and thus inhibits STAT1 signaling. With other words, arginine methylation protects the STATs from binding to PIAS1 and deactivation. The methylation of the highly conserved R31 residue in STAT1 by the protein arginine methyl-transferase PRMT1 was found to be required for IFN type I induced transcription <sup>35</sup>. PIAS 1 binding of STAT1 seems to protect STAT1 from dephosphorylation by TC-PTP/TC45. So arginine methylation of STAT1 regulates STAT1' dephosphorylation <sup>91</sup>. In addition to PIAS1, PIASy also interacts with STAT1 and seems to function as corepressor of STAT1.

Very recently the PIAS1 KO mouse has been reported by Liu et al. Tyrosine phosphorylation of STAT1 induced by IFN $\alpha$  or IFN $\gamma$  and likewise of STAT2 by IFN $\beta$ , was not altered in PIAS1-/- cells. Gene activation analysis showed that PIAS1 selectively regulates a subset of IFN $\gamma$  or IFN $\beta$  target genes. Due to PIAS1 inhibitorial function, the immune response to viral and bacterial infections was enhanced in these PIAS1 deficient mice <sup>92</sup>.

It has been reported that PIAS proteins have E3 ligase activity for SUMO-ylation mediated by the RING finger domain. However in the PIAS1 -/- thymocytes no defect was observed in SUMO3 or SUMO1 protein modification <sup>92</sup>. SUMO (small ubiquitin-related modifier) has been found added to target proteins by special protein-protein interactions. This is regulated by SUMO E3 ligases <sup>93</sup>. How SUMO-ylation of STAT inhibits its activation is not yet understood.

#### *Protein tyrosine phosphatases*

PTPs are active both in the cytoplasm and the nucleus. SHP1 and SHP2 are cytoplasmic PTPs, which can dephosphorylate Jaks and receptors. SHP1 has been shown to directly bind and dephosphorylate Jak2 <sup>89</sup>. Also SHP2 seems to be a regulator of Jak2 activity. Dephosphorylation of Jak2 by SHP2 protects Jak2 from SOCS1 mediated ubiquitination and degradation <sup>94</sup>. PTP1b specifically inhibits JAK2 and Tyk2 <sup>23</sup>. Although TC-PTP/TC45 (T-cell protein tyrosine phosphatase 45 kDa isoform) is known as a nuclear PTP, there is also evidence that it is involved in the dephosphorylation of Jak1 and Jak3. It was shown that it can bind to Jak1 and Jak3. Furthermore cells from mice deficient for TC-PTP/TC45 show increased phosphorylation of Jak1, STAT1 and STAT5 depending on the stimulation. Jak2 phosphorylation was not affected <sup>95</sup>. Nuclear tyrosine phosphatases TC-PTP/TC45 was identified to dephosphorylate specifically phosphorylated STAT1 in the nucleus. In TC-PTP null mouse embryonic fibroblasts (MEFs) the dephosphorylation of STAT1 is defective, as well as the dephosphorylation of STAT3, but not of STAT5 and 6. Reconstitution with TC-PTP/TC45, but not with TC48, the other TC-PTP isoform, could repair this defect <sup>96</sup>.

#### **1.2.6 Specificity and diversity in signaling**

Diversity and specificity are decisive factors in the determination of the outcome response in the complexity of intercellular signaling. The different cytokines induce specific and distinct biological responses in different types of cells by activating different members of the Jak and STAT families. However, even in the same type of cell, the responses to a certain cytokine can vary depending on the location of the cell and the condition of its



microenvironment. The cell specificity of cytokine action through the Jak-STAT pathway is determined at several levels, which are obviously influenced by one another <sup>97</sup>.

To start with, specificity is reached through the selective activation of the different STATs by specific ligands. This is achieved through the selective binding of different STAT family members to phosphotyrosine docking sites on receptors <sup>46, 98</sup>. This was shown by domain swapping experiments the docking sites <sup>98</sup> and with the STAT SH2 domains <sup>46</sup>. STAT2 constructed with the SH2 domain of STAT1 could be activated by IFN $\gamma$ , whereas the STAT1 constructed molecule including the STAT2' SH2 domain could not. When the tyrosine residues which phosphorylation is required for dimerization and nuclear translocation of the STATs, with surrounded sequence of STAT1 (Y701) and STAT2 (Y690) were swapped, the STAT1'SH2 domain was required to induce phosphorylation of the STAT protein by IFN $\gamma$  <sup>46</sup>. Using a phosphopeptide library to determine the sequence specificity of the receptor binding sites (i.e. peptides) for the SH2 domains of STAT1 and STAT3, did show by Wiederkehr-Adam et al. that STAT1 preferentially binds peptides with a motif phosphotyrosine-(aspartic acid/glutamic acid)-(proline/arginine)-(arginine/proline/glutamine), whereby a negatively charged aa at +1 excludes a proline at+2 and vice versa. STAT3 preferentially binds peptides with a motif phosphotyrosine-(basic or hydrophobic)-(proline or basic)-glutamine <sup>99</sup>.

Another level of specificity is determined by the specific binding of activated STAT dimers to slightly different response elements. Variations of the inner nucleotides between the different palindromic GAS-like motifs, have been shown to influence the binding affinity towards specific STAT dimers. For example STAT1 homodimer binds to the GAS element in the promoter of the Fc $\gamma$ R1 gene, whereas the STAT3 homodimer does not <sup>100</sup>. Furthermore, it seems that the ability of STATs to bind cooperatively to tandem GAS elements (which are 6-10 bp apart) also contributes to DNA binding specificity <sup>82, 101</sup>.

### 1.3 Biological functions of STAT proteins

The biological role of each individual STAT protein has been examined through the study of knockout mice.

#### *STAT1*

STAT1 KO mice are highly susceptible to microbial and viral infections and tumor formation due to defective IFN responses. These mice failed to induce transcription of STAT1 target genes in response to both IFN $\alpha/\beta$  and IFN $\gamma$ . They also failed to induce ISGs in response to IFN $\alpha$  <sup>102</sup>. It is also demonstrated that STAT1-deficient mice exhibit a higher incidence of spontaneous and chemically induced tumors. This can be explained through STAT1 roles in upregulation of proapoptotic genes (caspases<sup>103</sup>) and its role in the regulation of expression of proteins involved in antigen presentation (MHC class II) and thus affecting the immunogenicity of the tumor <sup>104</sup>. Furthermore, it is shown that STAT1 interacts with p53 to enhance DNA damage-induced apoptosis. In addition, STAT1 could suppress Mdm2 protein in STAT1-deficient cells. Mdm2 protein interacts with p53 to induce its degradation <sup>105</sup>.

---

### *STAT2*

STAT2 is the only member that does not bind to GAS elements. Its biological function is not well understood so far, however since it is activated by IFN $\alpha/\beta$  it is clear that it plays a critical role in promoting antiviral immune response. STAT2 knockout mice are, like STAT1 KO susceptible to viral infections. Studies in these mice suggested that STAT2 regulates the basal levels of STAT1 expression in MEFs, since upregulation of STAT1 in response to IFN $\alpha$  is impaired. This was not the case in macrophages <sup>106</sup>. STAT1/STAT2 double knockouts are completely unresponsive to all IFNs and show more susceptibility to infection than either of the single knockouts.

### *STAT3*

STAT3 is activated by many cytokines. STAT3 KOs are embryonically lethal at day 7.5. However the generation of tissue-specific knockouts using the Cre-lox method has revealed STAT3' role in a wide variety of tissues <sup>107</sup>. The lack of STAT3 in skin showed that it is important in the migration of keratinocytes and is essential during the hair cycle and wound healing <sup>108</sup>. STAT3 deficient T-cells exhibit loss of proliferative response to IL-6, which has previously been shown to suppress apoptosis in these cells <sup>109</sup>. Furthermore do STAT3-deficient T-cells show an impaired IL-2-mediated IL-2 receptor (IL-2R) alpha chain expression <sup>110</sup>. The lack of STAT3 in liver results in an impaired acute phase response, caused by a defective STAT3 induced expression of fibrinogen, haptoglobin, serum amyloid (SAP), serum amyloid A1 (SAA) and proteinase inhibitor  $\alpha$ 2-macroglobulin <sup>72</sup>. STAT3 does also play an essential role in the normal glucose homeostasis by downregulation of the expression of gluconeogenic genes like phosphoenolpyruvate carboxykinase-1 (PCK-1) and glucose 6-phosphatase (G6PC). Mice with liver-specific STAT3 deficiency showed insulin resistancy associated with increased hepatic expression of PCK-1 and G6PC genes <sup>111</sup>. Liver partial hepatectomy in STAT3 liver-specific KO mice showed that STAT3 promotes cell cycle progression and cell proliferation during liver regeneration. Activation of MAPK signaling was normal in these livers <sup>112</sup>. In thymus, it impairs the postnatal maintenance of thymic architecture and thymocyte survival <sup>113</sup>. Mice deficient for STAT3 in macrophages and neutrophils are more susceptible to endotoxin shock with an increased production of inflammatory cytokines such as TNF alpha, IL-1, IFN gamma, and IL-6 by the macrophages and neutrophils probably due to impaired IL-10 suppressive effects on this production in these mice <sup>114</sup>. Deletion of STAT3 in mammary glands results in delayed apoptosis that occurs during cyclical mammary gland involution <sup>115</sup>. Selective targeting of the full length STAT3 $\alpha$  and truncated STAT3 $\beta$  splice variants showed specific functions for both isoforms. Mice lacking STAT3 $\beta$  are hypersensitive to endotoxin-induced inflammation <sup>116</sup>. In liver-specific STAT3 isoform KO mice it was reported that STAT3 $\beta$  is not a dominant negative factor, since its expression can rescue the embryonic lethality of a complete STAT3 deletion. Both isoforms can induce acute phase proteins. STAT3 $\alpha$  however is responsible for regulation of the IL-6 response and of the IL-10 anti-inflammatory function in macrophages <sup>117</sup>.

### *STAT4*

Since IL-12 activates STAT4, the STAT4 knockout mouse does display defective IL-12 responses; i.e. impaired T-helper-cell type I (Th1) differentiation and therefore impaired IFN $\gamma$  production and cell-mediated immunity <sup>118</sup>. Because of the defective Th1 response these animals are resistant to Th1 mediated autoimmune diseases like arthritis and diabetes <sup>119</sup>.

### *STAT5*

The two STAT5a and STAT5b proteins are approximately 95% identical in aa sequence. Mice deficient for only STAT5a <sup>120</sup> or STAT5b <sup>121</sup> have revealed specific and limited functions for the two STAT5 proteins individually <sup>122</sup>. Through analyses of these single knockouts has been revealed that STAT5a is important in prolactin, GM-CSF and IL-2 signaling. STAT5a KO mice show no effect on body growth or serum IGF-1 (mediator of the somatic effects of GH) levels <sup>122</sup>. In liver is STAT5a, together with STAT5b the most important mediator activated by GH <sup>123</sup>. STAT5b is important in controlling somatic growth in mice. It is as well regulating sexually dimorphic gene patterns, which exhibits itself in STAT5b KOs by GH mediated loss of male-characteristic body growth rates and male specific liver gene expression of cytochrome P450 (CYP) steroid hydroxylases. Levels of male specific CYP2D9 and testosterone 16 $\alpha$ -hydroxylase were decreased in these knockouts and levels of female liver specific CYP3a, CYP2B and testosterone 6 $\beta$ -hydroxylase were increased. In female mice are both STAT5a and STAT5b required for the constitutive expression of hepatic female specific GH-regulated, CYP2B, as well as several CYP-catalyzed testosterone hydroxylase activities <sup>124, 125</sup>.

STAT5a is furthermore required for mediating prolactin signaling and mammary gland development and lactogenesis <sup>120</sup>. STAT5a/5b double knockout females are infertile, caused by an altered corpus luteum development. This is in contrast to single STAT5a or 5b deficient mice, which are fertile, suggesting that the function of the STAT5 proteins may be redundant <sup>122</sup>.

### *STAT6*

STAT6 is required for the induction of IL-4 dependent gene expression leading to type II T-helper-cell (Th2) differentiation and IL-4 dependent B-cell proliferation. In addition, has it been demonstrated that STAT6 is important for the functions mediated by IL13, which is related to IL4. IL4 and IL13 have been shown to induce the production of IgE, which is a major mediator in an allergic response. STAT6 activation might therefore be involved in IL4- and IL13-mediated disorders such as allergy <sup>126 127</sup>. This was proven in STAT6 deficient mice, which display a reduced pathology in asthma. Furthermore is it described that STAT6 deficiency is associated with enhanced tumor immunity, since natural killer T-cells (NKT-cells) and IL-13, produced by NKT-cells and signaling through the IL-4R-STAT6 pathway, are necessary for down-regulation of tumor immunosurveillance <sup>128</sup>.

---

### 1.3.1 Impact of STATs in disease

Since STAT proteins display a wide range of functions in many biological aspects, they are consequently involved in or mediating pathological processes.

Many viruses have developed mechanisms to inhibit the anti-viral immunity actions of IFNs through disruption of IFN induced Jak-STAT signaling.

Hepatitis C virus (HCV) inhibits IFN signaling downstream of STAT phosphorylation <sup>129</sup>. Duong et al. showed that acceleration of the negative feedback loop of Jak-STAT signaling, through an increased upregulation of PP2Ac, is responsible for decreased binding of activated STAT1 to the DNA and inhibition of signaling <sup>130</sup>. In vitro and in vivo studies to demonstrate HCV interference with IFN $\alpha$  induced Jak-STAT signaling are described in chapter 2 and 3. Interference with IFN induced Jak-STAT signaling in many different ways as mechanism of viral persistence, is also reported for other viruses as simian virus 5 <sup>131</sup>, herpes simplex virus type 1 (HSV-1) <sup>132</sup>, hepatitis B virus (HBV) <sup>133</sup>, Sendai virus <sup>134</sup>, human parainfluenza virus type 2 <sup>135</sup>, adenovirus <sup>136, 137</sup>, human papilloma virus (HPV) <sup>138, 139</sup>, Epstein-Barr virus (EBV) <sup>140</sup>, cytomegalovirus (CMV) <sup>141</sup> and paramyxoviruses like mumps virus <sup>142, 143</sup>, measles virus <sup>144</sup> and Nipah virus <sup>145</sup>.

Other examples of diseases caused by a defective signal transduction through the Jak-STAT pathway are X-linked combined immunodeficiency (XCID) and X-linked severe combined immunodeficiency (XSCID). In both diseases Jak3 activation is impaired due to mutations of the IL-2R $\gamma$  chain. C-terminal truncations of this receptor chain completely prevent Jak3 binding and results in development of XSCID. In XCID the Jak3 association with the receptor is only reduced due to a point mutation in IL-2R $\gamma$  chain. Mutational Jak3 deficiency has also been detected in patients with the less severe form SCID <sup>9 146</sup>.

STAT3 might be involved in the pathogenesis of Crohn's disease. Mice with tissue-specific deletion of STAT3 during haematopoiesis showed Crohn's disease-like pathogenesis and intestinal T-cells from patients with Crohn's disease express constitutively activated STAT3 <sup>147, 148</sup>.

Dysregulation of STAT signaling pathways has been demonstrated to contribute malignant cellular transformations by promoting cell cycle progression and/or cell survival. Constitutive activation of Jak and STAT proteins has been reported in a large and growing number of malignant cell lines and human cancers <sup>5, 149</sup>. Constitutive activation of STATs is often associated with malignant transformation induced by oncogenes coding for oncogenic tyrosine kinases like members of the Src, Abl or Ras family. Also a constitutive active STAT3 (STAT3-C; substitution of two cysteine residues in the SH2 domain) could function as oncogene independently of a tyrosine kinase oncogene. This molecule is capable of driving transcription and induces cell transformation <sup>150</sup>. Constitutively activated STAT3 and STAT5 participate in oncogenesis through upregulation of genes encoding apoptosis inhibitors like Mcl-1, Bcl-X<sub>L</sub> and Bcl-2 to promote cell survival <sup>151, 152</sup> and cell cycle regulators like cyclins D1, 2, 3 and A, c-myc, cdc25A to promote cell cycle G1 to S phase transition <sup>153, 154</sup> and inducers of angiogenesis like VEGF <sup>155</sup>.

## 1.4 Hepatitis C virus (HCV)

Hepatitis C virus is a small, enveloped, positive single-stranded RNA virus that belongs to the Flaviviridae Family and the genus Hepacivirus. Based on sequence similarities the different HCV strains are divided into 6 different genotypes (nr 1-6) and a large group of subtypes (a, b, ect.). The most important way of transmission is by direct blood contact. The initial infection is usually asymptomatic. Between 40-85% of infected patients do not clear the virus and develop chronic HCV <sup>156, 157</sup>. More than 170 million people worldwide are chronically infected <sup>157, 158</sup>. Chronic HCV patients can develop progressive liver fibrosis, cirrhosis with as result portal hypertension and liver failure (approx. 10-20% of cases after 10-20 years) and finally hepatocellular carcinoma (HCC) (75% of cirrhosis cases after 20-30 years, incidence of 1-4% per year) <sup>156, 157, 159</sup>.

HCV infected patients are treated with a combination therapy of pegylated IFN $\alpha$ -2a or 2b and ribavirin. Pegylation of IFN $\alpha$  increases the half life of IFN $\alpha$  from 5-6 hours to several days. The virological response is defined by a reduction of HCV RNA in serum and ideally by the absence of detectable HCV RNA by qualitative RT-PCR. HCV genotypes 1 and 4 show a 40-60% response rate after 48 weeks of combined antiviral treatment whereas genotype 2 and 3 show a 75-85% response rate <sup>156</sup>.

Although a HCV-specific immune response is generated, there is not enough control over viral replication to terminate persistent infection or to resolve chronic infection. There is evidence that both CD4+ and CD8+ T-cell responses are crucial for the clearance of viral load. In chronic infection, T-cell responses are to HCV significantly impaired <sup>160</sup>. It has been hypothesized that HCV avoids the induction of a strong innate or adaptive immune response during early infection. It was believed that the vigor and quality of the antiviral CD8+ T-cell response determines the outcome of acute HCV infection. However, studies in chimpanzee have shown that the clearance of HCV, derived from an infectious full-length HCV genotype 1b cDNA, was not correlated with T-cell responses. Two of four infected chimpanzees cleared the infection to undetectable levels for more than 12 months, but all four displayed weak and transient Thelper-cell responses during acute infection <sup>161</sup>. The production of a protecting antibody response to HCV following acute infection is delayed. Crossreactive neutralizing antibodies against heterologous HCV viruses seem to appear only between 33 and 111 weeks of infection. Before this period only strain-specific neutralizing antibodies are thought to be generated <sup>162</sup>.

### 1.4.1 Genomic organization of HCV and functions of viral proteins

The HCV genome (approximately 9.6 kb) contains a single long open reading frame encoding a polyprotein precursor of approximately 3100 aa that is post-translationally cleaved by both host and viral proteases to produce 10 structural and nonstructural proteins (Figure 5) <sup>163-165</sup>. The structural proteins which are coding at the N-terminal of the polyprotein include the nucleocapsid core protein, envelope glycoproteins E1 and E2 and p7. The nonstructural region encodes for NS2, NS3, NS4a, NS4b, NS5a and NS5b <sup>166</sup>. The nucleocapsid core protein forms together with the HCV RNA the HCV nucleocapsid. In addition has experimentally been suggested that HCV core

protein plays a role in gene transcription, cell proliferation, cell death, cell signaling, lipid metabolism and host immune responses <sup>167</sup>. The E1 and E2 envelope glycoproteins are believed to be essential for host-cell entry by binding to receptors and inducing fusion with a host-cell membrane. The p7 protein belongs to the viroporin family and can form an ion channel and might therefore play a role in viral particle release and maturation <sup>168</sup>. The nonstructural proteins are involved in polyprotein processing and viral replication. The junction between NS2 and NS3 encodes for a NS2-NS3 zinc-dependent metalloproteinase. The N-terminal of NS3 encodes for a serine proteinase, and the C-terminal region of NS3 includes RNA helicase and NTPase activities. NS4b is an integral membrane protein that appears to play a role in the formation of the replication complex <sup>169</sup>.

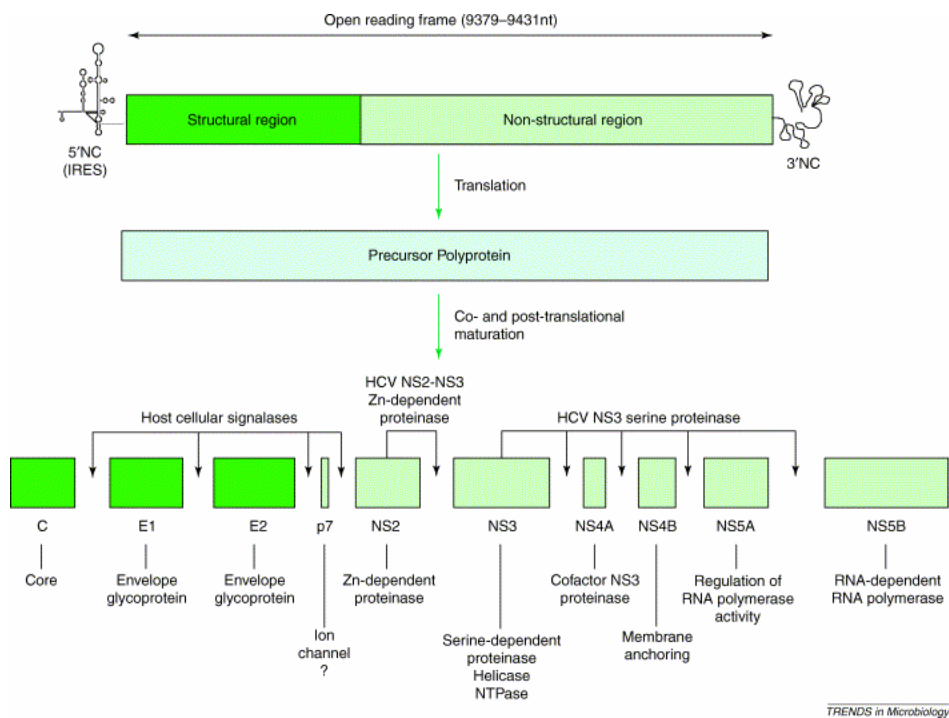


**Figure 5. Schematic organization of the Hepatitis C virus (HCV) genome.** The genome is depicted with the 5' containing the IRES and the 3' non-translated region (NTR or NC, non-coding in this picture). The open reading frame of the polyprotein is depicted as rectangle showing the process of translation and positions of post-translational cleavage sites by arrows. The individual functional HCV proteins and their functions are listed at the bottom. Picture is taken from a publication by JM Pawlowsky <sup>157</sup>.

NS5a is a polyphosphorylated protein of unknown function. NS5a has been reported to be involved in the inhibition of the antiviral actions of IFN by interacting with PKR, in transcriptional activation and in regulation of cell growth and cellular signaling pathways. Recent structural analyses of NS5a revealed that NS5a contains a membrane anchor domain that is likely involved in specific interactions essential for the assembly of the HCV replication complex <sup>170</sup>. NS5b is the RNA-dependent RNA polymerase and belongs to the family of tail-anchored proteins. NS5b C-terminal membrane

insertion sequence traverses the phospholipid bilayer as a transmembrane segment and believed to be a target for specific inhibitors <sup>171</sup>.

### 1.4.2 HCV polyprotein processing and replication

The HCV replication system is only partly understood, however based on its similarity to other Flaviviridae has the following model been proposed. The envelope glycoprotein complex E1-E2 is expressed on the surface of the HCV particle. Because the HCV particles have been shown to associate with low density lipoproteins (LDL) in serum, it has been suggested that HCV infection may occur through binding of LDL with the LDL receptor. Furthermore has the LDL receptor been shown to mediate HCV internalization by binding to virion-associated LDL particles <sup>172</sup>. However they did not show that these interactions lead to productive infection.

Sequences in the 5' and 3' termini of plus-strand RNA viruses harbor cis-acting elements important for efficient translation and replication. After entering the cell the viral protein translation is initiated by the ribosome binding to the internal ribosomal entry site (IRES) in the 341-nucleotide-long 5' non-translated region (NTR). The IRES is located downstream of an about 40-nucleotide-long sequence of unknown function. This 40-nucleotide long sequence was characterized to be required for RNA replication, deletions introduced into the 5' terminal 40 nucleotides abolished RNA replication but only moderately affected translation <sup>173</sup>. The 5' and 3' NTRs are highly conserved in all genotypes and an interesting subject for investigations concerning the development of antiviral therapies against HCV infection <sup>174</sup>.

The polyprotein is subsequently synthesized and co- and posttranslational cleaved by cellular and viral proteases at the level of the endoplasmic reticulum.

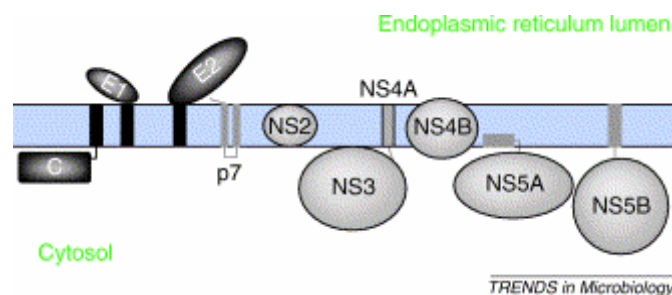


**Figure 6. Schematic representation of the polyprotein processing and the location of the HCV proteins relative to the endoplasmic reticulum membrane.**

The structural proteins (C, core protein; E1 and E2, envelope glycoproteins and p7) and the nonstructural proteins (NS2, NS3, NS4A, NS4B, NS5A and NS5B) are shown. Picture is taken from a publication by JM Pawlowsky <sup>157</sup>.

The structural proteins are cleaved by host-cell signal peptidases. The nonstructural proteins are produced by cleavage by NS2-NS3 zinc-dependent metalloproteinase, located at the NS2-NS3 junction, which separates NS2 from NS3. The NS3 serine proteinase, located at the N-terminal of NS3, is in association with NS4a, responsible for the cleavage of the remaining NS

---

proteins <sup>175</sup>. A schematic representation of the anchor regions of the HCV proteins within the endoplasmic reticulum membrane is shown in Figure 6.

In tetracycline-regulated cell lines inducibly expressing the entire HCV polyprotein has been demonstrated that intracellular membrane changes, called membranous web, were induced by the expression of all structural and nonstructural proteins in context of the entire HCV polyprotein. All HCV proteins were found to be associated with a membranous web, which consists of small vesicles embedded in a membranous matrix. Formation of the membranous web seems to be induced by the NS4b protein. A similar structure has also been found in the infected livers of chimpanzees <sup>176</sup>. Fluorescence in situ hybridization (FISH), EM-in situ hybridization and metabolic labeling with 5'-bromouridine 5'-triphosphate in presence of actinomycin D showed that the membranous web is the site of viral RNA synthesis and therefore represents the replication complex of HCV <sup>177</sup>. The HCV positive strand RNA is used as template for the synthesis of a negative strand RNA, which will serve as a template for the synthesis of positive strand RNA molecules that are through interaction with core proteins encapsidated in newly formed virions or serve as mRNA to generate viral proteins. The immature viral nucleocapsid particles are released to the ER lumen and are then transported to the Golgi apparatus where the envelope glycoproteins mature (glycosylation) and the final viral particles are formed. Subsequently are the viral proteins released from the cell through the ER membrane and cytoplasm <sup>157, 167, 178</sup>.

#### **1.4.3 Models to study HCV escape of immune response**

HCV has a replication rate of about  $10^{10}$ - $10^{12}$  new virions per day <sup>179</sup>. The high replication rate, in combination with the absence of any HCV polymerase proofreading ability, gives rise to viral quasispecies, which provide a mechanism for escaping host immune responses. The genetic instability of HCV also makes it difficult to develop vaccines. Furthermore it is probably that HCV viral proteins interfere with the host cellular functions by down-regulating processes unfavorable and up-regulating processes favorable for virus replication and persistence. Since a high percentage of infected patients do not respond to combined treatment of pegylated IFN $\alpha$  and ribavirin, it is necessary to investigate host-virus interaction and the mechanisms behind resistance against antiviral response and treatment by IFN $\alpha$  <sup>157, 165</sup>.

Since cells and small animals can not be infected with HCV, serving as model for replicating HCV, several models has been developed to study HCV viral proteins interference with IFN response and HCV viral structure and life cycle <sup>180</sup>. Continuous human osteosarcoma cell lines allowing tetracycline-regulated expression of the full length HCV open reading frame have been developed by Moradpour et al. <sup>181</sup>. A replicon system to study HCV replication was developed by Lohmann et al. <sup>182</sup>. They developed subgenomic and full-length replicons consisting of the 5' end of HCV including the IRES and 12 codons of the core protein, which is fused in frame with a neomycin resistance gene, the EMCV IRES to drive translation of the HCV structural and/or nonstructural proteins and the 3'NTR of HCV. The chimpanzee is the only animal model for HCV infection. However they have a very high viral clearance rate, thus are this not useful models to study persistent infection <sup>183</sup>. HCV transgenic mice have been raised expressing single HCV viral proteins <sup>184, 185</sup> or in



combinations<sup>186, 187</sup>. Also mouse models expressing all HCV viral proteins have been developed (see Chapter 2)<sup>129</sup> and HCV infected mice with human livers<sup>188</sup>.

Novel therapies for HCV include use of specific immunoglobulins against HCV<sup>189</sup>, DNA vaccines on its own or in combination with cytokines<sup>190</sup> and targeting of IRES mediated translation to block HCV replication<sup>191</sup>.

## 1.5 Liver cell regeneration

### 1.5.1 Liver

The liver is the largest organ of the human body. Its weight makes about 2.5% of the body weight in a human adult. The human liver consists of a main left and right lobe and two accessory lobes. The mouse liver contains three lobes, a middle, left and right lobe, from which the middle lobe is divided in two parts. Two-third of the liver cells are hepatocytes, they are responsible for glucose metabolism and uptake of lipids, amino acids and vitamins. Other cells include biliary epithelial cells, hepatic stellate cells and Kupffer cells, which are liver specific macrophages. The functional unit of the liver is the acinus, consisting of hepatic cells in between two terminal venules. The blood is supplied into the terminal portal venule and released into the sinusoids; from there the blood is collected in the central venule of the acinus and transported out of the liver via the hepatic veins.

### 1.5.2 Regulation of liver regeneration

Under normal physiological circumstances only a small percentage (0.0012% to 0.01%) of the hepatocytes proliferate, however after toxic injury or surgical resection the proliferative ability of the remaining hepatocytes is enormous. Within two weeks (after a loss of up to two thirds) the liver mass will grow back to its original size without losing its specific functions. The liver has the unique capacity to regulate its growth and mass. Studies with hepatic resections in larger animals and humans have shown that the regenerative response is proportional to the amount of liver removed and even proportional to the body size of where the liver mass is placed in, in case of a transplantation. So the size of the liver mass can be regulated positively as well as negatively<sup>192, 193</sup>. The experimental model to study liver regeneration is partial hepatectomy (PH), developed by Higgins and Anderson<sup>194</sup>, in which two-thirds of the liver of mouse or rat is removed. The excised lobes do not regrow; instead do the remaining lobes enlarge, undergoing compensatory hyperplasia<sup>195</sup>. Regeneration is induced by extrahepatic signals, which are probably a combination of interacting hormones (e.g. insulin, glucagon, growth hormone and glucocorticoids), growth factors (epidermal growth factor (EGF), transforming growth factor $\alpha$  and  $\beta$  (TGF $\alpha$  and  $\beta$ ), hepatocyte growth factor (HGF)) and cytokines (IL-1, IL-6, TNF $\alpha$ ,) <sup>195</sup>. When primed hepatocytes progress from the G<sub>0</sub> phase of the cell cycle to G<sub>1</sub>, move to the S phase and undergo mitosis. The first peak of DNA synthesis occurs in mice and rat at 24 to 40 hours after PH and at 180 to 200 hours in human<sup>193</sup>. The following priming model has been proposed for the factors involved in the response to PH to induce regeneration. Directly after PH are TNF $\alpha$  and IL-6 secreted in response to gut-derived lipopolysaccharide. They induce hepatocyte to respond to growth factors (G<sub>0</sub> to G<sub>1</sub>). The growth factors (HGF,

---

TGF $\alpha$  and EGF) allow hepatocytes to progress through the cell cycle (G1 to S). Insulin and epinephrine are growth promoting hormones and support the activity of the growth factors. Growth inhibitory factors activin A and TGF $\beta$  are down regulated during liver cell regeneration by suppressors of growth inhibitors LAP (latency associated peptide), inhibitor of TGF $\beta$  and follistatin, inhibitor of activin <sup>192</sup>.

Within 30 min after PH immediate early genes (like transcription factors c-myc, c-fos, c-jun and C/EBP $\beta$ ) are induced, several of these are target genes of STAT3 and NF $\kappa$ B <sup>196</sup>. STAT3 is activated by IL-6, and NF $\kappa$ B by TNF $\alpha$ . Liver regeneration studies in IL-6 and TNFR1 deficient mice showed high mortality after PH and impaired DNA synthesis in hepatocytes. The regeneration was delayed but in the surviving animals did the liver mass recover completely <sup>197</sup>. Mice overexpressing human IL-6 from Chinese hamster ovary cells showed massive hepatocyte proliferation and hepatomegaly <sup>198</sup>. Blindenbacher et al. showed that IL-6 was not required for liver cell proliferation since some KO animals did regenerate normally without IL-6 substitution. STAT3 target genes cyclin D1 and c-myc were not induced in these animals, and cell cycle progression was thought to take place with help of compensatory cyclin D3-CDK6 activation. The more important role of IL-6 in liver cell regeneration is induction of acute phase response. By acute phase protein activation induces IL-6 protective, i.e. anti-apoptotic pathways in hepatocytes <sup>199</sup>. IL-6 can induce expression of acute phase proteins through two kind of responsive elements, type I and type II. Type I IL-6 responsive elements are binding sites for CAAT/enhancer binding protein (C/EBP) transcription factor and have been identified on the class I genes for haptoglobin,  $\alpha$ 1-acid glycoprotein (AGP), hemopexin (Hpx), complement component 3 (C3), C-reactive protein (CRP), serum amyloid A (SAA), serum amyloid P (SAP). Class II genes, like  $\alpha$ 2-macroglobulin ( $\alpha$ 2M), fibrinogen, haptoglobin and  $\alpha$ 1-antitrypsin are regulated by type II IL-6 response elements (i.e. GAS-like response elements), which can be bound by STAT3. GAS-like motifs have also been identified on class I gene promoters <sup>72, 200</sup>.

New models to study liver regeneration make use of hematopoietic stem cells (HPCs) or bone marrow mesenchymal stem cells, of which has been proven that they are capable of generating many different types of cells, including hepatocytes. Production of hepatocytes from these stem cells, injected in mice with injured livers should lead to liver repopulation <sup>201</sup>. Bone marrow stem cells have however a very low capacity to generate hepatocytes in injured livers <sup>202-204</sup>. The most successful examples of hepatocyte generation from bone marrow stem cells are the production of hepatocytes in cultures of multipotent adult progenitor cells (MAPCs) <sup>205, 206</sup> and the repopulation of livers in fumarylacetoacetate hydrolase (FAH)-deficient mice by transplanted HSCs <sup>207</sup>.

## 1.6 Aim of this thesis

In general, the aim of this thesis was to understand in more detail the interference of HCV with Jak-STAT signaling and to develop new gain-of-function models to study the role of STAT signaling in liver pathophysiology.

Previous studies have suggested that interference of HCV proteins with IFN $\alpha$  induced signaling through the Jak-STAT pathway could contribute to resistance to IFN $\alpha$  treatment and enable HCV to escape the IFN $\alpha$  induced antiviral defense and so establish chronic infection. Such interference was shown in human osteosarcoma-derived cell lines expressing the entire HCV genotype 1a open reading frame under control of a tetracycline dependent promoter. When viral proteins were expressed in these cells, IFN induced DNA binding of STATs was inhibited and led to an impaired upregulation of IFN $\alpha$  target genes<sup>217</sup>. Here, we analyzed interferon induced signal transduction through the Jak-STAT pathway in transgenic mice that express HCV proteins (genotype 1b) in their liver cells, to confirm and get further insight in these previous *in vitro* found observations. Virus challenge experiments with LCMV were used to demonstrate the functional importance of Jak-STAT inhibition. Footpad swelling assays and vesicular stomatitis virus challenge experiments were used to exclude a defect immune response in the HCV transgenic mice (*chapter 2*). On the other hand we aimed to identify the HCV gene product(s) responsible for the observed inhibition of Jak-STAT signaling. For this purpose, we established a comprehensive panel of the osteosarcoma-derived and tetracycline-regulated cell lines allowing the expression of HCV genotype 1a or 1b structural and genotype 1a nonstructural proteins either alone or in different combinations. IFN $\alpha$  induced STAT activation was analyzed and compared in the diverse cell lines with EMSAs and Western blots (*chapter 3*).

We aimed to develop conditional gain-of-function mouse models to study the function of STAT1, STAT3 or STAT5a in various pathophysiological conditions, like HCV infection, cell regeneration or oncogenesis in liver. Therefore we have generated conditionally active forms of these STAT proteins, designed to be activated independently of their natural ligands and to mimic STAT signaling (i.e. fusion proteins between STAT proteins and the modified ligand binding domain of the estrogen receptor). In addition, for each STAT fusion protein three mutants were generated to study its functionality and ability to be activated. First, the wild-type and mutant fusion proteins for STAT1 and STAT3 were expressed in mouse embryonic fibroblasts in order to compare and analyze their ability to be activated and to mimic STAT signaling (*chapter 4*). Next, the transgenic mice were generated, designed to express wild-type STAT3 or SH2 domain mutant STAT5a fusion proteins under control of the liver-specific albumin promoter. The transgenic founders and F1 offspring were identified by PCR (*chapter 5*).



## **Expression of Hepatitis C Virus Proteins Inhibits Interferon Alpha Signaling in the Liver of Transgenic Mice**

Simone T.D. Stutvoet <sup>1</sup>, Alex Blindenbacher <sup>1</sup>, Francois Duong <sup>1</sup>, Lukas Hunziker <sup>2</sup>, Xueya Wang <sup>1</sup>, Luigi Terracciano <sup>3</sup>, Darius Moradpour <sup>4</sup>, Hubert E. Blum <sup>4</sup>, Tonino Alonzi <sup>5</sup>, Marco Tripodi <sup>5,6</sup>, Nicola La Monica <sup>7</sup>, and Markus H. Heim <sup>1,8</sup>

1. Department of Research, University Hospital Basel, CH-4031 Basel, Switzerland
2. Institute for Experimental Immunology, University Hospital, CH-8091 Zurich, Switzerland
3. Institute of Pathology, University Hospital Basel, CH-4031 Basel, Switzerland
4. Department of Medicine II, University Hospital Freiburg, D-79106 Freiburg, Germany
5. Istituto Nazionale Malattie Infettive I.R.C.C.S. "L. Spallanzani", Roma, Italy
6. Fondazione "Istituto Pasteur Cenci-Bolognetti", Dipartimento di Biotecnologie Cellulari ed Ematologia, Università di Roma La Sapienza, I-00161 Roma, Italy
7. Istituto di Ricerche di Biologia Molecolare P. Angeletti, I-00040 Pomezia, Italy
8. Department of Gastroenterology, University Hospital Basel, CH-4031 Basel, Switzerland

S.T.D.S., A.B., F.D. and L.H. contributed equally to this work

---

## Abstract

Hepatitis C virus (HCV) is a major cause of chronic liver disease, cirrhosis and hepatocellular carcinoma worldwide. The majority of patients treated with interferon alpha do not have a sustained response with clearance of the virus. The molecular mechanisms underlying interferon resistance are poorly understood. Interferon induced activation of the Jak-STAT signal transduction pathway is essential for the induction of an antiviral state. Interference of viral proteins with the Jak-STAT pathway could be responsible for interferon resistance in patients with chronic HCV.

We have analyzed interferon induced signal transduction through the Jak-STAT pathway in transgenic mice that express HCV proteins in their liver cells. STAT activation was investigated with Western blots, immunofluorescence and electrophoretic mobility shift assays (EMSA). Virus challenge experiments with LCMV were used to demonstrate the functional importance of Jak-STAT inhibition.

STAT signaling was found to be strongly inhibited in liver cells of HCV transgenic mice. The inhibition occurred in the nucleus and blocked binding of STAT transcription factors to the promoters of interferon stimulated genes. Tyrosine phosphorylation of STAT proteins by Janus kinases at the interferon receptor was not inhibited. This lack in interferon response resulted in an enhanced susceptibility of the transgenic mice to infection with a hepatotropic strain of LCMV.

Interferon induced intracellular signaling is impaired in HCV transgenic mice. Interference of HCV proteins with interferon induced intracellular signaling could be an important mechanism of viral persistence and treatment resistance.

## Introduction

The majority of patients infected with HCV develop chronic liver disease that may progress to cirrhosis and hepatocellular carcinoma<sup>208-210</sup>. The mechanisms by which the virus evades clearance by the host immune system despite a polyclonal and multispecific T-cell response and the presence of antibodies against all viral proteins are poorly understood<sup>211</sup>. There is good evidence in hepatitis B virus and lymphocytic choriomeningitis virus infection that noncytolytic, cytokine-mediated antiviral mechanisms play a key role in viral clearance from liver cells<sup>212, 213</sup>. Interferons (IFNs) induce an antiviral state in hepatocytes through the transcriptional induction of several dozens of target genes in the cell nucleus. After binding to their cognate receptors on the cell membrane, IFNs activate the Jak-STAT signal transduction pathway<sup>18, 65</sup>. Type I IFNs (IFN $\alpha$  and  $\beta$ ) bind to heterodimeric receptors consisting of IFN $\alpha$  receptor 1 and 2 (IFNAR1, IFNAR2). Ligand binding results in activation of two receptor-associated protein tyrosine kinases, Jak1 and Tyk2. The activated receptor kinase complex then recruits and activates signal transducer and activator of transcription 1 (STAT1), STAT2 and STAT3<sup>2, 214</sup>. STAT1 and STAT2 combine with a third transcription factor, p48 or interferon response factor 9 (IRF9), to form interferon stimulated gene factor 3 (ISGF3)<sup>18</sup>. ISGF3 binds to interferon stimulated response elements (ISREs) in the promoters of IFN stimulated genes (ISGs). Alternatively, the IFN activated STAT1 and STAT3 can form homodimers or STAT1-STAT3 heterodimers. These STAT dimers bind a different class of response elements, the gamma activated sequence (GAS) elements. Once bound to the promoters of ISGs, STATs induce the transcription of genes involved in the generation of an antiviral state<sup>1, 65</sup>. Signaling through the Jak-STAT pathway is of critical importance, since most IFN induced cellular effects are lost upon deletion of STAT1 in mice<sup>102, 215</sup> or in cell lines<sup>51</sup>. Therefore, interference with Jak and STATs could be a mechanism of viral persistence, and indeed, viruses such as adenovirus, cytomegalovirus, mumps virus and HBV have been shown to interfere with Jak-STAT signaling<sup>133, 137, 216</sup>. We hypothesized that interference with IFN signaling could enable HCV to escape the innate immune system. In previous work we have found evidence for such an interference with Jak-STAT signaling in human osteosarcoma cell lines with an inducible transgene comprising the complete open reading frame (ORF) of a HCV genotype 1a isolate<sup>181, 217</sup>. When viral proteins are expressed in these cells, IFN induced activation of ISGF3 is blocked and the activation of the STAT1/3 dimers is inhibited. Here, we report our analysis of IFN induced Jak-STAT signaling in liver cells of mice that express HCV proteins from a transgene with a liver specific promoter. We have found a strong inhibition of ISGF3 activation in these mice. When infected with lymphocytic choriomeningitis virus strain WE (LCMV-WE), the transgenic mice could not control the viral replication and suffered from a severe hepatitis. An inhibition of the interferon induced antiviral defenses in hepatocytes might enable HCV to establish a chronic infection in the majority of patients, and could contribute to resistance to treatment with IFN $\alpha$ .

---

## Materials and Methods

### Animals

A 9.0 kb cDNA fragment derived from plasmid pCD(38-9.4)<sup>218</sup> that covers the HCV ORF (aa 3 to 3010) was used for the generation of the transgenic mice. The HCV cDNA was inserted into a *A1AT* minigene by homologous recombination in bacterial cells<sup>219</sup>. Donor plasmid p(PucII-V ex *A1AT*) was first generated. This construct carries exons II, IV and V and intron IV of the *A1AT* gene, and it contains a multiple cloning site between exon II and exon IV. The HCV cDNA, spanning from nt 339 to 9416, flanked by two *Pac* I sites was then inserted into the *Pac* I site of plasmid p(PucII-V ex *A1AT*) such that the transgene ORF starts from the ATG of *A1AT* (in exon II), coding a fusion protein formed by 32 additional aa at the N-terminus of the HCV polyprotein. DH1 cells were used for the homologous recombination using as acceptor the recombinant cosmid containing the entire *A1AT* gene as described<sup>220</sup>. Transgenic C57BL/6 were generated by pronuclear microinjection in one-cell stage embryos of inbred C57BL/6 by BRL (BRL, Füllinsdorf, Switzerland) as described<sup>221</sup>. Genotype analysis was performed by Southern blot analysis on 10 µg of total genomic DNA extracted from tail specimens using a HCV cDNA fragment as probe (spanning E2-NS3). A full description of the mice will be published elsewhere. The inbred C57BL/6 control mice were purchased from the same provider that generated the transgenic mice (BRL; Füllinsdorf, Switzerland). Mice were bred in a specific pathogen free environment under standard conditions. For all experiments described in this manuscript, 7 to 14 week old animals were used, and controls and transgenic mice were age and sex matched. The study was approved by the animal care committee of the Kanton Basel.

### Northern blot

RNA was isolated from frozen tissues using Trizol reagent (Life Technologies) according to the manufacturer's instructions. Total RNA (20µg) was used in Northern blot analysis. HCV cDNA fragment including regions E2-NS3 and a 28S ribosomal RNA fragment were used as probe and labeled by random priming.

### Western blots

For the Western blot analysis whole cell extracts were prepared from the middle lobe of the mouse liver. The lobe was homogenized in lysis buffer ( 50 mM Tris pH 8, 280 mM NaCl, 0.5% NP40, 0.2 mM EDTA, 2 mM EGTA, 10% glycerol, 100 µM NaVO<sub>4</sub>, 1 mM PMSF, and proteinase inhibitors), incubated 30 minutes on a rotating wheel at 4 °C, and centrifuged at 14'000 x g for 5 minutes. To analyze the liver extracts for the presence of HCV core protein, 75 µg of total protein per sample was loaded onto a 12 % SDS-PAGE gel. The membranes were probed with the murine monoclonal antibody C7-50 directed against a conserved, linear epitope in the aminoterminal region of the HCV core protein<sup>222</sup>. For Western blot analysis of STAT phosphorylation, 100 µM NaVO<sub>4</sub> was added to the lysis buffer. Tyrosine phosphorylation of STAT1 and STAT3 was tested using the phospho-STAT1 specific antibody 9171S and the phospho-STAT3 specific antibody 9173S (New England BioLabs, Inc., Beverly, Massachusetts). Total amounts of STAT1 and STAT3 were determined with polyclonal antibodies sc346 and sc482, respectively (both from Santa Cruz



Biotechnology, Inc., Santa Cruz, California). For cytoplasmic/nuclear extracts, mouse livers were homogenized in 200  $\mu$ l of Buffer A containing 20 mM Hepes pH 7.6, 10 mM NaCl, 3 mM MgCl<sub>2</sub>, 0.1% NP-40, 10% glycerol, 0.2 mM EDTA and 1 mM DTT. After centrifugation at 2000 rpm for 5 min, supernatant (cytoplasmic extracts) was removed and the pellet was washed with 200  $\mu$ l of Buffer B containing 20 mM Hepes pH 7.6, 0.2 mM EDTA, 20% glycerol and 1 mM DTT, and then centrifuged at 3000 rpm for 5 min. The pellet was then resuspended in 150  $\mu$ l of Buffer C containing 20 mM Hepes pH 7.6, 400 mM NaCl, 0.2% EDTA, 20% glycerol and 1mM DTT. This nuclear extract was cleared by centrifugation and used for Western blot analysis.

### **Immunostaining of liver sections**

Cryosections were prepared at a thickness of 7  $\mu$ m and fixed in 4% paraformaldehyde. They were then permeabilized with 0.1% Triton X-100, blocked with 3% BSA, and incubated overnight at 37°C with phospho-STAT1 specific antibody 9173S (New England Biolabs, Inc., Beverly, Massachusetts) or anti-core monoclonal antibody C7-50<sup>222</sup>. After several washes, sections were incubated with secondary antibodies labeled with Cy3 or with FITC for 90 min at RT (Molecular Probes, Inc., Eugene, Oregon). Nuclei were stained with Hoechst stain diluted to 1/200 and sections were mounted with Fluorsave Reagent (Calbiochem, La Jolla, California).

### **Electrophoretic mobility shift assays (EMSA)**

Mice were injected with the indicated doses of murine IFN $\alpha$  (Calbiochem, La Jolla, California) or TNF $\alpha$  (Sigma, Buchs, Switzerland) into the tail vein. The animals were euthanized 20 minutes later. Nuclear extracts and EMSA were done as described previously<sup>223</sup>. The oligonucleotides used have the following sequences: ISRE = 5'-GAAAGGGAAACCGAAACTGAAGC-3', m67 = 5'-CATT TCCCGTAAATCAT-3', NFkB consensus site = AGTTGAGGGGACTTTCCCA GGC-3'. The experiments were repeated several times, using also murine IFN $\alpha$  from a different provider (Sigma, Buchs, Switzerland).

### **LCMV infections**

LCMV-WE was originally obtained from Dr. F. Lehmann-Grube (Hamburg, Germany) and was propagated on L929 cells. C57BL/6 and B6 HCV transgenic mice were infected i.v. with LCMV strain WE with the indicated dose. Virus titers in the liver were determined in an LCMV infectious focus assay as previously described<sup>224</sup>. For the LCMV footpad swelling reaction, mice were infected with 200 PFU LCMV-WE into the hind footpad and the swelling was measured daily with a spring-loaded caliper. Assays for serum concentration of alanine aminotransferase (ALT) and aspartate aminotransferase (AST) were performed at the Department of Clinical Chemistry, University Hospital Zurich, using photometric assays on a Hitachi 747 autoanalyzer (Tokyo, Japan).

---

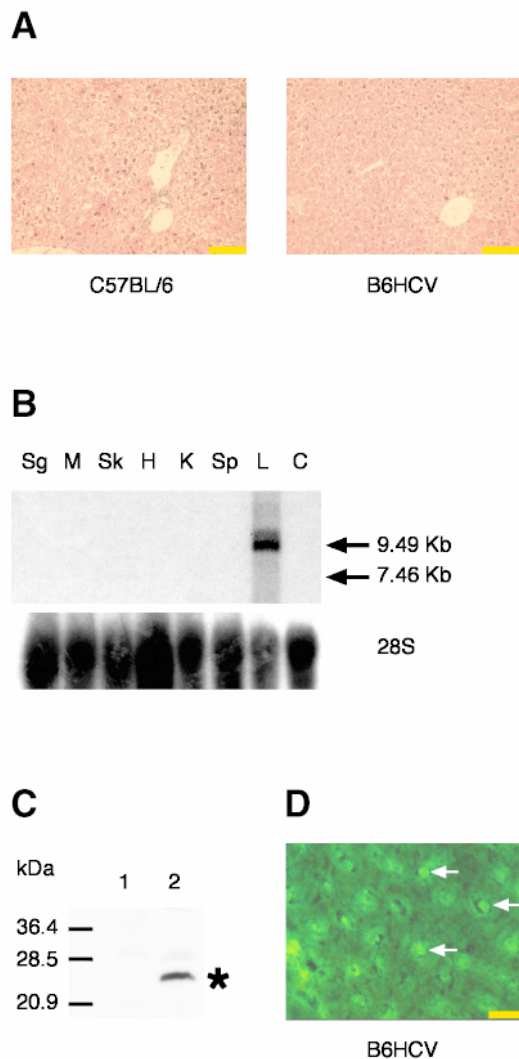
## Results

### HCV transgenic mice

To assess the effects of HCV proteins on IFN induced intracellular signaling in liver cells *in vivo*, we have generated a transgenic C57BL/6 mouse line carrying the entire ORF of a HCV genotype 1b isolate <sup>163</sup> under the control of an  $\alpha$ 1-antitrypsin promoter. The transgenic mice were designated B6HCV. B6HCV mice are healthy. With advanced age, more than 70% of the mice develop fatty liver, and, interestingly, a diffuse T-cell infiltration is observed in more than half of the mice. These observations are the subject of a separate manuscript. Since both liver steatosis and lymphocyte infiltrates could potentially influence signaling through the Jak-STAT pathway, we used for all our experiments 7 to 14 week old animals. In these younger mice, analysis of formalin fixed liver sections showed no inflammatory infiltrates or liver steatosis (Figure 1A). Controls were age and sex matched. In liver cell extracts of B6HCV mice a single full length mRNA transcript of the transgene of approximately 10kb can be detected by Northern blot (Figure 1B), and strong expression of HCV core protein was found by Western blot (Figure 1C). The core protein is fused on its N-terminus to 32 aa of  $\alpha$ 1-antitrypsin, and has a calculated molecular weight of 24 kDa. We could not detect additional HCV proteins by Western blot. Immunostaining of liver sections showed HCV core expression in hepatocytes (Figure 1D).

Similar to findings in other transgenic mice, the expression level of the transgene is not uniform. In some hepatocytes, no core protein can be detected, while others show strong signals. Core protein is found both in the cytoplasm and the nucleus of hepatocytes. The number of hepatocyte nuclei that stained positive was counted in liver sections from three mice. The mean percentage of nuclei containing core protein was 29% (with a standard error of the mean of 6%). Nuclear localization of the HCV core protein is a debated issue. While some authors have found core protein only in the cytoplasm <sup>225</sup> others have found an additional nuclear localization of the protein *in vitro* <sup>226</sup> and in transgenic mice *in vivo* <sup>184</sup>. In our transgenic mouse model, the high expression level of core protein in a subgroup of hepatocytes might allow the detection of core protein in the nucleus. Alternatively, the fusion of the first 32 aa from  $\alpha$ 1-antitrypsin to the N-terminus of core protein might have changed the subcellular distribution of core.

**Figure 1. Expression of HCV core protein in liver cells of B6HCV mice.** (A) Formalin fixed liver sections of C57BL/6 and of B6HCV mice were stained with hematoxylin-eosin according to standard procedures. Neither inflammatory infiltrates nor liver steatosis is present in these 14-week-old animals. The yellow size bars indicate 100  $\mu$ m. (B) Liver specific expression of the A1AT-HCV transgene. Northern blot analysis was performed using RNA extracted from 1 month old transgenic mouse tissues probed with a HCV specific probe. 20  $\mu$ g of total RNA were loaded per lane. A probe for the 28S ribosomal RNA was used as an internal control. Sg, salivary glands; M, muscle; Sk, skin; H, heart; K, kidney; Sp, spleen; L, liver of transgenic mice; C, control = liver of wild type mouse. (C) Liver cell extract from a C57BL/6 (lane 1) and a B6HCV mouse (lane 2) were analyzed for the presence of HCV core protein by Western blot. The asterisk indicates the core protein. The positions of the molecular weight markers are indicated to the left. (D) HCV core protein can be detected by immunostaining in liver cells of B6HCV mice. Core protein is present both in the cytoplasm and in the nucleus (arrows). The size bars indicate 20  $\mu$ m.



### IFN induced Jak-STAT signaling

In a first set of experiments B6HCV and control C57BL/6 mice were injected with murine IFN $\alpha$  (mIFN $\alpha$ ) into the tail vein (Figure 2A). The animals were euthanized 20 minutes later. Nuclear extracts were prepared from liver cells and tested for ISGF3 induction by electrophoretic mobility shift assays (EMSA) using an ISRE oligonucleotide probe. A total of 12 control mice and 16 B6HCV mice were used 4 independent experiments with 5 to 10 mice each. In C57BL/6 mice a strong ISGF3 shift was detected after treatment with 1000 IU mIFN $\alpha$ /g body weight, whereas the same dose was ineffective in B6HCV mice (Figure 2A, lanes 6, 7 and 8, respectively). This inhibition of STAT signaling could be overcome by higher doses of mIFN $\alpha$ . The intravenous (i.v.) injection of 4000 IU mIFN $\alpha$ /g body weight induces a strong STAT activation as shown by EMSA with the m67 probe (Figure 2B). The inhibition of STAT signaling is not due to non specific toxic effects of the viral proteins, since signaling of tumor necrosis factor  $\alpha$  (TNF $\alpha$ ) through NF $\kappa$ B was not inhibited (Figure 2C).

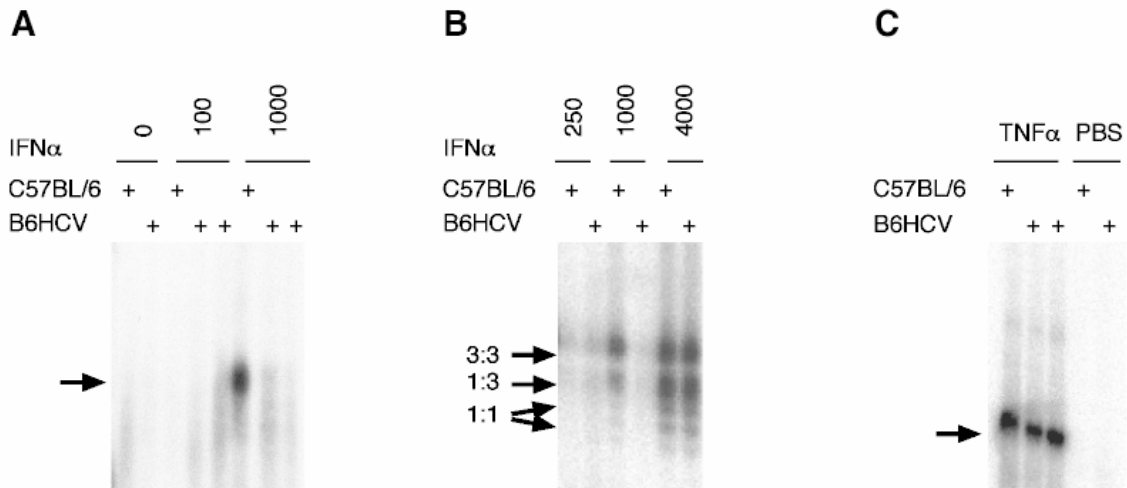
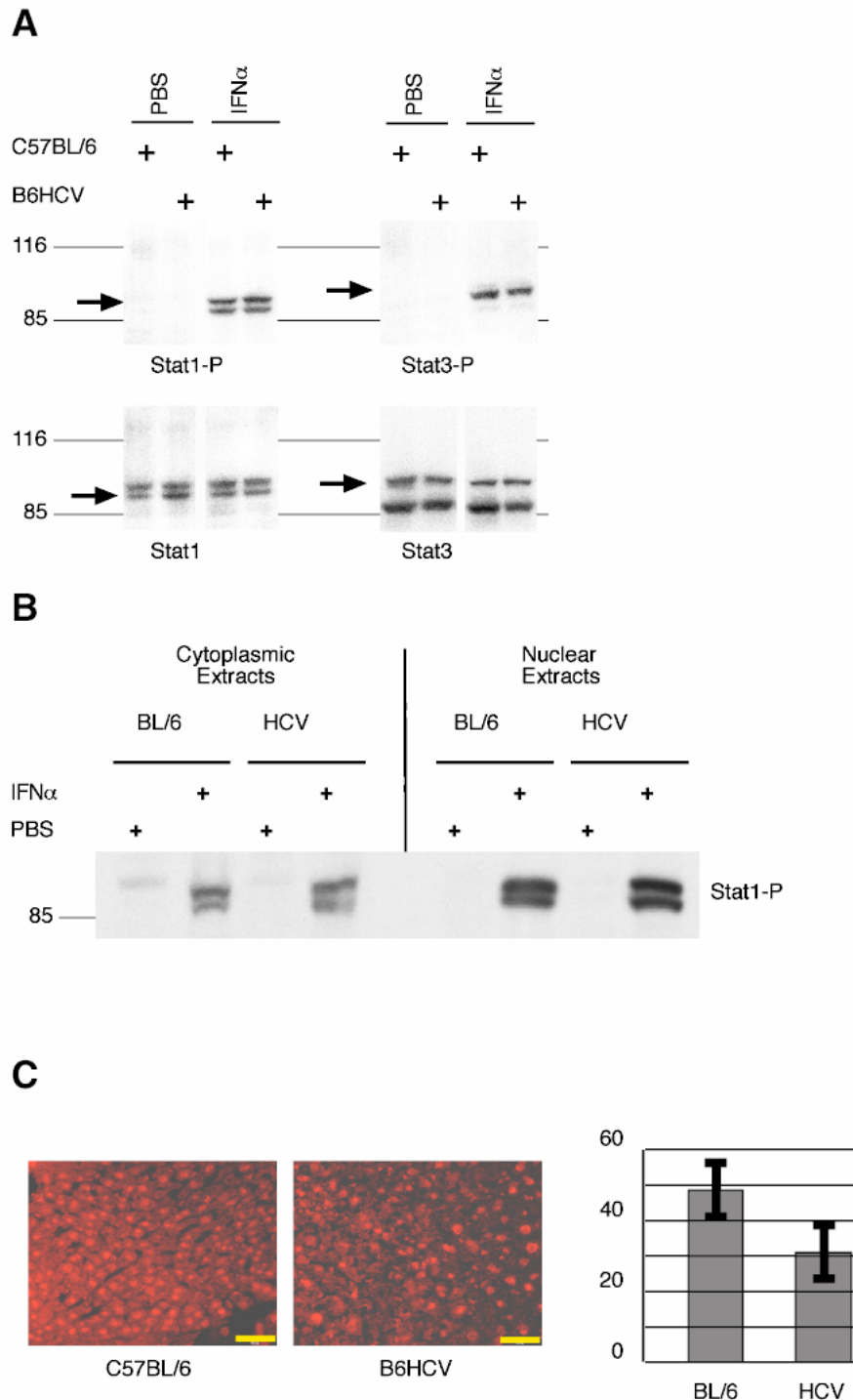


**Figure 2. Activation of STATs after intravenous cytokine injections in B6HCV and C57BL/6 mice.** (A) Nuclear extracts from liver cells were tested by EMSA with the ISRE oligonucleotide. An ISGF3 shift (arrow) is readily detected in C57BL/6 mice injected with 1000 IU mIFN $\alpha$ /g body weight, but not in B6HCV mice. C57BL/6 and B6HCV mice were injected with PBS, 100 IU mIFN $\alpha$ /g body weight, or 1000 IU mIFN $\alpha$ /g body weight as indicated. (B) EMSA with the m67 oligonucleotide. The positions of gel shift complexes containing STAT3 homodimers, STAT1-STAT3 heterodimers, and STAT1 homodimers are indicated. No induction of STAT gel shift complexes can be detected in both C57BL/6 and B6HCV mice after injection with 250 IU mIFN $\alpha$ /g body weight (lanes 1 and 2, respectively). Injection of 1000 IU mIFN $\alpha$ /g body weight induces STAT dimers in a C57BL/6 mouse (lane 3) but not in a B6HCV mouse (lane 4). In both the C57BL/6 (lane 5) and the B6HCV mouse (lane 6), STAT gel shifts are induced by 4000 IU mIFN $\alpha$ /g body weight. (C) TNF $\alpha$  induced NF $\kappa$ B activation is not impaired in B6HCV mice. EMSA with NF $\kappa$ B consensus oligonucleotide. Injection of 5 ng TNF $\alpha$ /g body weight results in NF $\kappa$ B shifts (arrow) in both a C57BL/6 mouse (lane 1) and in two B6HCV mice (lanes 2 and 3). PBS controls are shown in lane 4 (C57BL/6) and lane 5 (B6HCV).

The absence of ISGF3 and STAT1 and STAT3 homodimer gel shift complexes could result from a lack of activation of STATs through tyrosine phosphorylation at the IFN $\alpha$  receptor kinase complex. The phosphorylation of STATs on a single tyrosine residue carboxy-terminal of their SH2 domain is required for dimerization and nuclear translocation<sup>48</sup>. In HCV protein containing liver cells of B6HCV mice this decisive STAT activation event could be impaired through a downregulation of IFNAR1, IFNAR2, Jak1, Tyk2 or the STATs, or through the induction of suppressor of cytokine signaling 1 or 3 (SOCS1 or SOCS3)<sup>227</sup>. However, tyrosine phosphorylation of STAT1 and STAT3 after injection of 1000 IU mIFN $\alpha$ /g body weight is not impaired in the liver of B6HCV mice compared to C57BL/6 control mice (Figure 3A). This observation is in accordance with our previous findings in inducible cell lines *in vitro*<sup>217</sup>.

**Figure 3. Tyrosine phosphorylation and nuclear translocation of STATs.** (A) Tyrosine phosphorylation of STATs is not impaired in B6HCV mice compared to C57BL/6 mice. Mice were injected i.v. with PBS or with 1000 IU mIFN $\alpha$ /g body weight and euthanized 20 minutes later. The arrows indicate STAT1 and STAT3, respectively. The position of the 116 kDa and 85 kDa size markers is shown.



**(B)** Nuclear import of phospho-STAT1 is not inhibited in B6HCV mice. Cytoplasmic as well as nuclear extracts were prepared from livers of control mice and HCV transgenic mice 20 min after injection with PBS or 1000 IU mIFN $\alpha$ /g body weight as indicated. Tyrosine phosphorylated STAT1 was detected by Western blot with phospho-STAT1 specific antibodies. **(C)** Phospho-STAT1 nuclear translocation is impaired in B6HCV mice. The scale bar represents 50  $\mu$ m. Hepatocytes with phospho-STAT1 nuclear localization were counted under a fluorescent microscope. Five C57BL/6 mice and four B6HCV mice were analyzed. For each animal, ten areas were randomly chosen for counting. About 2000 cells were counted per animal. The histogram shows the average percentage of cell nuclei that stain positive with the phospho-STAT1 specific antibody 9171S in C57BL/6 and B6HCV mice, respectively. The error bars represent the 95% confidence interval for the mean values.

---

Viral proteins could also impair the nuclear translocation of phosphorylated STATs. Such a block in nuclear import in the presence of a normal STAT1 tyrosine phosphorylation at the receptor-kinase complex would result in an accumulation of phospho-STAT1 in the cytosol and a relative lack phospho-STAT1 in the nucleus. However, in both controls and B6HCV mice, most phosphorylated STAT1 molecules were found in nuclear extracts and not in cytoplasmic extracts (Figure 3B). We conclude that nuclear translocation is not significantly impaired in liver cells of HCV transgenic mice. Alternatively, viral proteins could stimulate the dephosphorylation of STATs in the nucleus through the upregulation of one or more as yet unidentified phosphatases. To address this issue with a more quantitative method than western blot detection of phospho-STAT1 in cytoplasmic and nuclear extracts, we stained cryosections from livers of five C57BL/6 and four B6HCV mice, respectively, with a phosphospecific STAT1 antibody (Figure 3C), and counted the number of cells that showed nuclear localization of phosphorylated STAT1. All mice have been injected i.v. with 1000 IU mIFN $\alpha$ /g body weight and euthanized 20 minutes later. About 2000 cells were counted for each mouse. The average percentage of phospho-STAT1 positive nuclei was 48.0% in C57BL/6 mice (standard deviation = 8.3, standard error of the mean = 3.7), but only 31.3% in B6HCV mice (standard deviation = 7.9, standard error of the mean = 2.3) (Figure 3C). The absence of detectable STAT gel shifts in nuclear extracts from B6HCV mice could be explained by this reduction of nuclear phospho-STAT1, since the sensitivity and detection limit of the EMSA with liver cell nuclear extracts is not known. Alternatively, the DNA binding of phosphorylated STAT1 complexes could be inhibited by viral proteins or by endogenous inhibitors such as protein inhibitor of activated STAT1 (PIAS1) that would be upregulated in the liver cells of B6HCV mice. By Western blots with PIAS1 antibodies we could not detect increased expression of PIAS1 in liver cells of B6HCV mice (data not shown). However, yet unknown inhibitors of STAT DNA binding could be involved in the observed inhibition of STAT gel shifts.

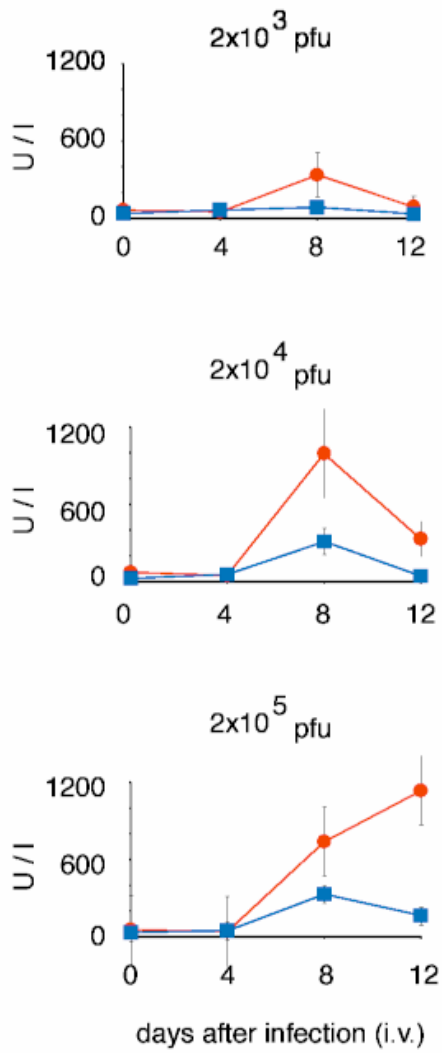
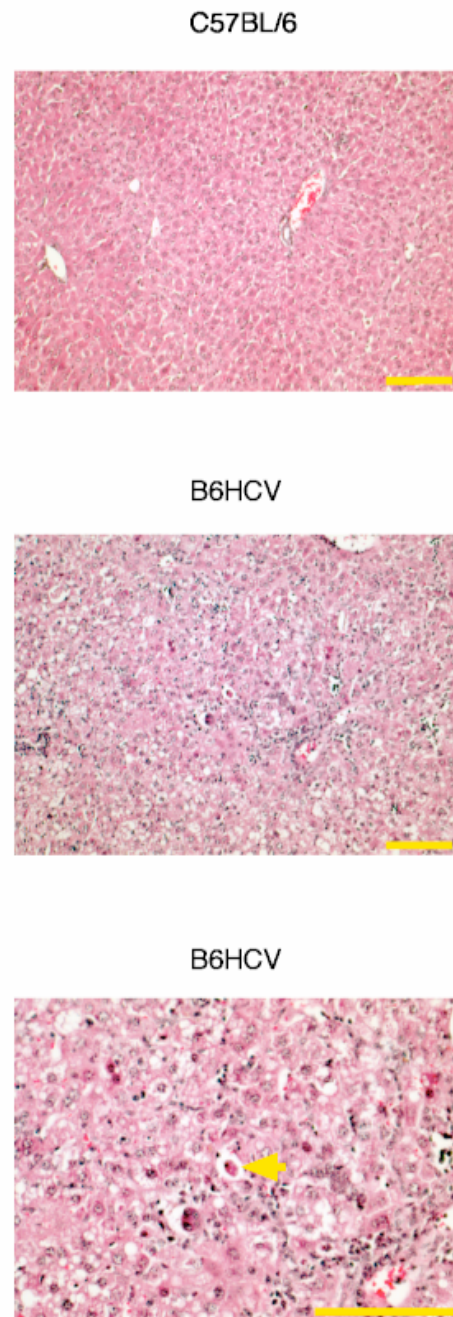
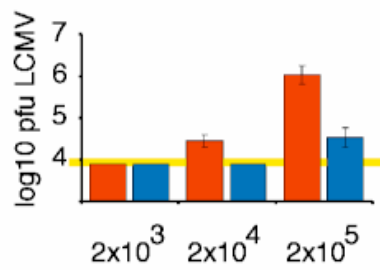
### **Impaired antiviral response *in vivo***

We next tested the consequences of impaired IFN signaling for host resistance to a viral infection. Susceptibility to LCMV has been shown to be greatly increased in mice that lack IFNAR1<sup>61</sup>. The hepatotropic strain LCMV-WE is a non-cytopathic RNA virus that causes a dose-dependent immunopathology. The liver damage is mediated by a cytotoxic T cell response<sup>228</sup>. We hypothesized that the inhibition of IFN signaling by HCV proteins in liver cells of B6HCV transgenic mice would increase the viral replication, and consequently result in an increased immunopathological liver inflammation. Therefore, transgenic and control mice were injected i.v. with various doses of the hepatotropic lymphocytic choriomeningitis virus strain WE (LCMV-WE). LCMV-WE infects hepatocytes, Kupffer and sinusoidal endothelial cells<sup>229</sup>. In support of our hypothesis, B6HCV mice suffered a more severe hepatitis (Figure 4).

After injection of  $2 \times 10^4$  pfu LCMV or  $2 \times 10^5$  pfu LCMV C57BL/6 controls had only a slight increase of serum amino transferase levels at day 8 after infection with a return to normal values at day 12 (Figure 4A). The liver histology of C57BL/6 mice showed a minimal mononuclear infiltrate in liver sinusoids at day 8, and a normal liver at day 12 (Figure 4B). On the contrary, B6HCV mice

had very high amino transferase values and liver histology showed a more severe hepatitis with diffuse hydropic swelling and ballooning of hepatocytes, diffuse intrasinusoidal mononuclear infiltrates and apoptotic hepatocytes (Figure 4).

**Figure 4. Increased susceptibility of B6HCV mice to LCMV-WE infection. (A)** B6HCV (red circles) and C57BL/6 (blue rectangles) mice were injected i.v. with the indicated doses of LCMV-WE. Serum alanine amino transferase (ALT) values (U/L) were determined at day 0, 4, 8 and 12. Three mice each were used per group and per LCMV-WE dose. The rectangles and circles represent mean values; the bars show the standard error of the mean. **(B)** All C57BL/6 and B6HCV mice were euthanized 12 days after i.v. injection of  $2 \times 10^5$  pfu of LCMV. Formalin fixed liver sections were stained with hematoxylin-eosin according to standard procedures. Representative samples are shown. Whereas C57BL/6 mice show no signs of hepatitis, a moderately severe hepatitis with slight lobular disarray, diffuse intrasinusoidal mononuclear infiltrates and apoptotic hepatocytes (arrow) are seen in B6HCV mice. The yellow size bars indicate 100  $\mu\text{m}$ . **(C)** Virus titers were measured 12 days after infection with the indicated doses. Results from B6HCV mice are shown in red, controls in blue. Two mice each were used per group and LCMV-WE dose. The bars are standard error of the means. The assay has a limit of detection at 4.2 log<sub>10</sub> pfu (shown as yellow bar). After injection of  $2 \times 10^3$  pfu in both groups and after injection of  $2 \times 10^4$  pfu in controls, the values were below the limit of detection.

**A****B****C**

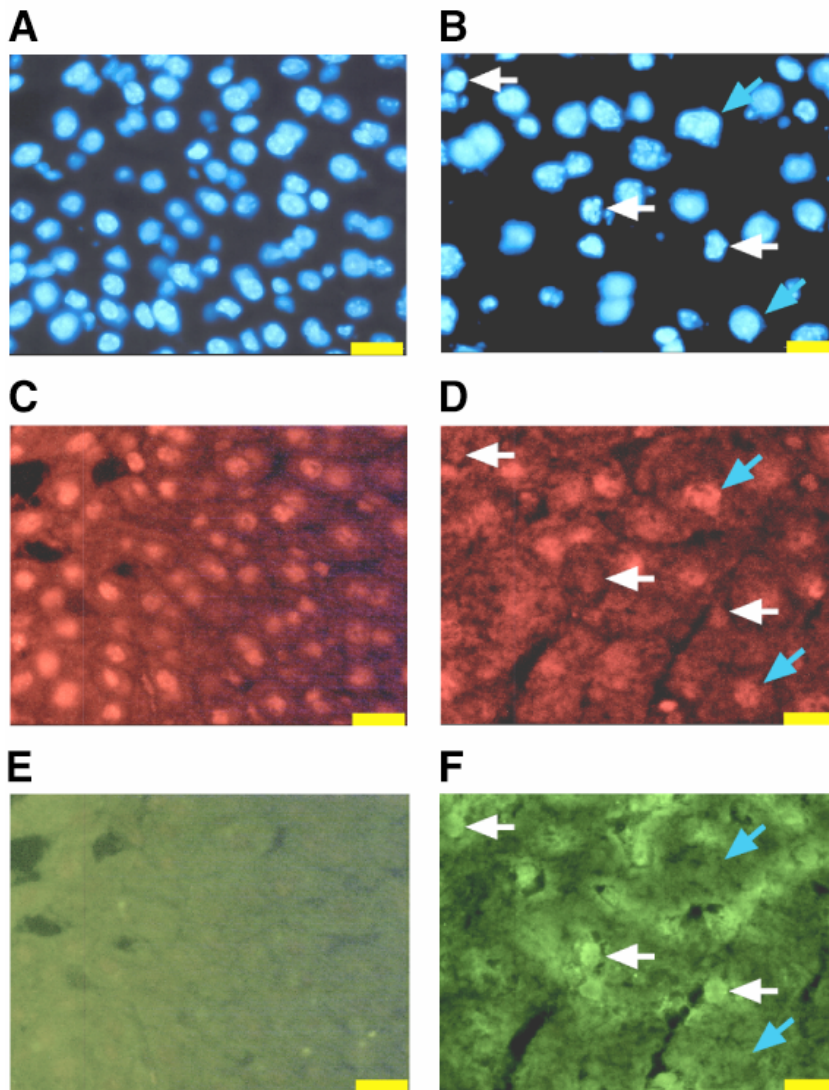


A likely explanation for the observed difference between controls and HCV transgenic mice is our finding of an increased LCMV replication in livers of B6HCV mice (Figure 4C). When measured 12 days after i.v. infection of  $2 \times 10^5$  pfu LCMV, the difference in viral replication was up to one hundred fold. This increased viral replication is most probably a consequence of the inhibition of the IFN induced antiviral defense caused by the interference of HCV proteins with the Jak-STAT pathway. Alternatively, the transgene insertion could have incidentally resulted in an ineffective CTL response against LCMV, causing an insufficient CTL mediated control of LCMV replication. However, local infection with LCMV resulted in a normal CTL mediated immunopathology in HCV transgenic mice, as shown by footpad-swelling after injection of 200 pfu LCMV-WE in the foot of B6HCV and control mice. Both groups showed a similar increase of 150-170% 8 days after infection (data not shown). Further evidence for an unimpaired immune response in B6HCV mice was obtained with VSV challenge experiments. Infection of mice with vesicular stomatitis virus (VSV), a neurotropic rhabdovirus with a high mortality rate in mice lacking the IFN $\alpha$  receptor <sup>61</sup>, was controlled by an equally efficient immune response in both C57BL/6 and B6HCV mice. Of three B6HCV and three control mice infected with  $2 \times 10^6$  pfu VSV, all survived (data not shown). In an observational study with 12 B6HCV and 12 control mice infected with various dosis of LCMV-WE, 6 of 12 B6HCV mice and 2 of 12 controls died between 10 and 12 days after infection. The death of the controls is in the range of the CTL mediated immunopathology usually observed in wild-type mice (around 10-15% mortality). In the case of the B6HCV mice we believe that the liver disease contributed to the excess mortality.

### **Interference of viral proteins with nuclear localization of STATs**

Our observation of a nuclear localization of the HCV core protein in about 30% of the hepatocytes (Figure 1C) and the 35% reduction of phospho-STAT1 localized in the nucleus after IFN $\alpha$  treatment in B6HCV mice as compared to C57BL/6 mice (Figure 3C) suggested that the two phenomena might be interdependent. We therefore performed double staining experiments of liver sections from C57BL/6 and B6HCV mice after mIFN $\alpha$  treatment. Interestingly, most cells that were strongly stained with antibodies to HCV core protein had no detectable phospho-STAT1 in the nucleus (Figure 5B, D and F).

**Figure 5. Double immunostaining for HCV core protein and phospho-STAT1 in C57BL/6 and B6HCV after injection of mIFN $\alpha$ .** (A) Hoechst stain of C57BL/6 mouse liver section. (B) Hoechst stain of B6HCV mouse liver section. (C) phospho-STAT1 staining, C57BL/6, (D) phospho-STAT1 staining, B6HCV. (E) HCV core protein staining, C57BL/6, (F) HCV core protein staining, B6HCV. As expected, no HCV core protein could be detected in C57BL/6 mice. In B6HCV mice, approximately 30% of hepatocytes show HCV core protein nuclear localization and its presence in the nucleus is negatively correlated with the presence of activated STAT1. The white arrows show nuclei of hepatocytes that stain positive for HCV core but negative for phospho-STAT1. The blue arrows show hepatocytes with nuclear staining for phospho-STAT1 but without nuclear staining for HCV core. The yellow size bar indicates 20 $\mu$ m.



## Discussion

In order to establish a persistent infection in humans, HCV must, at least to a degree, evade the antiviral cellular defense mechanisms induced by IFNs. The very same defense strategies could also contribute to the observed resistance to IFN based treatments in the majority of patients with chronic hepatitis C. Over the last years, several groups have reported that HCV proteins NS5A or E2 can interfere with the IFN induced antiviral effector protein PKR<sup>230-232</sup>. These results have been obtained by biochemical methods using purified proteins or by analyses of transfected mammalian or yeast cells, and the significance of these findings for chronic hepatitis C in patients remains to be determined. As an alternative to the inhibition of antiviral effector systems the virus could already interfere with IFN induced signaling and thereby prevent the induction of these systems. Since Jak-STAT signaling is required for IFN induction of an antiviral state, such an inhibition could be a very efficient defense strategy for HCV. We report here that HCV proteins expressed from a

transgene in mouse liver cells indeed inhibit signaling through the Jak-STAT pathway.

Since HCV can not be propagated in cultured cells and small animal models for chronic hepatitis C are still not available, we have generated a transgenic mouse that constitutively expresses the entire ORF of a genotype 1b HCV isolate. These mice provide an opportunity to study interference of HCV proteins with IFN induced signaling or with IFN induced effector systems in liver cells *in vivo*. They have some properties that should be kept in mind. First, the expression level of the HCV transgene in hepatocytes is heterogeneous. We do not have an explanation for the patchy staining of hepatocytes, but similar staining patterns have been reported in other transgenic mouse lines<sup>186, 187</sup>. We detect strong signals with core specific antibodies in about 30% of hepatocytes. However, it is likely that viral proteins are expressed in more than 30% of hepatocytes, but at a lower level not detectable by immunofluorescence. Second, the core protein contains 32 additional amino acids from the N-terminus of  $\alpha_1$ -antitrypsin. It is unlikely that the observed inhibition of Jak-STAT signaling is caused by novel properties specific to the fusion protein, since we have observed an inhibition of Jak-STAT signaling in cell lines that express the core protein in its regular form<sup>217</sup>. Third, we have little information on the other viral proteins. We can not detect them by Western blot, and can therefore not know if they are correctly cleaved from the HCV polyprotein precursor and present in undetectably low concentrations, or if they are completely absent. This is an important caveat, because even a low amount of viral proteins could still have a major impact on cellular processes such as signaling. In fact it is known that HCV protein expression levels in human liver samples from patients with chronic hepatitis C are generally low, often not detectable by Western blots.

The functional importance of impaired IFN induced signaling through the Jak-STAT pathway is demonstrated in the virus challenge experiments with LCMV-WE. We show here for the first time that expression of HCV proteins in hepatocytes has an influence on the course of a viral infection in an animal. B6HCV mice are clearly more susceptible to LCMV induced hepatitis than the controls. The most likely explanation for the more severe hepatitis and the increased mortality in B6HCV mice is the increased viral replication in liver cells and thereby the increased CTL mediated lysis of infected hepatocytes. We believe that hepatocytes that express HCV proteins do not mount an effective antiviral defense against LCMV, because the endogenous IFN that binds to its receptors on the surface of hepatocytes can not signal to the nucleus.

In a recent report, expression of HCV core protein in liver cells after infection with a replication defective recombinant adenovirus coding for core was found to induce normal immune response against adenovirus<sup>233</sup>. In the same report, HCV core transgenic mice were shown to mount a normal CTL response against adenovirus. The authors concluded that core protein has no immunomodulatory effect on virus-induced cellular immunity. Experiments performed by another group using core-E1-E2 transgenic mice that were infected with replication defective adenovirus found also an intact cellular and humoral immune response against adenovirus<sup>234</sup>. The authors concluded that HCV core and envelope proteins do not inhibit the hepatic antiviral mechanism in general. In agreement with these reports we also find a normal immune response against LCMV in our HCV transgenic mice. B6HCV mice have a normal footpad-swelling assay after local injection of 200 pfu LCMV-

---

WE in the foot as well as an unimpaired immune response against the neurotropic rhabdovirus VSV. However, when challenged with the replication competent hepatotropic LCMV-WE virus, B6HCV mice show a profound defect in the control of viral replication because of the defect of the IFN stimulated antiviral intracellular defense. Because the immune response is intact, B6HCV mice suffer a stronger and often fulminant hepatitis. In patients with chronic hepatitis C, liver histology usually does not show a similar degree of necroinflammatory changes. Indeed, for the host response against HCV, clearance of the virus without destruction of liver cells has been suggested to be an important mechanism<sup>179</sup>. It depends on IFN $\alpha$  induced non-cytopathic clearance through the induction of intracellular antiviral defense mechanisms in hepatocytes<sup>212, 213</sup>. An inhibition of IFN induced intracellular signaling by viral proteins would prevent the induction of an antiviral state and allow an active viral replication despite the presence of a strong cellular immune response.

Our data provide evidence that the inhibition of STAT signaling occurs at the level of DNA binding of the activated STAT transcription factors. We found an intact tyrosine phosphorylation of STAT1 and STAT3 (Figure 3A), indicating a functional IFN receptor and a normal activity of the receptor associated kinases Jak1 and Tyk2. For this reason, an upregulation of the well-known pathway inhibitor SOCS1 and SOCS3 is unlikely, and indeed, we found no such induction of SOCS1 or SOCS3 (data not shown). Next, nuclear import of STATs could be inhibited by viral proteins. A block in nuclear import in the presence of normal STAT activation at the receptor kinase complex could lead to an accumulation of phosphorylated STAT1 in the cytoplasm. However, we could not detect such an accumulation in cytoplasmic extracts of B6HCV mice. In the nucleus, STAT dephosphorylation is an important mechanism for the termination of STAT signaling. Viral proteins could induce nuclear phosphatases. The phospho-STAT1 immunostaining experiments (Figure 3C) provide evidence for such an increased dephosphorylation of STATs, since the number of nuclei with a positive phospho-STAT1 signal is reduced. Finally, STAT signaling can be blocked at the level of DNA binding. So far, the only protein known to interfere with DNA binding of activated STATs is PIAS1, and we could not detect an upregulation of PIAS1 by Western blot (data not shown). However, the strong inhibition of DNA binding found in the gel shift assays (Figure 2) indicates, that a direct or indirect interference of viral proteins with DNA binding is an important mechanism HCV induced inhibition of Jak-STAT signaling.

As outlined above, we can not unequivocally identify the specific viral protein(s) that is (are) responsible for the observed inhibition of the Jak-STAT pathway. Our immunofluorescence results suggest a role of core protein in the inhibition of the Jak-STAT pathway in our transgenic mice. We found core protein expression in the nucleus of about 30% of the hepatocytes, and, interestingly, most of those very same hepatocytes did not have the active, tyrosine phosphorylated form of STAT1 in the nucleus. The core protein itself could stimulate a rapid dephosphorylation of STATs in the nucleus. Alternatively, high expression levels of core might just be an indicator of an above average expression of the entire viral transgene. In this case, the inhibition of Jak-STAT signaling could be caused by any other viral protein(s). Whatever the mechanism, hepatocytes with detectable core protein in the nucleus show a lack of phosphorylated STAT1 in the nucleus.

The same mechanism of interference with the Jak-STAT pathway could take place in chronic viral hepatitis. IFN would then be actively inducing an antiviral state only in hepatocytes that are not infected by HCV or have very low cellular viral loads with concomitant low expression levels of viral proteins. It is a matter of an ongoing debate what percentage of hepatocytes is actually infected by HCV in chronic hepatitis C. Published data indicate that viral replication and gene expression takes place in less than 20 percent of hepatocytes <sup>235</sup>. In view of these data one may speculate that IFN treatment in patients with chronic hepatitis C actually induces an antiviral state in uninfected hepatocytes only, while the patient's own HCV specific CD8 positive cytotoxic T lymphocytes would have to clear the virus by attacking infected hepatocytes. On the other hand, high doses of IFN can overcome the block of IFN $\alpha$  induced Jak-STAT signaling in our mouse model (Figure 2B). Interestingly, a similar observation has been made in patients infected with HCV. It has been shown that treatment with higher IFN $\alpha$  doses results in a higher response rate in patients with chronic hepatitis C <sup>236</sup>. Higher doses apparently could overcome the resistance against IFN $\alpha$  treatment in about 15% of patients <sup>236</sup>. Adverse effects of IFN $\alpha$ , however, limit the dose that can be administered to about 100 IU/g body weight three times per week. In this context, a more promising strategy to overcome viral interference with IFN signaling would be to search for compounds that counteract the effects of viral proteins on Jak-STAT signaling.

In summary, we have found a functionally important inhibition of IFN $\alpha$  induced signaling through the Jak-STAT pathway in liver cells of HCV transgenic mice *in vivo*. Interference with this intracellular signaling pathway reduces the amount of phosphorylated STAT1 in the nucleus of cells expressing viral proteins and results in a loss of binding of STAT transcription factor complexes to their cognate response elements in the promoters of ISGs. This mechanism could contribute to escape from the antiviral effects of endogenous IFNs and thereby to HCV persistence in infected individuals. Moreover, it might contribute to the poor response to IFN based therapies in the majority of HCV infected patients. Strategies aimed at restoring IFN signaling in infected liver cells might allow to more successfully treating patients in the future.

### Acknowledgments

We would like to thank Rolf Zinkernagel, George Thomas, Francesco Negro and Gennaro Ciliberto for stimulating discussions and reading of the manuscript.

This work was supported by Swiss National Science Foundation grants 3231-054973 and 3100-052626, Swiss Cancer League grant 922-09-1999, Roche Research Foundation grant 90-1999, the Astra-Fonds and the Stiftung für Gastroenterologische Forschung. D.M. and H.E.B. are supported by grant Mo 799/1-2 from the Deutsche Forschungsgemeinschaft. M.T. is supported by the AIRC (Associazione Italiana Ricerca sul Cancro), by progetto strategico 2000 "Epatite C" Ministero della Sanità and by MURST (Ministero della Ricerca Scientifica e Tecnologica), Italy.



**Expression of Hepatitis C Virus  
Structural Proteins Inhibits  
Interferon-alpha Induced Signaling  
through the Jak-STAT Pathway**

Simone T.D. Stutvoet,<sup>\*</sup> Elke Bieck,<sup>\*,†</sup> Hubert E.  
Blum,<sup>†</sup> Markus H. Heim,<sup>\*,2</sup> and Darius  
Moradpour<sup>†,1</sup>

<sup>\*</sup>Department of Research, University Hospital Basel,  
CH-4031 Basel, Switzerland

<sup>†</sup>Department of Medicine II, University of Freiburg,  
D-79106 Freiburg, Germany

---

## **Abstract**

The mechanisms of hepatitis C virus (HCV) persistence and resistance to interferon $\alpha$  (IFN $\alpha$ ) are poorly understood. We have shown previously that expression of the HCV polyprotein inhibits IFN $\alpha$  induced signal transduction through the Jak-STAT pathway. The aim of this study was to identify the HCV protein(s) responsible for this inhibition. Using a comprehensive panel of tetracycline-regulated cell lines inducibly expressing individual HCV proteins alone or in different combinations, we found that the combined structural proteins strongly and the core protein alone partly inhibited Jak-STAT signaling. As previously observed in cell lines inducibly expressing the entire HCV polyprotein, inhibition occurred downstream of STAT tyrosine phosphorylation and resulted in an impaired upregulation of IFN $\alpha$  target genes. Interference with IFN $\alpha$  induced signaling through the Jak-STAT pathway may represent an escape strategy of HCV contributing to viral persistence and resistance to IFN $\alpha$ . Ultimately, elucidation of the molecular mechanism involved may open possibilities to design more effective therapies for chronic hepatitis C.



## Introduction

Hepatitis C virus (HCV) infection is a major cause of chronic hepatitis, liver cirrhosis, and hepatocellular carcinoma worldwide. A protective vaccine does not exist to date and therapeutic options are still limited<sup>237</sup>. At present, pegylated interferon alpha (IFN $\alpha$ ) in combination with ribavirin is the treatment of choice for chronic hepatitis C. However, only about 40% of patients infected with HCV genotype 1 experience a sustained response<sup>238</sup>. The mechanisms underlying viral persistence and resistance to IFN $\alpha$  therapy are poorly understood<sup>211, 239, 240</sup>. In general, the IFN-induced cellular antiviral response is the first line of innate defense against viral infections. In order to establish a productive infection, therefore, viruses must first overcome the IFN-induced mechanisms blocking viral replication<sup>241, 242</sup>.

The complete signal transduction pathway from the IFN receptors to the nucleus has been identified over the past several years (reviewed in<sup>9</sup>), and viral interference with IFN-induced signaling can now be studied in detail. Type I IFNs (IFN $\alpha$  and  $\beta$ ) bind to heterodimeric type I IFN receptors consisting of IFN $\alpha$  receptor I (IFNARI) and IFNARII. Ligand binding results in activation of two cytoplasmic protein tyrosine kinases associated with IFNARI and IFNARII, Tyk2 and Jak1. The activated kinases then phosphorylate tyrosine residues of the receptors. These phosphotyrosines are consecutively bound by the Src homology 2 (SH2) domains of signal transducer and activator of transcription 1 (STAT1), STAT2 and STAT3. The STATs are then tyrosine phosphorylated, and form hetero- or homo-dimers through mutual SH2 domain-phosphotyrosine interactions. STAT3 and STAT1 form homodimers, designated serum inducible factor A (SIF-A) and SIF-C, respectively, and a STAT1-STAT3 heterodimer, SIF-B. STAT1 can also dimerize with STAT2, and this STAT1-STAT2 heterodimer associates with a third DNA binding protein, ISGF3 $\gamma$ -p48 (IRF-9), to form interferon-stimulated gene factor 3 (ISGF3). Binding of these STAT factors to their cognate sequences in the promoter regions of target genes results in enhanced gene transcription. Among others, STAT1, STAT2, and ISGF3 $\gamma$ -p48 (IRF-9) have been identified as IFN $\alpha$  induced target genes. A number of regulatory mechanisms of the Jak-STAT signal transduction pathway have recently been identified. The activity of the Jak kinases is controlled by receptor associated phosphatases and by the family of suppressors of cytokine signaling (SOCS). Binding of STAT dimers to DNA can be inhibited by protein inhibitors of activated STATs (PIAS). STATs are deactivated by an as yet unknown nuclear phosphatase and by protein degradation through the ubiquitin-proteasome pathway. At any of the steps outlined above, viral proteins could interfere with the Jak-STAT pathway and inhibit induction of antiviral effector proteins.

We have shown previously that expression of the entire HCV polyprotein in tetracycline-regulated cell lines inhibits IFN $\alpha$  induced signal transduction through the Jak-STAT pathway<sup>217</sup>. Inhibition occurred downstream of STAT tyrosine phosphorylation, led to an impaired upregulation of IFN $\alpha$  target genes<sup>217</sup>, and resulted in an inhibition of antiviral IFN effector functions<sup>243</sup>. More recently, these observations were confirmed and extended in HCV-transgenic mice *in vivo*<sup>129</sup>.

The aim of this study was to identify the HCV gene product(s) responsible for the inhibition of Jak-STAT signaling. For this purpose, we established a comprehensive panel of cell lines allowing the regulated expression of HCV

---

structural and nonstructural proteins either alone or in different combinations. Using this well-characterized cell culture system, we demonstrate that expression of the HCV structural proteins inhibits IFN $\alpha$  induced signaling through the Jak-STAT pathway.

## Materials and Methods

### Expression constructs

Fragments comprising the core protein (aa 1-191) or the entire structural region (core-E1-E2-p7; aa 1-809) of a functional HCV H strain consensus cDNA were amplified by PCR from pBRTM/HCV1-3011con<sup>244</sup>; generously provided by Dr. Charles M. Rice, Center for the Study of Hepatitis C, Rockefeller University, New York, NY) using forward primer GAG36 (5'-GAGAATTCCGTGCACCATGAGCACGAATCCTAAACC-3'; *Eco*RI site underlined, HCV translation initiation codon boldface;<sup>181</sup> and reverse primers Crev (5'-GCTGTCTAGATTAGGCTGAAGCGGGCACGGTCAGGC-3'; *Xba*I site underlined, engineered stop codon boldface) or 809-rev (5'-GCTGTC TAGATTATGCGTATGCCCGCTGAGGCAACGCCAG-3'; *Xba*I site underlined, engineered stop codon boldface), respectively. The amplification products were digested with *Eco*RI and *Xba*I and cloned into the *Eco*RI-*Xba*I sites of pUHD10-3<sup>245</sup> to yield plasmids pUHDCcon and pUHDCp7con, respectively. These constructs allow expression of the core protein or of the entire structural region of HCV genotype 1a under the transcriptional control of a tTA-dependent promoter.

The *Hin*DIII-*Xba*I fragment of pcDNA5-9-1<sup>222</sup>, comprising the core coding region (aa 1-191) of a genotype 1b isolate, designated TH<sup>246 247</sup>, was ligated into the *Eco*RI-*Xba*I sites of pUHD10-3 after fill-in with Klenow polymerase of the 3' recessed termini resulting from *Hin*DIII and *Eco*RI digestion to yield plasmid pUHDTHC.

Fragments comprising the NS3-NS4B and NS4B-NS5B region of the HCV H consensus cDNA were amplified by PCR from pBRTM/HCV1-3011con using primer pairs GCA45 (5'-GCACGAATTCACCATGGCGCCCATCACGGCGTACGCCAGCAGAC-3'; *Eco*RI site underlined, engineered translation initiation codon boldface;<sup>175</sup> - 4Brev (5'-GCTGTCTAGATTAGCATGGAGTGGTACACTCCGAGCTTATCC-3'; *Xba*I site underlined, engineered stop codon boldface;<sup>169</sup> and 4Bfwd (5'-GAGAATTCACCATGTCTCAGCACTTACCGTACATCGA GCAAGGG-3'; *Eco*RI site underlined, engineered translation initiation codon boldface;<sup>169</sup> - NS5Brev (5'-GCTGTCTAGATCATCGGTTGGGGAGGAGGTAGATGCCTACC-3'; *Xba*I site underlined, HCV stop codon boldface;<sup>248</sup>, respectively, followed by digestion of the amplification products with *Eco*RI-*Bsu*36I and *Bsu*36I-*Xba*I, respectively, and ligation of both fragments into the *Eco*RI-*Xba*I sites of pUHD10-3<sup>245</sup> to yield plasmid pUHDNS3-5Bcon. This construct allows expression of the nonstructural proteins 3-5B derived from a functional genotype 1a cDNA under the transcriptional control of a tTA-dependent promoter.

### **Tetracycline-regulated cell lines**

Tetracycline-regulated cell lines were generated as previously described<sup>249 169 222 181 246 248 175</sup>. In brief, the constitutively tTA-expressing, U-2 OS human osteosarcoma (ATCC HTB-96)-derived founder cell line UTA-6<sup>250</sup>; (generously provided by Dr. Christoph Englert, University of Würzburg, Germany) was cotransfected by a modified calcium phosphate precipitation protocol<sup>251</sup> with pUHDTHC, pUHDCcon, pUHDCp7con, or pUHDNS3-5Bcon, respectively, and pBabepuro<sup>252</sup>, followed by selection with G418 and puromycin. Double-resistant clones were isolated and screened for tightly regulated HCV protein expression by immunofluorescence microscopy and immunoblot analyses.

The following previously described cell lines were also used in this study: UTHCNS3-43 cells allow the inducible expression of the entire structural region including a functional NS2-3 autoprotease derived from the genotype 1b TH cDNA<sup>246</sup>. UNS3-4A-24 cells<sup>175</sup> allow the inducible expression of the NS3-4A complex derived from a prototype HCV H strain cDNA<sup>164</sup>. UHCVcon-57<sup>248</sup>, UNS4Acon-27 (Moradpour et al., unpublished data), UNS4Bcon-4 and -52<sup>169</sup>, UNS5Acon-26, -29, -37 and -46<sup>249</sup>, and UNS5Bcon-8 cells<sup>248</sup> allow the inducible expression of the entire polyprotein, NS4A, NS4B, NS5A, or NS5B, respectively, derived from a functional HCV H consensus cDNA<sup>244</sup> (Fig. 1A).

Cells were cultured in DMEM supplemented with 10% fetal bovine serum, 50 U/ml penicillin G, 50 µg/ml streptomycin, 500 µg/ml G418, 1 µg/ml puromycin, and 1 µg/ml tetracycline. For induction of viral protein expression, cells were cultured in the absence of tetracycline for 24 h before IFN $\alpha$  stimulation.

### **Reagents and antibodies**

Human IFN- $\alpha$ 2b (Intron A<sup>®</sup> Essex Chemie AG, Lucerne, Switzerland) was a gift of Essex Chemie AG. Antibodies against STAT1 (S21120) and ISGF3 $\gamma$ -p48 (IRF-9) (I29320) were from Transduction Laboratories (Lexington, KY). A polyclonal antiserum against Tyr<sub>701</sub>-phosphorylated STAT1 (9171S) was from Cell Signaling Technologies (New England Biolabs, Beverly, MA). The HCV core protein-specific mAb C7-50 has been described<sup>222</sup>. MAb 384 against E1 was kindly provided by Dr. Michinori Kohara, The Tokyo Metropolitan Institute of Medical Science, Tokyo, Japan. MAbs A4 and A11 against E1 and E2, respectively, were generous gifts of Dr. Jean Dubuisson, Institut Pasteur de Lille, Lille, France and Dr. Harry Greenberg, Stanford University, Stanford, CA. MAb 11H against NS5A<sup>249</sup> was kindly provided by Dr. Jan Albert Hellings, Organon Teknika BV, Boxtel, The Netherlands.

### **Indirect immunofluorescence microscopy**

Indirect immunofluorescence microscopy was performed as described previously<sup>222 181</sup>. In brief, cells grown as monolayers on glass cover slips were fixed with 2% paraformaldehyde, permeabilized with 0.05% saponin, and incubated with primary antibodies in phosphate-buffered saline containing 3% bovine serum albumin and 0.05% saponin. Bound primary antibody was revealed with fluorescein isothiocyanate-conjugated goat F(ab')<sub>2</sub> fragment to mouse IgG F(ab')<sub>2</sub> (Cappel, Durham, NC). Cover slips were mounted in SlowFade (Molecular Probes, Eugene, OR) and examined with a Zeiss Axiovert photomicroscope equipped with an epifluorescence attachment.

---

## EMSA

After treatment with IFN $\alpha$ , cells were lysed in low salt buffer (20 mM Hepes pH 7.9, 10 mM KCl, 1 mM EDTA, 1 mM EGTA, 0.2% NP-40, 10% glycerol, 0.1 mM Na<sub>3</sub>VO<sub>4</sub>, 1 mM PMSF, 1 mM dithiothreitol, 2  $\mu$ g/ml aprotinin, 1  $\mu$ g/ml leupeptin, and 1  $\mu$ g/ml pepstatin) at 4 °C for 10 min. After centrifugation for 30 s at 12,000 x *g*, supernatants (= cytoplasmic extracts) were immediately frozen on dry ice, and pellets were extracted with high salt buffer (same as low salt, except for 420 mM NaCl and 20% glycerol) for 30 min at 4 °C. Samples were cleared by centrifugation at 12,000 x *g* at 4 °C. Supernatants were aliquoted, frozen on dry ice and stored at -70 °C. For EMSA, nuclear extracts (2  $\mu$ l) were incubated for 20 min at RT in 20 mM HEPES, pH 7.9, 4% Ficoll, 1 mM MgCl<sub>2</sub>, 40 mM KCl, 0.1 mM EGTA, 0.5 mM dithiothreitol, and 160  $\mu$ g/ml poly[dI-dC]-poly[dI-dC] with 1 ng of <sup>32</sup>P-labeled oligonucleotides. Samples were separated on a 5% non-denaturing polyacrylamide gel at 400 V for 4 h at 4 °C. Gels were then dried and exposed for 10-20 h to a storage phosphor screen. Quantitation was performed using NIH Image 1.62 software, and the sum of arbitrary density values of STAT1:3 heterodimer and STAT1 and STAT3 homodimers was normalized to the nonspecific bands ran on the same gel. The following oligonucleotides corresponding to STAT response element sequences were used: ISRE (interferon stimulated response element) = 5'-GAAAGGGAAACCGAAACTGAAGC-3'; SIE-m67 (mutated serum inducible element) = 5'-CATTTCCCGTAAATCAT-3'.

## Protein extraction and Western blotting

For the preparation of whole cell extracts, cells were lysed in a buffer containing 50 mM Tris-HCl, pH 8.0, 280 mM NaCl, 0.5% NP-40, 0.2 mM EDTA, 2 mM EGTA, 10% glycerol, 0.1 mM Na<sub>3</sub>VO<sub>4</sub>, 1 mM PMSF, 2  $\mu$ g/ml aprotinin, 1  $\mu$ g/ml leupeptin, and 1  $\mu$ g/ml pepstatin A. SDS-polyacrylamide gel electrophoresis and Western blot were performed according to standard protocols<sup>253</sup>. Quantitation was performed using NIH Image 1.62 software and arbitrary density values were normalized to the nonspecific bands run on the same gel.



---

## Results

### Tetracycline-regulated cell lines

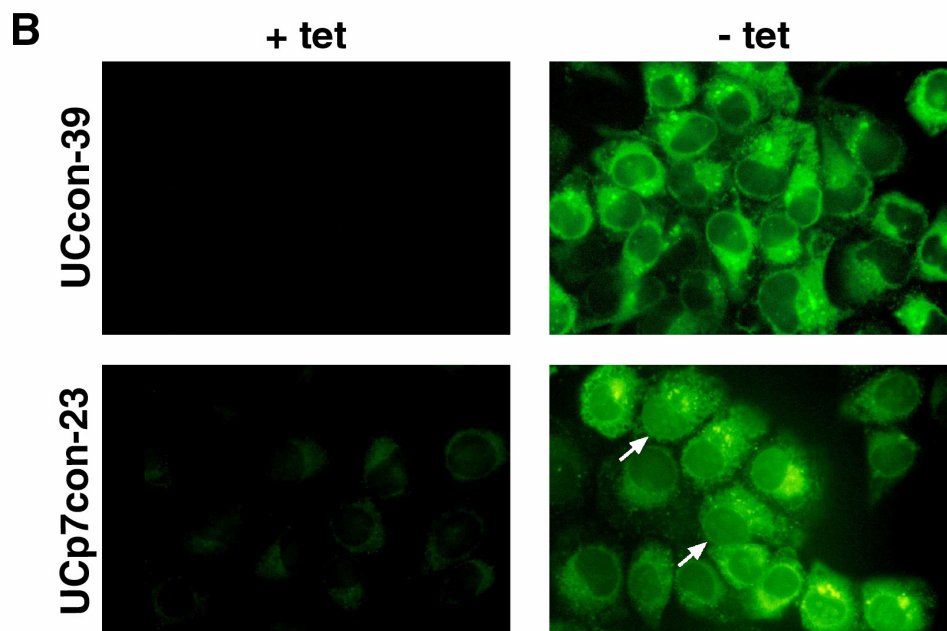
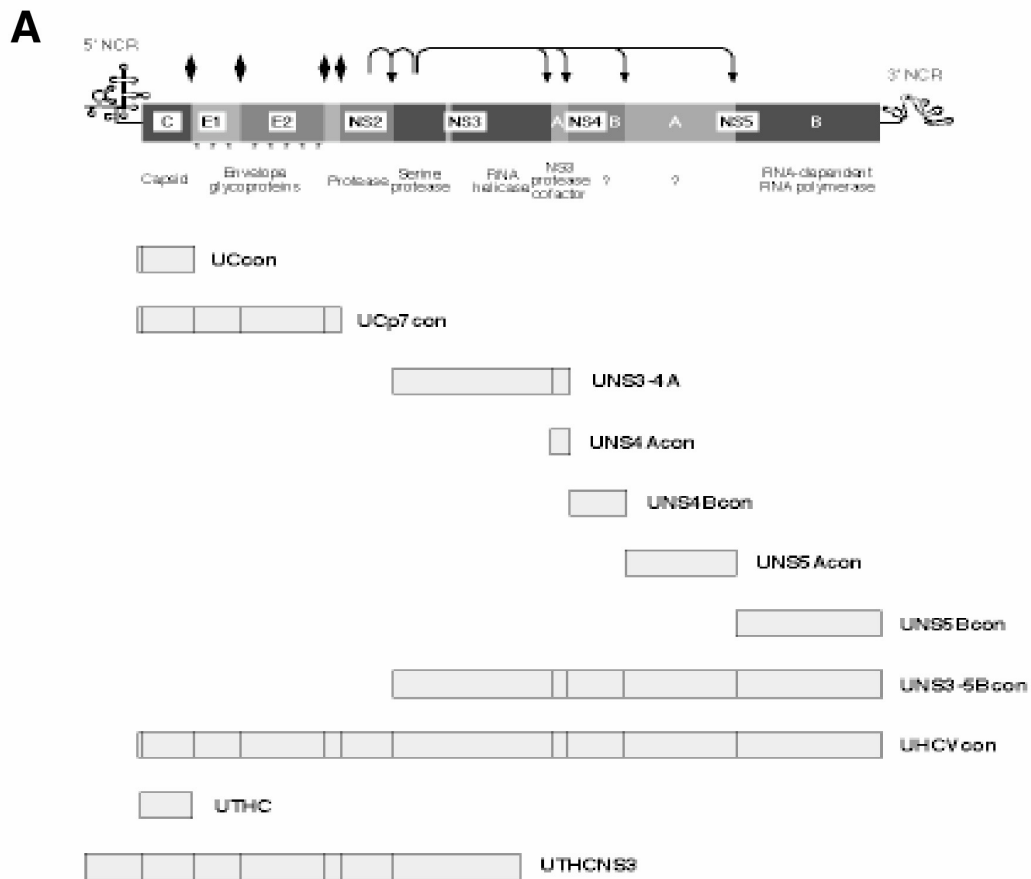
A tetracycline-regulated gene expression system was used to establish U-2 OS human osteosarcoma-derived cell lines inducibly expressing the core protein derived from HCV genotype 1a and 1b cDNAs as well as the entire structural or nonstructural region derived from genotype 1a. Screening of G418- and puromycin-resistant clones resulting from transfection of the tetracycline-controlled transactivator (tTA)-expressing founder cell line UTA-6 with the constructs pUHDTHC, pUHDCcon, pUHDCp7con, or pUHDNS3-5Bcon allowed the isolation of several tightly regulated UTHC, UCcon, UCp7con, and UNS3-5Bcon cell lines, respectively (Figure 1A). In general, the suffix "con" denotes cell lines harboring segments of an infectious HCV H consensus cDNA<sup>244</sup> and the numbers following cell line designations indicate independent clones. Cell lines UTHC-10 and -17 (both medium expression), UCcon-18 (low-medium expression) and -39 (high expression, regulation by tetracycline slightly leaky), UCp7con-9 (high expression), -10, and -23 (both medium expression), as well as UNS3-5Bcon-27 (medium expression), -33 (high expression), and -35 (medium expression) were used in this study. These cell lines were maintained in continuous culture for more than 12 months and over 50 passages with stable characteristics. Additional previously characterized cell lines used in this study are specified in Figure 1A and in the Materials and Methods section.

Indirect immunofluorescence analyses of UTHC, UCcon, and UCp7con cells with the HCV core-specific monoclonal antibody (mAb) C7-50 revealed the typical cytosolic reticular and granular staining pattern<sup>222</sup> (Figure 1B). In addition, core protein was found on the surface of round cytoplasmic structures corresponding to lipid droplets<sup>176 222</sup> and, somewhat surprisingly, in the nucleus of UCp7con cells (Figure 1B). An estimated 2-5% of the total core protein expressed in these cells was found in the nucleus where it accumulated in the nucleoli. Interestingly, nuclear core protein was found only in UCp7con and UHCVcon<sup>176 248</sup>, but not in UCcon (Figure 1B), UTHC (data not illustrated), and UTHCNS3 cells<sup>246</sup>.

### Figure 1. Tetracycline-regulated cell lines.

**(A)** Overview of the cell lines used in this study. The genetic organization and polyprotein processing of HCV are depicted at the top. Asterisks in the E1 and E2 region indicate glycosylation of the envelope proteins. Diamonds denote cleavages of the HCV polyprotein precursor by the endoplasmic reticulum signal peptidase and arrows indicate cleavages by HCV NS2-3 and NS3 proteases. UNS3-4A (Wölk *et al.*, 2000) cell lines were derived from a prototype HCV H cDNA (genotype 1a) (Grakoui *et al.*, 1993). UCcon (this work), UCp7con (this work), UNS4Acon (Moradpour *et al.*, unpublished data), UNS4Bcon (Hügler *et al.*, 2001), UNS5Acon (Brass *et al.*, 2002), UNS5Bcon (Schmidt-Mende *et al.*, 2001), UNS3-5Bcon (this work), and UHCVcon cell lines (Schmidt-Mende *et al.*, 2001) were derived from a functional HCV H consensus cDNA (Kolykhalov *et al.*, 1997). The cell lines UTHC (this work) and UTHCNS3 (Moradpour *et al.*, 1998b) were derived from a genotype 1b cDNA, termed TH (Moradpour *et al.*, 1998b; Wakita and Wands, 1994).

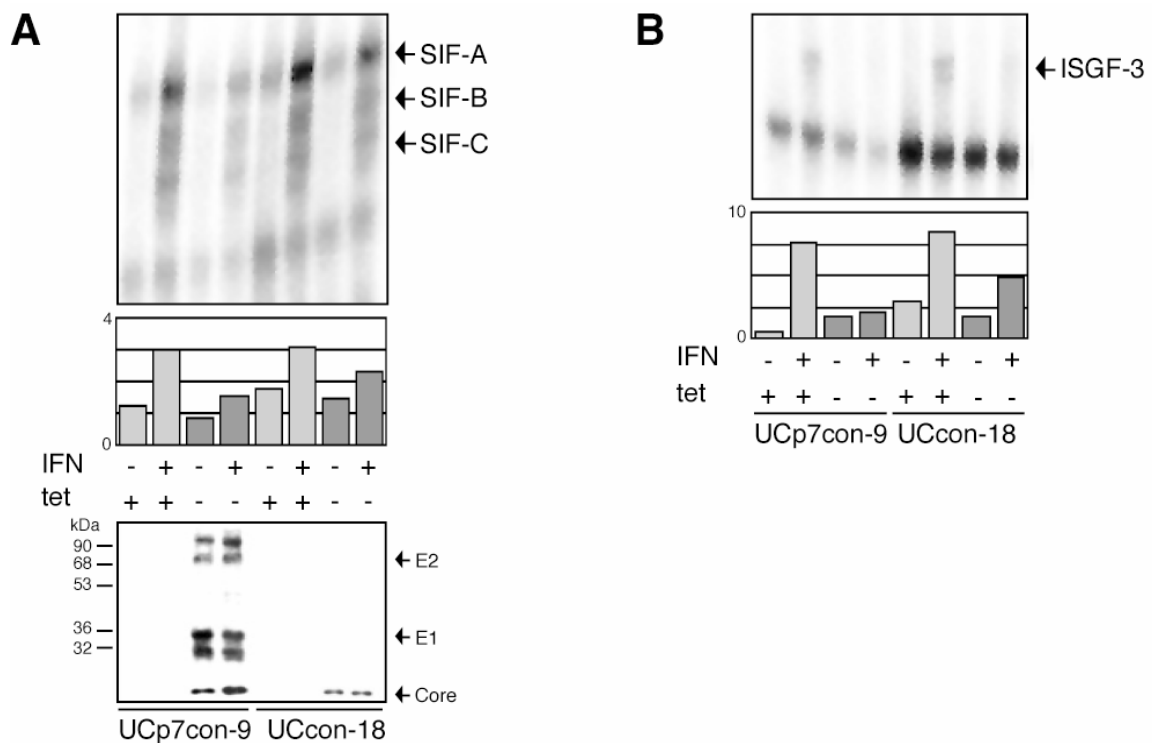
**(B)** Expression of HCV core protein in UCcon and UCp7con cell lines. UCcon-39 and UCp7con-23 cells were cultured for 24 h in the presence (+ tet) or absence (- tet) of tetracycline and subsequently processed for indirect immunofluorescence analysis with the HCV core-specific mAb C7-50. Arrows indicate nucle(ol)ar localized core protein.



## Expression of HCV structural proteins inhibits IFN $\alpha$ induced Jak-STAT signaling

To test for a possible interference of HCV proteins with IFN signal transduction, several independent clones of the inducible cell lines shown in Figure 1A were analyzed for IFN $\alpha$  induced SIF-A, -B, and -C as well as ISGF3 formation after derepression of the HCV cDNA. Subconfluent cell monolayers were cultured for 24 h in the presence or absence of tetracycline. Cells then either were left untreated or were stimulated for 20 min with 500 U/ml IFN $\alpha$ . Nuclear extracts were prepared and tested for STAT DNA binding activity by electrophoretic mobility shift assay (EMSA) using the m67 or interferon-stimulated response element (ISRE) oligonucleotide probes, respectively.

Western blot analyses of UCcon-18, UCp7con-9, UNS3-5Bcon-27, UTHC-10, and UTHCNS3-43 cells cultured in the presence or absence of tetracycline revealed HCV protein expression only in derepressed cells, as shown in Figure 2. As shown in Figure 2A and 2B, SIF-A, -B and -C as well as ISGF3 induction was inhibited in UCcon-18 and UCp7con-9 cells cultured in the absence of tetracycline. Figure 2 shows representative examples of experiments that were repeated 2-5 times with similar results (except for UCcon-18 IFN induced ISGF3, which was performed only once).





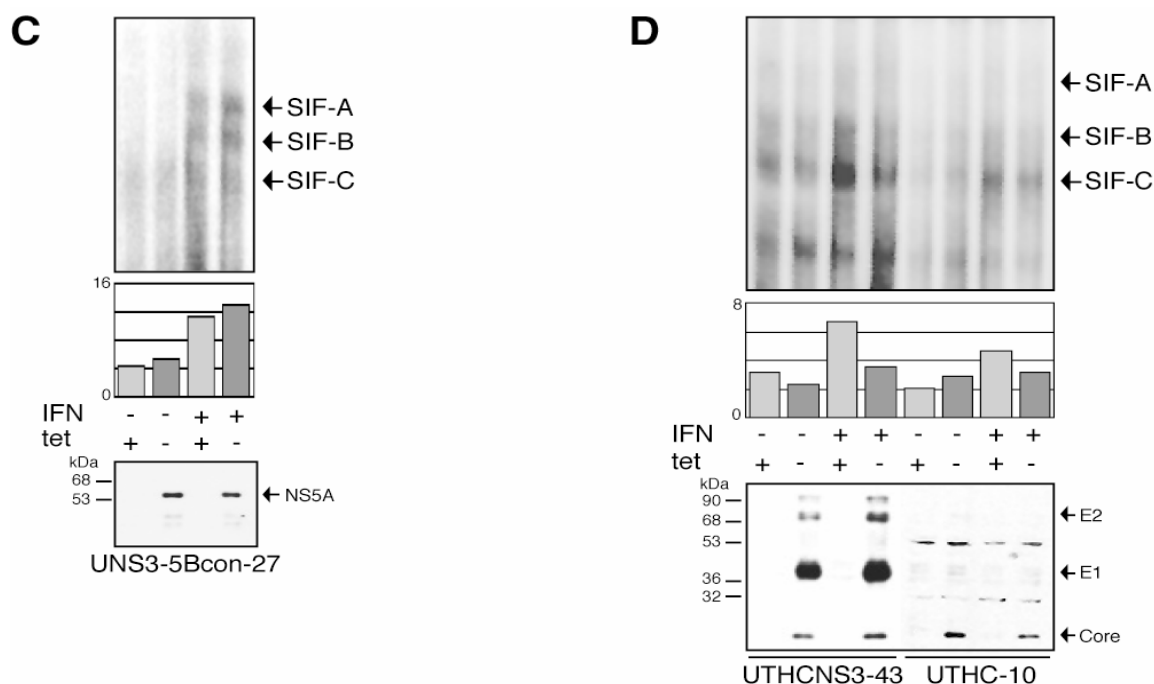


**Figure 2. Expression of HCV structural proteins inhibits IFN $\alpha$  induced Jak-STAT signaling.** UCcon-18, UCp7con-9, UNS3-5Bcon-27, UTHC-10, and UTHCNS3-43 cells were cultured in the presence (lanes indicated by tet +) or absence (lanes indicated by tet -) of tetracycline. Cells were then not treated (lanes indicated by IFN -) or stimulated for 20 min with 500 U/ml IFN $\alpha$  (lanes indicated by IFN +). Panels A, C and D demonstrate EMSAs with the m67 oligonucleotide probe. The positions of SIF-A, -B and -C are indicated by arrows. An example of an EMSA with the ISRE oligonucleotide probe is shown in panel B (using the same nuclear extracts as in panel A). Quantitation of EMSA signals was performed as described in the Materials and Methods section and arbitrary density values are depicted as bars. These values reflect the experiment shown in this figure and are included in the average  $\pm$  S.D. values specified in the Results section. Light grey bars represent cells cultured in the presence of tetracycline, dark grey bars cells cultured in the absence of tetracycline. Panels A, C and D include Western blot analyses, depicted below the EMSAs, of cytoplasmic extracts corresponding to the nuclear extracts. Ten  $\mu$ g of protein was loaded per lane (except for UTHC-10 cells where 40  $\mu$ g was loaded per lane). The positions of HCV proteins are indicated by arrows. Molecular weight markers in kDa are indicated on the left. **(A)** EMSA with nuclear extracts from UCp7con-9 and UCcon-18 cells and the m67 oligonucleotide probe. MAbs C7-50 against core protein as well as A4 and A11 against E1 and E2, respectively, were used for Western blot. **(B)** EMSA with the nuclear extracts from panel A and an ISRE probe. **(C)** EMSA with nuclear extracts from UNS3-5Bcon-27 cells and the m67 oligonucleotide probe. MAb 11H was used for the detection of NS5A by Western blot. **(D)** EMSA with nuclear extracts from UTHCNS3-43 and UTHC-10 cells and the m67 oligonucleotide probe. MAbs C7-50 against core as well as 384 and A11 against E1 and E2, respectively, were used for Western blot.

Quantitative analyses of all experiments performed demonstrated a  $30 \pm 11\%$  (average  $\pm$  S.D.) and  $33 \pm 12\%$  reduction of IFN induced SIF signals as well as a  $68 \pm 7\%$  and  $42\%$  reduction of IFN induced ISGF3 signals in UCp7con-9 and UCcon-18 cells, respectively, when compared to cells cultured in the presence of tetracycline (Figures 2A and 2B). As shown previously<sup>217</sup>, a low-level constitutive STAT3 activation was present even in unstimulated cells, whereas STAT1 was not detected in these control samples. In line with our previous

---

report <sup>217</sup>, inhibition of STAT activation by HCV structural proteins appeared to be more complete for ISGF3 as compared to SIF-A, -B, and -C. This is likely a consequence of a higher threshold activation level for EMSAs using the ISRE as compared to the m67 oligonucleotide probe. Analogous results were obtained in UCp7con-10 and -23 as well as in UCcon-39 cells expressing different levels of HCV structural and core proteins (data not illustrated).

By contrast, no inhibition of IFN $\alpha$  induced Jak-STAT signaling was observed in UNS3-5Bcon-27 cells which inducibly express the nonstructural region derived from the HCV H consensus cDNA clone (Figure 2C). Quantitative analyses actually demonstrated an 18 $\pm$ 10% increase of the signal as compared to cells cultured in the presence of tetracycline. However, this slight increase was not uniformly reproducible in independent clones, namely UNS3-5Bcon-33 and -35, expressing nonstructural proteins (data not illustrated). In addition, no inhibition of Jak-STAT signaling was observed in UNS3-4A-24, UNS4Acon-27, UNS4Bcon-4 and -52, UNS5Acon-26, -29, -37, and -46 as well as UNS5Bcon-8 cells. Thus, the HCV nonstructural proteins expressed in combination or alone did not interfere with IFN $\alpha$  induced signaling through the Jak-STAT pathway.

To extend the findings obtained with genotype 1a-derived proteins, we investigated the effect of structural proteins derived from a HCV genotype 1b cDNA, designated TH <sup>246</sup> <sup>247</sup>, on IFN $\alpha$  induced Jak-STAT signaling. As shown in Figure 2D, a comparable inhibition of SIF-A, -B and -C induction was found in UTHCNS3-43 cells expressing the entire structural region and in UTHC-10 cells which express the core protein alone. Quantitative analyses demonstrated a 32 $\pm$ 10% reduction in UTHCNS3-43 cells and a 25 $\pm$ 14% reduction in UTHC-10 cells expressing HCV structural and core proteins, respectively. Analogous results were obtained in UTHC-17 cells (data not illustrated). Thus, the inhibitory effect of HCV structural proteins was reproducible in two different viral isolates and was independent of nuclear localized core protein, because core was never found in the nucleus of UTHCNS3 cells.

### **Inhibition of Jak-STAT signaling by HCV structural proteins occurs downstream of STAT tyrosine phosphorylation**

To determine the level at which inhibition of Jak-STAT signaling occurs we next examined IFN $\alpha$  induced STAT1 tyrosine phosphorylation in UCp7con-9, UCcon-18, and UNS3-5Bcon-27 cells. For this purpose, cells were cultured for 24 h in the presence or absence of tetracycline, followed by stimulation for 20 min with 500 U/ml IFN $\alpha$ . Cytosolic cell extracts were subsequently analyzed by Western blot with a polyclonal antiserum specific for Tyr<sub>701</sub>-phosphorylated STAT1. As shown in Figure 3A, phospho-STAT1-specific signals showed the same intensity in repressed and derepressed cells, indicating that STAT1 phosphorylation was not affected by HCV proteins.

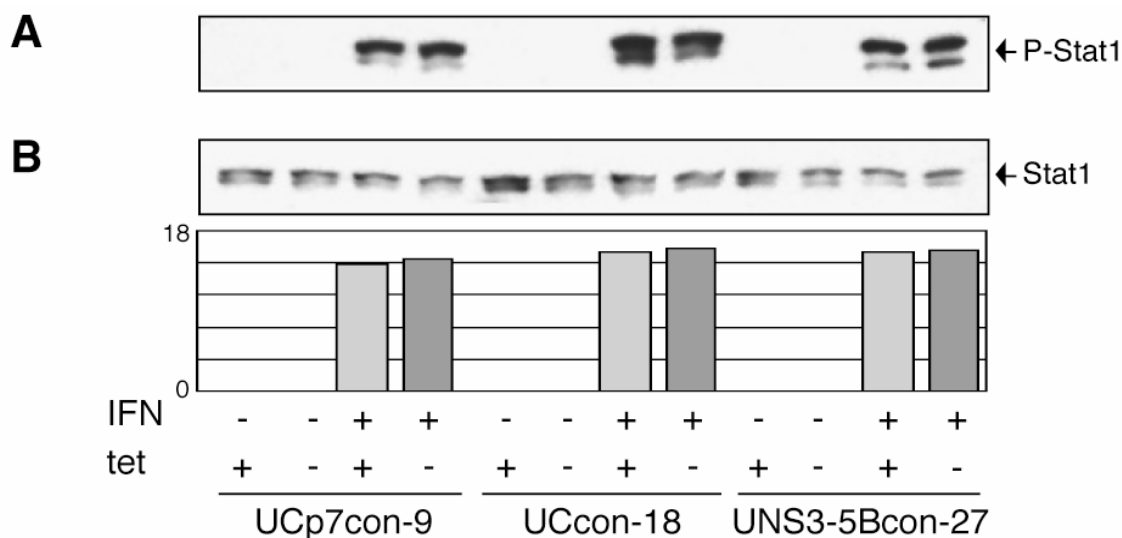


**Figure 3. Inhibition of Jak-STAT signaling by HCV structural proteins occurs downstream of STAT tyrosine phosphorylation.** UCp7con-9, UCcon-18, and UNS3-5Bcon-27 cells were cultured for 24 h in the presence or absence of tetracycline (tet + or tet -) and were then either not treated or stimulated for 20 min with 500 U/ml IFN $\alpha$  (IFN - or IFN +). Cytosolic extracts corresponding to 10  $\mu$ g protein per lane were analyzed by Western blot using **(A)** a polyclonal antiserum against Tyr<sub>701</sub>-phosphorylated STAT1 (P-STAT1) or **(B)** a mAb against STAT1. Quantitation of P-STAT1-specific Western blot signals was performed as described in the Materials and Methods section and arbitrary density values are depicted as bars. Light grey bars represent cells cultured in the presence of tetracycline, dark grey bars cells cultured in the absence of tetracycline.

In addition, we could not detect any quantitative difference for total STAT1, indicating that viral protein expression did not diminish intracellular concentrations of STAT proteins by either enhanced protein degradation or impaired gene expression (Figure 3B). Analogous results were obtained in UCp7con-10 and -23, UCcon-39, UNS3-5Bcon-33 and -35 as well as UTHCNS3-43 cells. We concluded from these experiments, that activation of STATs through tyrosine phosphorylation at the receptor-kinase complex was not inhibited by HCV proteins.

### **Inhibition of Jak-STAT signaling by HCV structural proteins results in impaired upregulation of IFN $\alpha$ target genes**

To examine the effect of HCV proteins on the expression of IFN $\alpha$  induced target genes, UCp7con-9, UCcon-18, and UNS3-5Bcon-27 cells were cultured for 24 h in the presence or absence of tetracycline, stimulated for 4 or 8 h with 100 U/ml IFN-alpha, and subsequently examined for the expression of IRF-9. As shown in Figure 4, the inhibition of Jak-STAT signaling in UCp7con-9 and UCcon-18 cells resulted in reduced upregulation of IRF-9. This experiment was repeated twice. Quantitative analyses showed that the signal was reduced by 29 $\pm$ 4% and 25 $\pm$ 6% in UCp7con-9 cells after 4 h and 8 h, respectively, and by 44 $\pm$ 4% after 4 h in UCcon-18 cells. In UCcon-18 cells the difference in upregulation of IRF-9 after 8 h was not significant. A similar inhibition was observed in the upregulation of the IFN $\alpha$  target gene STAT1 (data not shown).

By contrast, no decrease, or, in line with the EMSA data, even a slight increase was found in UNS3-5Bcon-27 cells. These observations indicate that the expression of HCV structural proteins affects not only IFN signaling but IFN $\alpha$  effector functions as well. Interestingly, the observed inhibition could be overcome by using a 5-fold increased concentration of IFN $\alpha$  (data not illustrated).

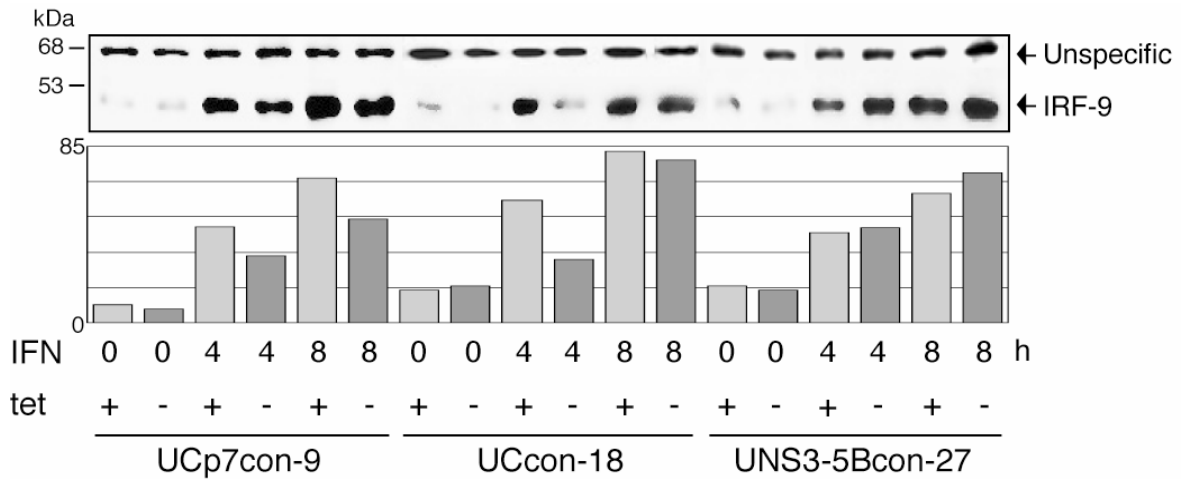


**Figure 4. Inhibition of Jak-STAT signaling by HCV structural proteins results in impaired upregulation of IFN $\alpha$  target genes.** UCp7con-9, UCcon-18, and UNS3-5Bcon-27 cells were cultured for 24 h in presence or absence of tetracycline (tet + or tet -) and were then either not treated (0 h) or stimulated for 4 h or 8 h with 100 U/ml IFN $\alpha$  (IFN). Whole cell extracts were analyzed by Western blot using a mAb against IRF-9. The position of IRF-9 is indicated by an arrow, a higher molecular weight nonspecific band can serve as an internal loading control. Quantitation of IRF-9-specific Western blot signals was performed as described in the Materials and Methods section and arbitrary density values normalized to the nonspecific bands are depicted as bars. These values reflect the experiment shown in this figure and are included in the average  $\pm$  S.D. values specified in the Results section. Light grey bars represent cells cultured in the presence of tetracycline, dark grey bars cells cultured in the absence of tetracycline.

## Discussion

The mechanisms by which HCV evades the host immune response to cause persistent infection in the majority of patients are poorly understood. Various strategies of immune evasion have been proposed, including, among others, down-regulation of major histocompatibility complex gene expression, viral interference with antigen processing and presentation, inhibition of cellular signaling pathways, and the generation of viral humoral and cellular immune escape variants<sup>211, 240, 254, 255</sup>. In this context, expression of HCV proteins was found not to interfere with major histocompatibility complex class I processing and presentation *in vitro*<sup>256</sup>.

We have shown previously that expression of the entire HCV polyprotein in U-2 OS human osteosarcoma-derived tetracycline-regulated cell lines inhibits IFN $\alpha$  induced signaling through the Jak-STAT pathway. To identify the HCV gene product(s) responsible for the observed inhibition of Jak-STAT signaling we generated a comprehensive panel of well-characterized cell lines allowing the regulated expression of HCV structural proteins either individually or in different combinations. In addition to the previously described inducible cell lines (reviewed in<sup>257</sup>), cell lines inducibly expressing the core protein derived from genotype 1a and 1b HCV cDNAs as well as the entire structural or nonstructural regions derived from a genotype 1a cDNA were generated for this study.

Using this panel of cell lines, we demonstrate that expression of the HCV structural region - and to a somewhat lesser extent of core protein alone - interferes with IFN $\alpha$  induced signaling through the Jak-STAT pathway. The findings obtained with genotype 1a-derived proteins were confirmed in genotype 1b. As previously found in the context of the entire HCV polyprotein, in the cell lines<sup>217</sup> and in the HCV transgenic mice (Chapter 2)<sup>129</sup>, inhibition occurred downstream of STAT tyrosine phosphorylation; i.e. the IFN $\alpha$ -induced binding of STAT1 transcription factor complexes to their response elements in the promoters of ISGs is inhibited, and resulted in an impaired upregulation of IFN target genes.

Duong et al. has recently showed in the HCV transgenic mouse, and in liver biopsies from HCV infected patients that this inhibition of IFN $\alpha$ -induced signaling might be the result of upregulation of the catalytic subunit of protein phosphatase 2A (PP2Ac). PP2Ac is overexpressed in liver extracts of HCV transgenic mice and expression of a constitutive active PP2A in Huh7 cells, resulted in inhibition of STAT1-DNA binding. This inhibition of STAT1-DNA binding was mediated by PP2Ac-induced hypomethylation of STAT1, which enhances its association with PIAS1 and prevents binding to DNA. So HCV viral protein expression can upregulate PP2Ac or can inhibit the PRMT1-induced-methylation of STAT1. The specific PTP for STAT1, TC-PTP was neither upregulated in HCV transgenic animals nor in liver biopsies from infected patients. The results indicate that patients with high PP2Ac expression levels are less responsive to IFN $\alpha$  treatment *ex vivo*<sup>130</sup>.

Proof that inhibition of STAT1-DNA binding, resulting from HCV induced STAT1 hypomethylation and increased PIAS1-STAT1 association, is the cause for IFN $\alpha$  treatment resistancy and thus an important mechanism how HCV

---

induces inhibition of Jak-STAT signaling, was given through the generation of the PIAS1-deficient mice <sup>92</sup>. The IFN antiviral activity, measured by expression of many IFN induced genes, was consistently enhanced in these mice. The PIAS1-deficient mice showed increased protection against pathogenic infection and an increased IFN-mediated antiviral response.

The observed degree of inhibition of STAT-DNA binding seems not to correlate with the inhibition of upregulation of ISGs (IRF-9 in Figure4). A similar observation was made for upregulation of PKR and 2'-5'-OAS in the HCV transgenic mice. Only a slight inhibition of upregulation of these genes could be shown (Chapter 2, unpublished data).

ISGs are upregulated in HCV infection, of which several have been analyzed for their ability to interfere with HCV replication. However the effector proteins that inhibit HCV replication have not yet been identified <sup>258, 259</sup>.

MxA, interferon inducible protein 44 (IFI-44) and IFI-56 were shown to be upregulated in HCV liver biopsies of patients compared to biopsies from non infected livers <sup>260</sup>. Upregulation of 2'-5'-OAS was shown in chimpanzees, and was correlated with an increase in level of HCV particles <sup>261</sup>. A DNA microarray study, in which hepatocytes from chimpanzee liver biopsies were probed for changes in gene expression during acute infection, revealed enormous fold upregulations of ISGs; p15/17, p27, IRF7, MxA and 2'-5'-OAS. <sup>262</sup>. Another study in infected chimpanzees showed that 2'-5'-OAS, STAT1 and MxA were induced <sup>263</sup>. PKR, MxA, 2'-5'-OAS and ISG15 were upregulated in liver biopsies from chronic HCV infected patients <sup>264, 265</sup>. However, neither of these cases shows a positive correlation between the mentioned ISGs induction and viral clearance.

This might be explained by the results obtained from a detailed gene activation analysis of 650 genes induced by IFNs in PIAS1-deficient macrophages. Only 9% of these interferon-inducible genes showed an induction. This suggests that PIAS1 specifically regulates a subset of interferon-induced genes <sup>92</sup>. It could be assumed that the ISGs found to be upregulated in the previous mentioned studies, are not regulated by PIAS1 and therefore are not inhibited in their upregulation during HCV infection. A HCV effector protein might be an interferon-induced protein regulated by PIAS1. Interferon-induced genes identified to be specifically regulated by PIAS1 are: GBP1 (guanylate binding protein), CXCL9 (CXC chemokine ligand 9), CXCL10, IFI203 (interferon-inducible gene 203) and LY6E <sup>92</sup>.

A surprising side aspect of this study was the presence of a minor proportion of core protein in the nucleus of UCp7con, but not UCcon cells. In cell lines expressing genotype 1b TH cDNA-derived structural proteins, core protein was found only in the cytoplasm <sup>222, 246</sup>. The reason for this discrepancy is not understood. Carboxyterminal truncation of the core protein results in nuclear translocation <sup>222</sup>. However, no smaller size core protein products were seen by Western blot (data not illustrated). In addition, a nonspecific toxic effect of overexpressed HCV structural proteins seemed unlikely because nucle(ol)ar core protein was found also in UCp7con and UHCVcon cells expressing low levels of viral proteins (data not shown).

Basu *et al.* recently presented data indicating an inhibitory effect of HCV core protein on ISGF3 formation <sup>266</sup>. However, in contrast to our study this effect

seemed to be the result of reduced STAT1 expression in HeLa cells stably transfected with HCV cDNAs. In this context, the availability of tightly regulated cell lines inducibly expressing different HCV proteins allows to verify effects in the same cell in the presence or absence of HCV proteins. Keskinen et al. used the in this chapter described cell lines, to show that only the combined expression of all structural proteins, but not by only core expression, allowed viral replication (of VSV) despite IFN $\alpha$  treatment of the cells <sup>267</sup>. With other words they show that the structural proteins impair IFN $\alpha$  antiviral activity.

The HCV nonstructural protein 5A has been reported to interfere with the activity of the double-stranded RNA activated protein kinase (PKR) and, thereby, to inhibit the IFN $\alpha$  response <sup>230, 268, 269</sup>. In this context, we found no inhibition of IFN $\alpha$  induced Jak-STAT signaling by NS5A in 4 independent UNS5Acon cell clones analyzed. This is in accordance with recent data published by Polyak *et al.* <sup>270</sup>. Interestingly, however, expression of the NS5A protein in cultured cells resulted in partial resistance to the antiviral effects of IFN $\alpha$  against IFN-sensitive viruses, such as vesicular stomatitis or encephalomyocarditis viruses <sup>271, 272, 273, 274, 231, 275</sup>. In line with observations made earlier in the context of the entire HCV polyprotein <sup>243</sup>, Pödevin *et al.* recently found no effect of NS5A expression on PKR activity in HuH-7 cells constitutively expressing different NS5A sequences <sup>274</sup>. Therefore, the inhibitory effect of NS5A may be mediated by PKR-independent mechanisms as well. Taken together, these observations indicate that HCV proteins may interfere with the IFN system by different mechanisms.

Among other members of the *Flaviviridae* family, bovine viral diarrhea virus was found to interfere with the IFN system to establish persistent infection <sup>276 277</sup>. Therefore, interference with the IFN system may be a common mechanism of *Flaviviridae* family members leading to persistent infection.

In conclusion, we show here that the HCV structural proteins interfere with IFN $\alpha$  induced signal transduction through the Jak-STAT pathway. Inhibition occurred downstream of STAT tyrosine phosphorylation and resulted in an impaired upregulation of IFN $\alpha$  target genes. A better understanding of the interactions between HCV and the IFN system may ultimately result in more effective therapies to inhibit HCV escape of the IFN-induced antiviral defense, and consequently to prevent establishment of chronic HCV infection.

### Acknowledgments

The authors express their sincere gratitude to Juliane Schmidt-Mende for help with the establishment of UNS3-5Bcon cell lines, Dr. François Duong for helpful discussions, Dr. Charles M. Rice for the HCV H prototype and consensus cDNAs, Dr. Christoph Englert for UTA-6 cells, Drs. Jean Dubuisson and Harry Greenberg for mAbs A4 and A11, Dr. Michinori Kohara for mAb 384, and Dr. Jan Albert Hellings for mAb 11H.

This work was supported by the Deutsche Forschungsgemeinschaft, Bonn, Germany (Mo 799/1-2 and Mo 799/1-3), the Bundesministerium für Bildung und Forschung, Bonn, Germany (01 KI 9951), the European Commission, Bruxelles, Belgium (QLRT-PL1999-00356), the Lucie Bolte Foundation, Dillingen/Saar, Germany, the Swiss National Science Foundation, Berne, Switzerland (3231-054973 and 3200-63838.00), the Swiss Cancer League, Berne, Switzerland (KFS 922-09-1999), Oncosuisse, Berne, Switzerland (OCS-01170-09-2001), the Roche Research Foundation, Basel, Switzerland (90-1999), and the Novartis Stiftung, Basel, Switzerland (01C43).





Chapter 4

**A fusionprotein between wild type murine STAT3 and the modified ligand-binding domain of the estrogen receptor can mimic activated STAT3 in the presence of 4-hydroxytamoxifen**

Simone T.D. Stutvoet, Elke Bieck, Sabina Hernandez Penna, and Markus H. Heim

Department of Research, University Hospital Basel,  
CH-4031 Basel, Switzerland

---

## Abstract

The role of STATs in liver pathophysiology has been studied so far mainly with loss-of-function models (e.g. IL-6 KO mice, IFN-receptor KO mice, STAT1 and STAT5 KO mice, inducible STAT3 KO mice).

To study the effects of enhanced activities of STATs, we generated fusion proteins between STAT1, STAT3 or STAT5a and the modified ligand-binding domain of the estrogen receptor. In addition, we generated several mutants of the fusion proteins to study the functionality of the fusion proteins and its ability to mimic activated STAT, when stimulated with 4-hydroxytamoxifen (4-HT).

Fusion proteins between wild-type mSTAT1, mSTAT3 or mSTAT5a and the ligand binding domain of the estrogen receptor were generated. For each STAT three mutants were generated; a SH2-domain (R602→K, R609→K or R618→K), a tyrosine phosphorylation site (Y701→F or Y705→F) and a serine phosphorylation site (S727→A) mutant. STAT1-ER constructs were transfected in STAT1  $\Delta/\Delta$  mouse embryonic fibroblasts (MEFs) and the STAT3-ER constructs in STAT3  $\Delta/\Delta$  MEFs, and stable transfected clones were selected.

STAT signaling was investigated after activation of cells with natural ligands (IFN, IL-6, LIF) and compared to effects generated by treatment of the cells with 4-hydroxytamoxifen (4-HT), a synthetic steroid drug that can dimerize and activate the STAT-ER proteins directly. The STAT1-ER fusion proteins appeared to be not functional. From the STAT3-ER fusion proteins only the wild type could be activated by 4-HT and was shown to mimic STAT3 activation.

STAT3<sub>wt</sub>-ER and STAT5aR618K-rER fusion protein construct are used to generate mice expressing the STAT-ER fusion proteins under the control of the albumin promoter.

## Introduction

The biological function of STAT proteins has been mainly studied with loss-of-function models, i.e. dominant negative forms of STATs or STAT deficient mice. However, there are a number of diseases where constitutive active STATs have been found. We therefore wanted to generate conditionally active forms of STAT proteins that can be activated independently of their natural ligands. To that aim, we constructed fusion proteins between STAT1, STAT3 or STAT5a and the modified ligand binding domain (LBD) of the estrogen receptor (ER). Such fusion proteins can be dimerized by 4-HT (4-hydroxytamoxifen). STAT1, 3 and 5a are chosen for the following reasons.

STAT1 is central for IFN signaling and both Hepatitis B and C virus are treated with IFN. Enhanced STAT1 signaling could be a possible way to target HCV interference with IFN $\alpha$  induced Jak-STAT signaling. Furthermore has STAT1 been shown to induce apoptosis<sup>103, 105</sup> and to inhibit cell growth<sup>278</sup>. Due to these properties is STAT1 described as tumor suppressor<sup>5, 279</sup> and it could be of importance during liver regeneration.

STAT3 activation is one of the earliest events in the regenerating liver and prolonged activation is positively correlated with hepatocyte regeneration and survival. However IL-6 was shown to be not required for liver cell proliferation since some KO animals did regenerate normally without IL-6 substitution. STAT3 target genes cyclin D1 and c-Myc were not induced, and cell cycle progression was thought to take place with help of compensatory cyclin D3-CDK6 activation. So it seemed that STAT3 activation is not required for cell cycle progression<sup>199</sup>. With gain-of-function model for STAT3 we would be able clarify further the role of STAT3 in the process resulting in a restored liver. STAT3 is reported to act as an oncogene<sup>150</sup> and can upregulate antiapoptotic genes and genes involved in cell cycle, indicating its role in oncogenesis<sup>149</sup>.

STAT5a is, like STAT3 also a promoter of cell proliferation, cellular transformation and inhibitor of apoptosis<sup>280</sup>. Especially because of its role in GH signaling in liver<sup>123</sup>, it would be interesting to study STAT5a in a gain-of-function model during liver regeneration or oncogenesis of e.g. hepatocellular carcinoma. A model for STAT5a would also be of use to examine whether STAT5a can protect hepatocytes against apoptosis in ischemia injuries during liver transplantation.

Conditionally active STAT models that have been generated make it possible to analyze the function of the STAT proteins in their correct physiological context. Fusion proteins between the modified (G525R) ligand binding domain of the estrogen receptor (aa 281-599) and the full length mSTAT1, 3 or 5a protein (i.e. mSTAT-ER) have been created. The fusion protein can be activated by the synthetic steroid ligand 4-HT only; the mutation of the glycine at position 525 abolishes the ability of the receptor to bind 17 $\beta$ -estradiol<sup>281</sup>. 4-HT binds to the modified ligand binding domain by forming two hydrogen bonds with E357 and R398, this result in the repositioning of ER's ligand binding domain helix 12 over the NR box coactivator site, which prevents binding of the NR box protein and activation of the estrogen response element (ERE). Moreover, this mutant does not have transactivation activity<sup>282</sup>. Upon binding with 4-HT, the ER ligand binding domain is phosphorylated on the tyrosine residue 541, which is thought to induce dimerization of the domains<sup>283</sup>, and consequently of the STAT-ER fusion protein. It is then able to translocate to the nucleus where it can induce

---

STAT specific target gene transcription. Matsuda et al. showed in cells that the fusion protein between STAT3 and the modified ligand binding domain of the estrogen receptor (mSTAT3-ER) can mimic activated STAT3 in the presence of 4-HT without cytokine signaling. With this model proof was given that STAT3 activation is sufficient to maintain an undifferentiated state of mouse embryonic stem (ES) cells <sup>284</sup>. In their hands, mSTAT3-ER could be tyrosine and serine phosphorylated by 4-HT or LIF, and it could bind to DNA when ES cells were stimulated. They also used this model to investigate the mechanism underlying the regulation of D-type cyclins during liver development. They showed that oncostatin M suppresses the expression of cyclins D1 and D2 in fetal hepatocytes in vitro and that this is mediated by STAT3 <sup>285</sup>. Other STAT-ER fusion proteins have been published by Kamogawa et al. and Milocco et al. A STAT6-ER fusion protein could induce transcription of an IL-4-responsive promoter upon 4-HT stimulation. Additional IL-4 stimulation enhanced DNA binding <sup>286</sup>. Fusion proteins between hSTAT1, STAT5a, STAT5b or STAT6 and the intact ligand binding domain of the estrogen receptor were reported to be activated upon estradiol, 4-HT and IFN $\gamma$  stimulation, however not to be phosphorylated on Y701 (for STAT1ER) <sup>287</sup>.

For the cloning of the models we used the mSTAT3-ER and mSTAT5a-rER constructs generated by Matsuda <sup>284</sup>. These constructs and mSTAT1 cDNA were used to clone the third construct; i.e. mSTAT1-ER.

In the published studies there was no proof presented that tyrosine phosphorylation and/or a functional SH-2 domain are required to establish a stable STAT-ER dimer and induce STAT specific transcription. Due to the results with the STAT6-ER fusion protein, it was suggested that dimerization and activation of the STAT-ER fusion proteins occurs without phosphorylation of the C-terminal STAT tyrosine residue <sup>286</sup>. It was also shown by all who published fusion proteins between STAT and the ligand binding domain of the ER, that the fusion protein could be activated, in addition to 4-HT, by cytokines. This would imply in an in vivo situation that the STAT-ER fusion proteins could be activated by any endogenous occurring ligand and activation responses would be difficult to control. If, as suggested, the dimerization of the fusion proteins is induced by the dimerization of its ER ligand binding domain upon 4-HT binding, then a mutation of the conserved arginine in the SH2 domain or of the tyrosine residue would not influence the functionality of the STAT-ER protein. As described, the conserved arginine in the SH2 domain is required for STAT recruitment to the receptor upon ligand binding and interactions between this arginine residue and the phosphorylated tyrosine residue is required for dimerization and activation of the STATs. Therefore, it is expected that these mutations would abolish the possibility that STAT-ER fusion proteins are activated by cytokines. To test this hypothesis and aiming to create a STAT-ER fusion proteins, which would be exclusively be activated by 4-HT, three mutants were designed for mSTAT1-ER, mSTAT3-ER and one for mSTAT5a-rER. A single amino acid mutation was introduced replacing arginine (R) 602 (mSTAT1), 609 (mSTAT3) or 618 (mSTAT5a) with a lysine (K), replacing tyrosine (Y) 701 (mSTAT1) or 705 (mSTAT3) with a phenylalanine (F) and serine (S) 727 with an alanine (A). The serine mutated fusion proteins will be used to test the functional significance of S727 phosphorylation on transcriptional activity in the context of STAT-ER fusion proteins.

The wild-type and mutant constructs for mSTAT1-ER and mSTAT3-ER were expressed in mouse embryonic fibroblasts (MEFs) deficient for STAT1 and STAT3, respectively, to determine the most optimal inducible mSTAT-ER fusion protein variant to use in an in vivo model.

Here we report our analysis of the activation of mSTAT1-ER and mSTAT3-ER fusion protein mutants compared to wild type, by either 4-HT, IFN $\gamma$  or IL-6 in MEF cell lines.

## Materials and Methods

### Plasmid construction

The wild type mouse STAT3-ER (mSTAT3<sub>wt</sub>-ER) and mSTAT5a-rER constructs ligated EcoRI-XhoI in the pCAGGS vector, were kindly provided by Dr. T. Yokota (Science University of Tokyo) (described in <sup>284</sup>). The plasmids contain a puromycin acetyltransferase gene driven by the SV40 early promoter, expressing a fusion protein between full length mSTAT3 or mSTAT5a and modified ligand binding domain of the estrogen receptor (aa 281-599) of mouse respectively rat (ER respectively rER).

The SH2 domain mutation (R618→K) in pCAGGS-mSTAT5a-rER was introduced using the QuikChange™ XL Site-directed mutagenesis kit (Stratagene, The Netherlands) and mutagenic primers designed forward (5'-A CCTTCCTGCTGAAGTTCAGTGAAGTTCGG-3'; mutation boldface) and reverse (5'-CCGAGTCACTGAACTTCAGCAGGAAGGT-3'; mutation boldface) complementary to opposite strands of pCAGGS-mSTAT5a-rER. With this method *pfuTurbo* DNA polymerase extends and incorporated the mutagenic primers during temperature cycling. Following temperature cycling, the product was treated with DpnI endonuclease, which is specific for methylated and hemimethylated DNA and was used to digest the parental DNA template and to select for mutation containing synthesized DNA. The vector DNA incorporating the desired mutation was then transformed into XL10-Gold ultracompetent bacterial cells.

The mSTAT3<sub>wt</sub>-ER cDNA was amplified from pCAGGS using forwardHindIII (5'-GCCAGTCGGGCCTCAAGCTTGGAGACAGTCGAGACC-3'; HindIII site underlined) and reverseApaI/mutated stop codon (5'-AGATCCACTAGT AGGGGCCCTGAGATCGTGTGG-3'; ApaI site underlined, mutated stop codon boldface) introducing primers. The PCR products were digested and cloned HindIII-ApaI into the pcDNA4/*myc*-His© (frame A) vector (Invitrogen, Carlsbad, CA) in frame with the *myc*-His-stop tag, generating pcDNA4mSTAT3<sub>wt</sub>-ER-*myc*-His.

Mutagenesis of pcDNA4mSTAT3<sub>wt</sub>-ER-*myc*-His, to introduce a SH2 domain (R609→K), a tyrosine phosphorylation site (Y705→F) or a serine phosphorylation site (S727→A) mutation, was performed according to the QuikChange™ XL Site-directed mutagenesis kit protocol and using the mutagenic primers designed forward (5'-CACCTTCCTACTGAAGTTCAGCGA GAGCAG-3'; R→K mutation boldface) and reverse (5'-CTGCTCTCGCTG AACTTCAGTAGGAAGGTG-3'; mutation boldface), forward (5'-TAGTGCTG CCCCCTTCCTGAAGACCAAG-3'; Y→F mutation boldface) and reverse (5'-

---

CTTGGTCTTCAGGAACGGGGCAGCACTA-3'; mutation boldface), and forward (5'-GACCTGCCGATG**CCCCCGCACTTTAG**-3'; S→A mutation boldface) and reverse (5'-CTAAAGTGC**GGGGGGCCATCGGCAGGTC**-3'; mutation boldface), respectively, complementary to opposite strands of the plasmid.

The mSTAT3<sub>wt</sub>-ER-*myc*-His, mSTAT3<sub>R609K</sub>-ER-*myc*-His, mSTAT3<sub>Y705F</sub>-ER-*myc*-His and mSTAT3<sub>S727A</sub>-ER-*myc*-His cDNAs were amplified from pcDNA4/*myc*-His using forward SpeI (5'-TATAGGGAGACCCAAGCTGACTAGTTAAGCTTGGAGACAG-3'; SpeI site underlined) and reverse NotI (5'-ATG GCTGGCAACTAGCGGCCGAGTCGAGGCTGATC-3'; NotI site underlined) introducing primers. The PCR products were digested and cloned SpeI-NotI into the pEFzeo vector <sup>288</sup> (gift from Dr. T. Decker, Vienna Biocenter), generating pEFmSTAT3<sub>wt</sub>-ER-*myc*-His ect.

The mSTAT1<sub>wt</sub> cDNA was amplified by PCR from pcDNA3 (XhoI-XhoI insert) (a gift from Dr. D.E. Levy, New York University school of medicine) using forward KpnI (5'-GGGAACGGAAGCATT**TGGTACCTCCAGGATGTCAC**-3'; KpnI site underlined) and reverse BamHI/mutated stopcodon (5'-GTCGCCAGAGAGAAATTCGGAT**CCATACTGTGCTCATCATACTG**-3'; BamHI site underlined, mutated stop codon boldface) introducing primers. The PCR products were digested and cloned in a pcDNA3 vector (Invitrogen).

To generate the mSTAT1<sub>wt</sub>-ER fusion construct, the modified ER ligand binding domain was amplified from the pCAGGS-mSTAT3<sub>wt</sub>-ER using forward BamHI including/insertion (5'-GTGCTACCTCCCCATGGATCCGGGCTCCGAGCCCGAATT-3'; BamHI site underlined, insertion boldface) including and reverse NotI introducing/stop codon including (5'-GGGAGATCCACTAGCGGCCGCT**CTCAGATCGTG**-3'; NotI site underlined, stop codon boldface) primers. The mER BamHI-NotI PCR fragment was digested and ligated in frame at the C-terminal of mSTAT1 in pcDNA3. This fusion protein (STAT1<sub>wt</sub>-ER) contains 11 extra amino acids (WIRAPSPNSDP), which are not present in either mSTAT1 or ER ligand binding domain, at the fusion point.

Mutagenesis of pcDNA<sub>3</sub>mSTAT1<sub>wt</sub>-ER, in order to introduce a SH2 domain (R602→K), a tyrosine phosphorylation site (Y701→F) or a serine phosphorylation site (S727→A) mutation, was performed according to the QuikChange™ XL Site-directed mutagenesis kit protocol and using the mutagenic primers designed forward (5'-AGGGACGTT**CCTGCTTAAATTCAGTGAGAGCTCC**-3'; R→K mutation boldface) and reverse (5'-GGAGCTCTCAC TGAATTTAAGCAGGAACGTCCCT-3'; mutation boldface), forward (5'-AAGC GAACTGGATTCATCAAGACTGAGTTG-3'; Y→F mutation boldface) and reverse (5'-CAACTCAGTCTTGATGAATCCAGTTCGCTT-3'; mutation boldface), and forward (5'-AACCTGCTTCCCATGGCTCCAGAGGAGTTTG-3'; S→A mutation boldface) and reverse (5'-CAAACCTCCTCTGGAGCCATGGGAA GCAGGTT-3'; mutation boldface), respectively, complementary to opposite strands of the plasmid.

The mSTAT1<sub>wt</sub>-ER, mSTAT1<sub>R602K</sub>-ER, mSTAT1<sub>Y701F</sub>-ER and mSTAT1<sub>S727A</sub>-ER cDNAs were amplified from pcDNA3 using forward SpeI introducing (5'-TAGGGAGACCCAAGCTTGGTA**ACTAGTGGATGTCACAGTGG**-3'; SpeI site underlined) and reverse NotI including (5'-TCTAGATGCATGCTCGAGCGG**CCGCTCTCAGATCG**-3'; NotI site underlined) primers. The PCR products

were digested and cloned SpeI-NotI into the pEFzeo vector, generating pEFmSTAT1<sup>wt</sup>-ER ect.

All sequences and mutations were confirmed using the DYEnamic Direct Cycle Sequencing system (Amersham Biosciences) or a ABI Prism™ DNA 3730 sequencer (Perkin Elmer, MA, USA).

### **Establishment of stable transfectants**

STAT1 deficient ( $\Delta/\Delta$ ) MEFs <sup>288</sup> (gift from Dr. T. Decker, Vienna Biocenter) were transfected in 10 cm culture dishes, using 2  $\mu$ g of pEFmSTAT1<sup>wt</sup>-ER, pEFmSTAT1<sup>R602K</sup>-ER, pEFmSTAT1<sup>Y701F</sup>-ER or pEFmSTAT1<sup>S727A</sup>-ER plasmid DNA and Effectene reagent according to the manufacturer's instructions (Qiagen, Hilden, Germany). Clones were selected with Zeocin (200  $\mu$ g/ml, Invitrogen). Individual clones, isolated by limiting dilution were characterized for comparable STAT1-ER expression to STAT1 expression in STAT3 deficient MEFs by western blotting.

STAT3 deficient ( $\Delta/\Delta$ ) MEFs <sup>289</sup> (kind gift from Prof. V. Poli, DiPartimento di Genetica, Torino) were transfected in 10 cm culture dishes, using 2  $\mu$ g of pEFmSTAT3<sup>wt</sup>-ER-*myc*-His, pEFmSTAT3<sup>R609K</sup>-ER-*myc*-His, pEFmSTAT3<sup>Y705F</sup>-ER-*myc*-His or pEFmSTAT3<sup>S727A</sup>-ER-*myc*-His plasmid DNA and Effectene reagent. Clones were selected with Zeocin (400 $\mu$ g/ml). Individual clones, isolated by limiting dilution were characterized for comparable STAT3-ER expression to STAT3 expression in STAT1  $\Delta/\Delta$  MEFs by western blotting.

Cells were cultured in DMEM GlutaMAX™ supplemented with 5% fetal bovine serum, 50 U/ml penicillin and 50  $\mu$ g/ml streptomycin (Gibco, Invitrogen AG, Switzerland).

### **Reagents and antibodies**

4-Hydroxytamoxifen (4-HT) (H-7904) was purchased from Sigma (St. Louis, Mo.) and used at a concentration of 1 $\mu$ M (except where indicated differently), recombinant human IL-6 was produced as described <sup>290</sup> and used at a concentration of 200 ng/ml. Murine IFN $\gamma$  (Gibco) was used at a concentration of 1000 U/ml and murine LIF (Sigma) at a concentration of 100 ng/ml.

Antibodies against STAT1 (sc-346) and ER $\alpha$  (sc-542) were from Santa Cruz Biotechnology, and against STAT3 from Zymed Laboratories Inc. (13-7000; CA, USA). Polyclonal antisera against Tyr705-phosphorylated STAT3 (07-391) or Ser727-phosphorylated STAT3 (9134S) were obtained respectively, from Upstate Biotechnology (Lake Placid, N.Y.) and Cell Signaling Technologies (New England Biolabs, Beverly, MA). The antibody against phosphorylated Jak1 (3331S) was from Cell Signaling Technologies, and against Jak1 (J24320) from Transduction Laboratories (Lexington, KY).

### **EMSA**

After treatment with 4-HT, hIL-6, mLIF or mIFN $\gamma$ , cells were lysed in low salt buffer (20 mM Hepes pH 7.9, 10 mM KCl, 1 mM EDTA, 1 mM EGTA, 0.2% NP-40, 10% glycerol, 0.1 mM Na<sub>3</sub>VO<sub>4</sub>, 1 mM PMSF, 1 mM dithiothreitol, 2  $\mu$ g/ml aprotinin, 1  $\mu$ g/ml leupeptin, and 1  $\mu$ g/ml pepstatin) at 4 °C for 10 min. After centrifugation for 30 s at 12,000  $\times$  g, supernatants (= cytoplasmic extracts) were immediately frozen on dry ice, and pellets were extracted with high salt buffer (same as low salt, except for 420 mM NaCl and 20% glycerol

---

and no NP-40) for 30 min at 4 °C. Samples were cleared by centrifugation at 12,000 x *g* at 4 °C. Supernatants were aliquoted, frozen on dry ice and stored at -70 °C. For EMSA, nuclear extracts (2 µl) were incubated for 20 min at RT in 20 mM HEPES, pH 7.9, 4% Ficoll, 1 mM MgCl<sub>2</sub>, 40 mM KCl, 0.1 mM EGTA, 0.5 mM dithiothreitol, and 160 µg/ml poly[dI-dC]-poly[dI-dC] with 1 ng of <sup>32</sup>P-labeled oligonucleotides. Samples were separated on a 5% non-denaturing polyacrylamide gel at 400 V for 5 h at 4 °C. Gels were then dried and exposed for 24 h to a storage phosphor screen. The following oligonucleotides corresponding to STAT response element sequences were used; SIE-m67 (mutated serum inducible element) = 5'-CATTTCCTCGTAAAT CAT-3'.

### **Protein extraction and Western blotting**

For the preparation of whole cell extracts, cells were lysed in a buffer containing 50 mM Tris-HCl, pH 8.0, 280 mM NaCl, 0.5% NP-40, 0.2 mM EDTA, 2 mM EGTA, 10% glycerol, 0.1 mM Na<sub>3</sub>VO<sub>4</sub>, 1 mM PMSF, 2 µg/ml aprotinin, 1 µg/ml leupeptin, and 1 µg/ml pepstatin A. SDS-polyacrylamide gel electrophoresis and Western blot were performed according to standard protocols <sup>253</sup>.

### **Protein extraction and Immunoprecipitation**

For the preparation of IP whole cell extracts, cells were lysed in a buffer containing 50 mM Tris-HCl, pH 7.5, 100 mM NaCl, 1 mM EDTA, 0.1% TX-100, 10 mM NaF, 1 mM Na<sub>3</sub>VO<sub>4</sub>, 1 mM PMSF, 2 µg/ml aprotinin, 1 µg/ml leupeptin, and 1 µg/ml pepstatin A. 50µg of total protein was incubated in a total volume of 300 µl with 3µl of anti-c-Myc (sc-42, Santa Cruz) antibody for overnight at 4 °C. Then protein A-Sepharose (Sigma) was added for 2.5 hours at 4 °C. After SDS-polyacrylamide gel electrophoresis and transfer onto nitrocellulose membrane, proteins were detected with the anti-c-Myc antibody. Blots were analyzed by densitometry using NIH image software.

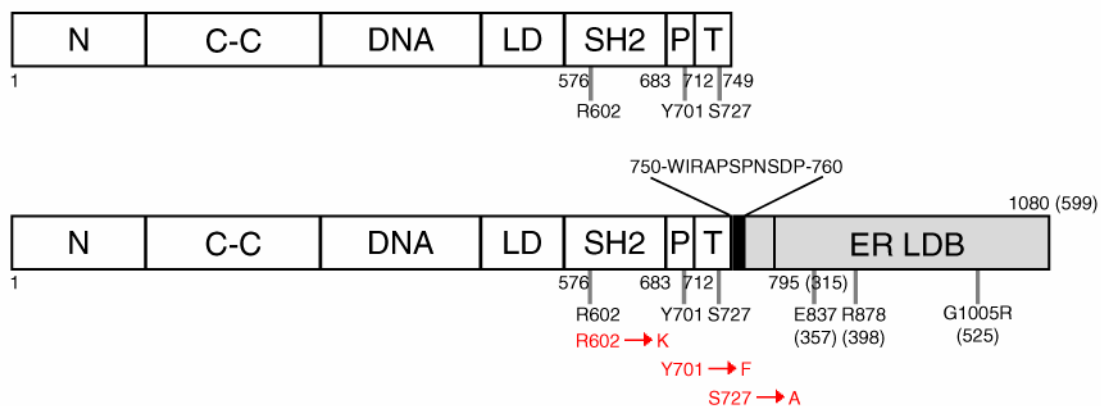


## Results and Discussions

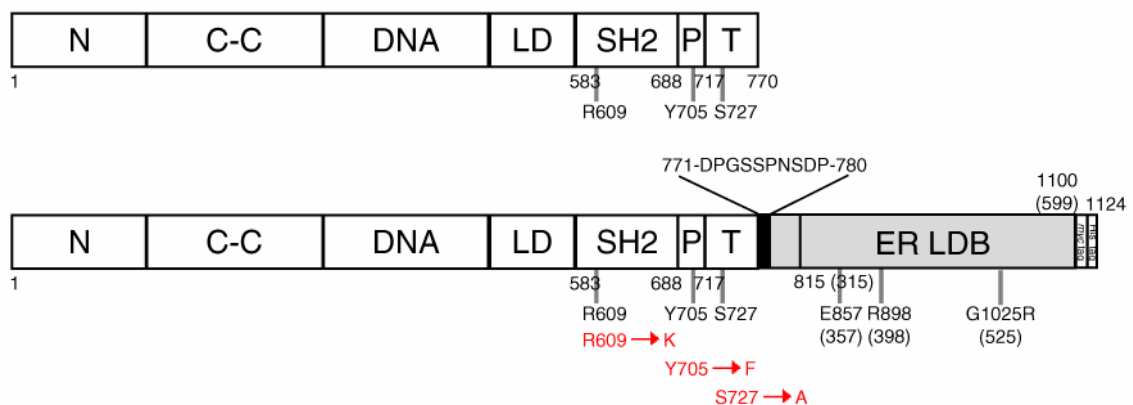
The pCAGGS-mSTAT3<sup>wt</sup>-ER and pCAGGS-mSTAT5<sup>awt</sup>-rER plasmids (a gift from Dr. Yokota) were used for cloning. mSTAT1<sup>wt</sup>-ER was composed out of the entire coding region of mouse STAT1 put together with the modified ER ligand binding domain amplified from pCAGGS-mSTAT3-ER. The constructs were transferred to another murine expression vector to enable them to be expressed in MEFs under Zeocin selection.

Three mutants of the mSTAT1<sup>wt</sup>-ER and mSTAT3<sup>wt</sup>-ER fusion protein constructs were generated; a SH2 domain mutant (R exchange for K); a tyrosine phosphorylation site mutant (Y to F); and a serine phosphorylation site mutant (S to A). Due to technical limitations of the mutagenesis procedure, it was possible to establish only the SH2 mutant of mSTAT5<sup>a</sup>-rER. The mSTAT5<sup>a</sup>-rER constructs were not expressed in cells, assuming that results for mSTAT1-ER and mSTAT3-ER would be as well valid for mSTAT5<sup>a</sup>-rER. Domain structures of STAT1, STAT3 and STAT5 in relation to their conditional active form (i.e. STAT-ER) are shown in Figure 1. The locations of the introduced mutations indicated in red writing.

### A



### B



**C**

**Figure 1. Schematical diagram showing the STAT1 (A), STAT3 (B) and STAT5a (C) domain structure in relation to their STAT-ER form.** Domains are labeled as follows: N= N-terminal domain, C-C= coil-coil domain, DNA= DNA binding domain, LD= linker domain, SH2= SH2 domain, P= phosphorylated tail segment, T= transactivation domain, ER LBD= ligand binding domain of the estrogen receptor alpha. The whole fragment taken from ER $\alpha$  (including the LBD) to generate the fusion protein is shown in grey. The linker between the STAT and the ER is depicted as a black rectangle, showing on top the linker's aa residue composition. The three STAT mutation sites are indicated. In the ER LBD two residues are indicated that enable the binding to 4-HT. The mutation modifying the ER LBD is also indicated. The numbers of the aa that render the domain boundaries are shown. Between brackets, the original aa residue numbers from the complete mouse ER $\alpha$  protein sequence.

## mSTAT3-ER fusion proteins

### *Cloning and mutagenesis procedures*

The mSTAT3<sub>wt</sub>-ER construct was amplified by PCR from the pCAGGS-mSTAT3<sub>wt</sub>-ER plasmid and transferred to a pcDNA4-*myc*-His vector. The pCAGGS vector contained many GC-rich sequences which interfered with the mutagenesis procedure. Mutagenesis of pcDNA4-mSTAT3<sub>wt</sub>-ER-*myc*-His was performed according to the QuikChange™ XL Site-directed mutagenesis kit protocol as described in the materials and methods section, using the mutagenic primers designed forward and reverse complementary to opposite strands of pcDNA4-mSTAT3<sub>wt</sub>-ER-*myc*-His.

Because of the incompatibility of the selection marker in pcDNA4-*myc*-His with the STAT3 $\Delta/\Delta$  MEFs, mSTAT3-ER-*myc*-His wild-type and mutant constructs were amplified by PCR from the pcDNA4-mSTAT3-ER-*myc*-His plasmids and transferred to the pEFzeo vector, which contains a Zeocin selection gene, designated pEFmSTAT3<sub>wt</sub>-ER-*myc*-His, pEFmSTAT3<sub>R609K</sub>-ER-*myc*-His, pEFmSTAT3<sub>Y705F</sub>-ER-*myc*-His and pEFmSTAT3<sub>S727A</sub>-ER-*myc*-His. These constructs were sequenced using forward and reverse primers at every 400 base pairs. In this way the sequencing results were confirmed by at least two primer readings. Sequencing results were compared to the NCBI GenBank. Some additional mutations have been discovered in the mutant fusion protein compared to the wild-type mSTAT3<sub>wt</sub>-ER-*myc*-His fusion protein. These are summarized in Table 1. K16E and T25S are described as variation in mSTAT3 by the GenBank.

	N	C-C	DNA	LD	SH2	P	T	ER LBD
mSTAT3 <sup>wt</sup> -ER	K16E, T25S							M925T, <b>G1025R</b>
mSTAT3 <sup>R609K</sup> -ER	K16E, T25S, N82D		G402D, L413P	P496L	G604D, <b>R609K</b>			<b>G1025R</b>
mSTAT3 <sup>Y705F</sup> -ER	K16E, T25S	L207P	N401S		M648V	S691G, <b>Y705F</b>		<b>G1025R</b>
mSTAT3 <sup>S727A</sup> -ER	K16E, T25S						<b>S727A</b>	N911I, <b>G1025R</b>

**Table 1. Summary of sequence analysis of the mSTAT3-ER-*myc*-His constructs.**

Amino acid substitutions revealed by sequencing of the pEFmSTAT3-ER-*myc*-His constructs. Confirmed aa mutations were summarized according to their location. Domains are labeled as in Figure 1.

Presented in bold script are the intentionally introduced mutations, in grey the mutations already present in mSTAT3<sup>wt</sup>-ER-*myc*-His construct and in normal script, the mutations introduced due to the mutagenesis procedure.

*Expression of pEFmSTAT3-ER-*myc*-His constructs in STAT3-deficient MEFs*

The pEFmSTAT3-ER-*myc*-His wild-type and mutant plasmids were introduced into STAT3 $\Delta/\Delta$  MEFs according to normal transfection procedures and stable transfectants were established. The expression level of the different mSTAT3-ER-*myc*-His clones in STAT3 $\Delta/\Delta$  MEFs is shown in Figure 2. The calculated size of mSTAT3-ER-*myc*-His is 124.8 kDa. Clones with an expression level, when possible, comparable to STAT3 expression in STAT1 $\Delta/\Delta$  MEFs, were chosen to use in functional assays; i.e. nr.10 for mSTAT3<sup>wt</sup>-ER, nr.71 for mSTAT3<sup>R609K</sup>-ER, nr.44 for mSTAT3<sup>Y705F</sup>-ER and nr.12 for mSTAT3<sup>S727A</sup>-ER.

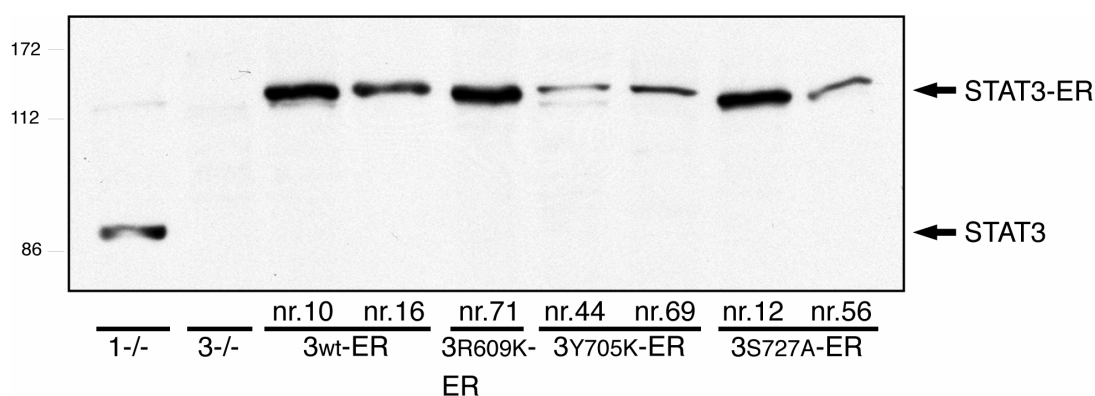


**Figure 2. Expression of the different pEFmSTAT3-ER-*myc*-His clones in STAT3-deficient MEFs.** Expression levels were analyzed by Western blotting using a monoclonal antibody against the STAT3 C-terminal. Whole cell lysates were prepared from untreated MEFs either transfected or left untransfected. Arrows indicate the positions of the STAT3 and STAT3-ER proteins. Lanes are labeled as follows: 1-/- = untransfected STAT1 $\Delta/\Delta$  MEFs, 3-/- = untransfected STAT3 $\Delta/\Delta$  MEFs, 3<sup>wt</sup>-ER = STAT3  $\Delta/\Delta$  MEFs transfected with pEFmSTAT3<sup>wt</sup>-ER-*myc*-His ect.

### Activation of mSTAT3-ER-myc-His fusion proteins

The different cell lines expressing wild-type or mutant mSTAT3-ER-myc-His fusion proteins, were stimulated with 4-HT, hIL-6 or mLIF for 30 min or 1 hour. Nuclear and cytoplasmic extracts were prepared. The cytoplasmic extracts at the 30 min timepoint were analyzed in Western blotting using antibodies against the tyrosine705 and serine727 phosphorylation site of STAT3 and against STAT3. We show in Figure 3 that both 4-HT and hIL-6 stimulation did result in phosphorylation of tyrosine705 of mSTAT3<sub>wt</sub>-ER-myc-His fusion protein. hIL-6 stimulation results in even a stronger signal than after 4-HT stimulation (Figure 3A). 4-HT stimulation, but not IL-6 or LIF stimulation (LIF stimulation data not shown) of the STAT3-ER expressing MEF cell lines, did result in serine727 phosphorylation of the mSTAT3<sub>wt</sub>-ER-myc-His fusion protein (Figure 3B). Phosphorylation levels did not increase after 1 h of stimulation compared to the 30 min timepoint (data not shown). STAT3 expressed by STAT1-deficient MEFs could as well be tyrosine as serine phosphorylated by hIL-6, but not by 4-HT (4-HT stimulation not shown). Expression levels of STAT3 and STAT3-ER in the MEFs are shown in Figure 3C. We were neither able to demonstrate tyrosine nor serine phosphorylation of the mutant forms of STAT3<sub>wt</sub>-ER fusion protein by either 4-HT, IL-6 or LIF.

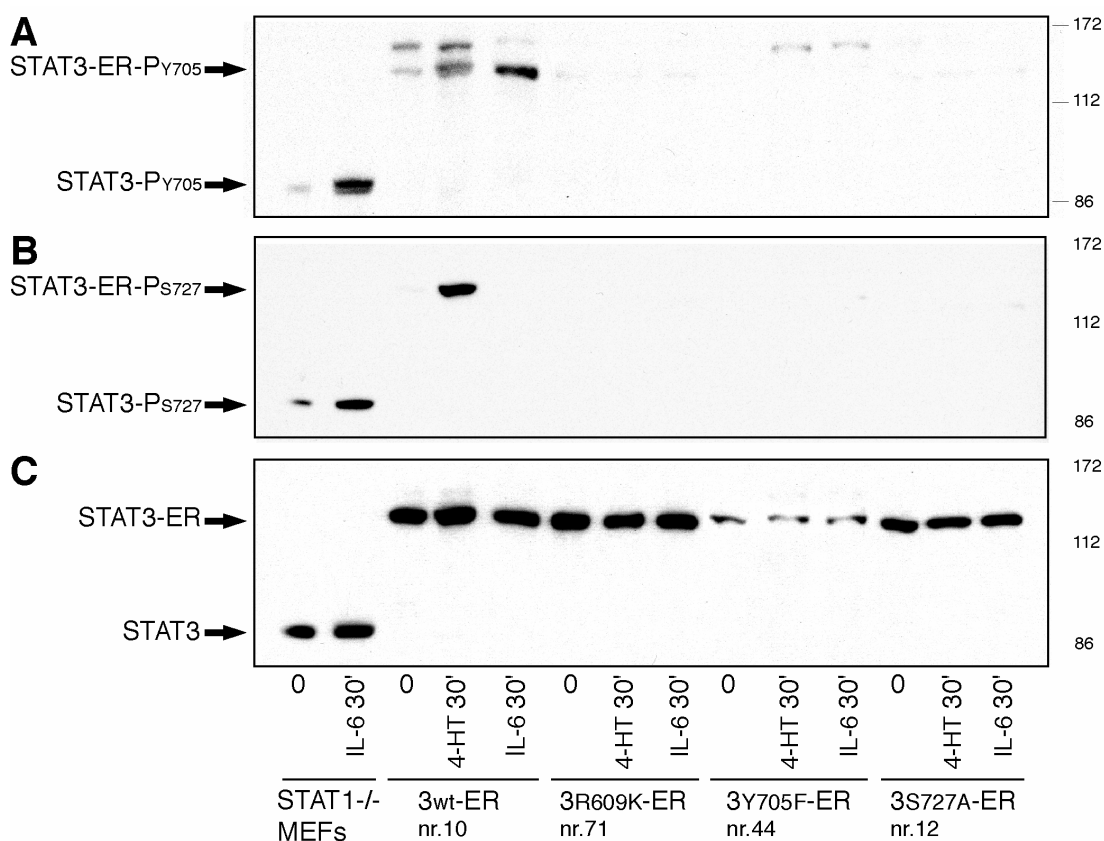


**Figure 3. Activation of STAT3 and STAT3-ER after stimulation with 4-HT or IL-6 in STAT1  $\Delta/\Delta$ , respectively STAT3  $\Delta/\Delta$  MEFs.** Tyrosine and serine phosphorylation of STAT3 and STAT3-ER. Cytoplasmic extracts were analyzed by Western blotting using 30  $\mu$ g of lysate. The membrane was probed with anti-phosphoserine727-STAT3 antibody (**B**), stripped, reprobred with anti-phosphotyrosine705-STAT3 antibody (**A**), stripped and

reprobed for a third time with anti-STAT3 antibody (C). The positions of (phosphorylated) STAT3 proteins are indicated by arrows. MEFs were either left untreated or treated for 30 min or 1h with 1 $\mu$ M 4-HT or 200 ng/ml hIL-6.

To determine whether the mSTAT3-ER-*myc*-His fusion proteins can function as DNA binding protein in response to 4-HT and cytokines, and to determine which or if one of the mutations would diminish this function, the nuclear extracts prepared in the same experiment as the previous described cytoplasmic extracts were analyzed by EMSA. Figure 4 shows that the mSTAT3wt-ER-*myc*-His fusion protein is able to bind DNA upon already 30 min of 4-HT stimulation, but not upon IL-6 stimulation.

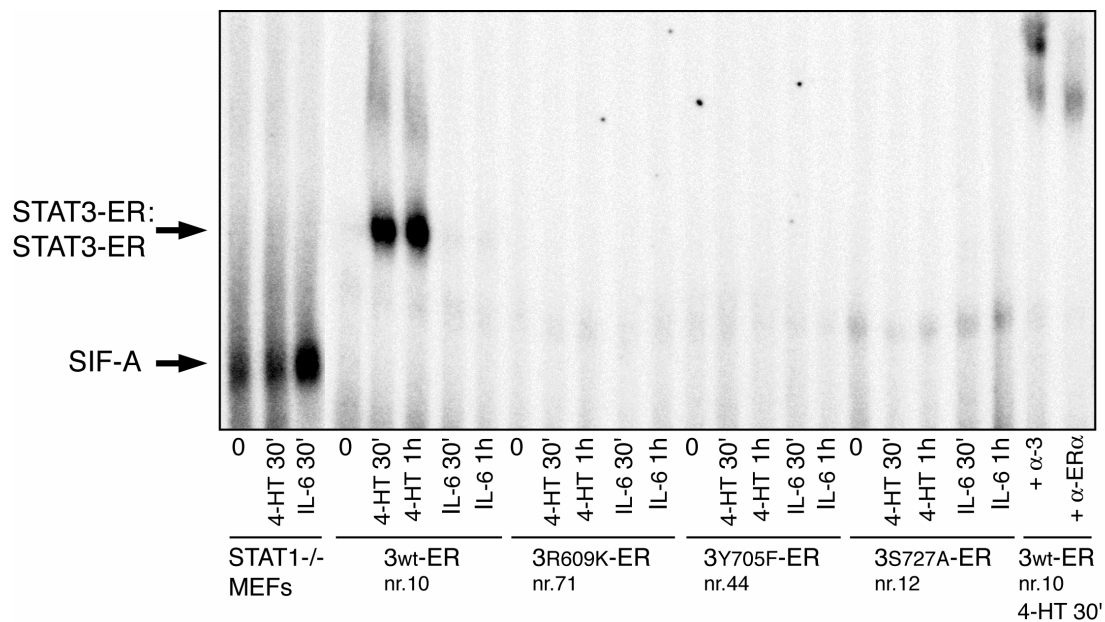


**Figure 4. DNA binding assay of STAT3 and STAT3-ER stimulated with 4-HT or IL-6 in STAT1  $\Delta/\Delta$ , respectively STAT3  $\Delta/\Delta$  MEFs.** Nuclear extracts, corresponding to the cytoplasmic extracts used for Figure 3, were analyzed by EMSA using the M67 oligonucleotide. SIF-A (i.e. STAT3:STAT3 homodimer) shift is detected in STAT1-deficient MEFs only when stimulated with 200 ng/ml hIL-6, but not when stimulated with 1  $\mu$ M 4-HT. STAT3wt-ER (=3wt-ER nr.10 in the Figure) could be activated by only 4-HT, but not by hIL-6. The position of the STAT3-ER: STAT3-ER dimer is indicated by an arrow. Samples of 4-HT-stimulated mSTAT3wt-ER-*myc*-His fusion protein could be shifted by either 1  $\mu$ l of polyclonal antibody against STAT3 (i.e.  $\alpha$ -3, sc-482, Santa Cruz) or by 1  $\mu$ l of an antibody against the LBD of ER $\alpha$  (sc-542).

Although this wild-type STAT3 fusion protein can be tyrosine phosphorylated upon IL-6 stimulation, it obviously is not able to dimerize and bind DNA. Otherwise it might be possible that IL-6 induced binding of the activated fusion protein occurs below EMSA detection level. Only IL-6 stimulation resulted in DNA binding of STAT3. We were not able to show DNA binding of the mutant forms of mSTAT3wt-ER fusion protein by either 4-HT, IL-6 or LIF (LIF activation data not shown). Several independent experiments confirmed these results.

### Target gene induction by mSTAT3<sup>wt</sup>-ER-myc-His fusion protein

To examine whether the mSTAT3<sup>wt</sup>-ER-myc-His fusion protein was able to induce transcription of STAT3 target genes, the upregulation of STAT3 target gene c-Myc<sup>291</sup> by 4-HT or IL-6 was analyzed. MEFs expressing the mSTAT3<sup>wt</sup>-ER-myc-His fusion protein were stimulated between 1 and 8 hours by either 4-HT or IL-6. As control normal 3T3 MEFs were stimulated with 4-HT and IL-6. Whole cell extracts were prepared and precipitated with anti-c-Myc antibody. Immunoprecipitates were separated on a Western blot and blotted against anti-c-Myc antibody. Figure 5A shows that 4-HT by activating mSTAT3<sup>wt</sup>-ER-myc-His can induce c-Myc protein expression in STAT3-deficient MEFs. In contrast, IL-6 stimulation of the fusion protein did not result in c-Myc protein upregulation (Figure 5B). In 3T3 MEFs c-Myc expression was induced by only IL-6 (data not shown). These results suggest that 4-HT activates the STAT3 pathway in STAT3-deficient MEFs expressing mSTAT3<sup>wt</sup>-ER-myc-His.

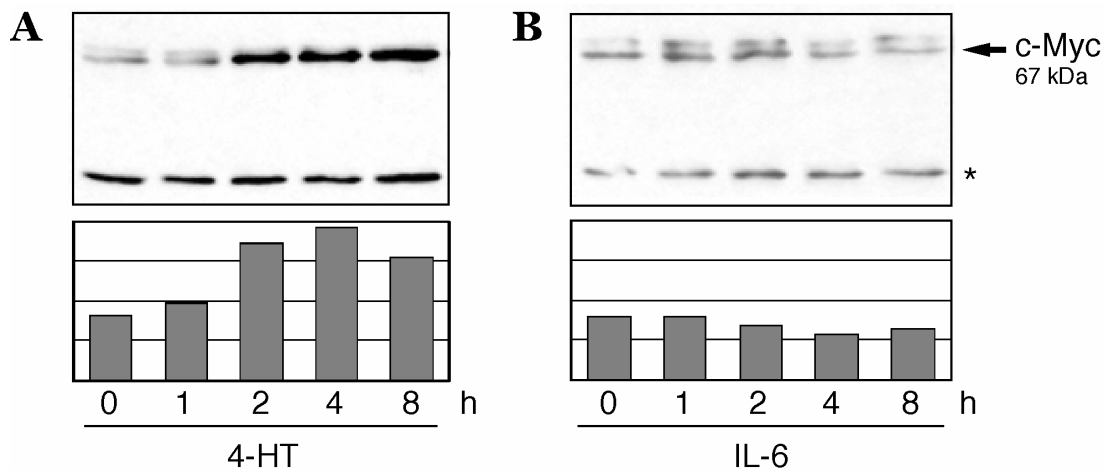


**Figure 5. Function of mSTAT3<sup>wt</sup>-ER-myc-His.** IP-Western blot analysis of STAT3 $\Delta/\Delta$  MEFs transfected with pEFmSTAT3<sup>wt</sup>-ER-myc-His (clone nr.10). Cells were grown to 80% confluency and starved for 48 h. Subsequently the cells were stimulated with (A) 1  $\mu$ M 4-HT or (B) 200 ng/ml hIL-6, for the timepoints indicated and IP whole cell extracts were prepared. 50  $\mu$ g of total protein was precipitated with an antibody against c-Myc (sc-42). Precipitates were analyzed by Western blotting using the same anti-c-Myc Ab. The arrow indicates the position of c-Myc protein and the asterisk the IgG heavy chain.

### Discussion

We did show that mSTAT3<sup>wt</sup>-ER fusion protein can be activated and mimic STAT3 signaling upon 4-HT stimulation. The mSTAT3<sup>wt</sup>-ER fusion protein can be tyrosine phosphorylated upon 4-HT, IL-6 or mLIF stimulation. This phosphorylation is concentration dependent in case of 4-HT (data not shown). Until up to 1h this signal does not increase or diminish. Despite tyrosine phosphorylation of the fusion protein by IL-6 or LIF no mSTAT3<sup>wt</sup>-ER DNA binding can be established upon cytokine stimulation, but only upon 4-HT stimulation. In a target gene induction assay we demonstrated that only 4-HT, but not IL-6 could induce c-Myc expression and not IL-6, in MEFs expressing mSTAT3<sup>wt</sup>-ER fusion protein. This might indicate that upon IL-6 stimulation

no stable fusion protein dimer and consequently DNA binding is established. Possible do the mSTAT3<sup>wt</sup>-ER fusion proteins dimerize as well upon cytokine stimulation, however lacking the 4-HT induced linking of the ER domains, are instable as dimer. We can not explain why Matsuda et al. can demonstrate LIF induced transcriptional activity of mSTAT3<sup>wt</sup>-ER, expressed in embryonic stem cells, in a luciferase assay and Northern blot analysis <sup>284</sup>. In addition, it was not understood why we observed S727 phosphorylation of mSTAT3<sup>wt</sup>-ER upon 4-HT, but not upon IL-6 stimulation. We were able though to induce serine727 phosphorylation on endogenous STAT3 in STAT1-deficient MEFs by IL-6, but not upon 4-HT stimulation. It is not known how 4-HT stimulation result in phosphorylation of either the tyrosine or serine residue. 4-HT binding to the modified LBD of the ER, induces phosphorylation of Y541 in this domain, although is not clear by which mechanism <sup>283</sup>. It might be that kinases responsible for this phosphorylation, are also able to phosphorylate tyrosine 705 and serine 727 of mSTAT3-ER. Therefore it might be that the serine phosphorylation in case of 4-HT stimulation is more a non-specific result than a regulated process.

On a first glance, one could conclude that the mSTAT3-ER fusion proteins are only functional with intact SH2 and phosphotyrosine domains, because the corresponding mutated forms are not active. However the presence of the additional mutations shown in Table 1 could also explain the non-functionality of these mutant mSTAT3-ER fusion proteins. We could, however exclude another potential reason for the activation defect of these fusion proteins, e.g. that the expression of these mutant proteins is toxic for cells. When the transfected cells were treated with LIF, STAT1 dimers were easily detectable by EMSA. Therefore, the receptor-kinase complex is fully functional. We also demonstrated that Jak1 can be phosphorylated upon IL-6 and LIF stimulation in these mutant fusion protein expressing MEFs, which implies a normal IL-6 and LIF induced signaling.

It is possible that some of the additional introduced mutations, as described in Table 1, interfere with STAT dimerization, phosphorylation and/or DNA binding, although they are not described in literature as such. Residues and/or regions described in literature to be important for STAT3 phosphorylation, dimerization, nuclear translocation or DNA binding (see introduction), are not impaired in these mutant fusion proteins, except for the ones intentionally introduced. An exception is the L207P mutation in mSTAT3<sup>Y705F</sup>-ER. Since it is in the second  $\alpha$  helix of the coiled-coil domain of mSTAT3, it could result in an inactive protein. Another proline mutation (L413P) in the DNA binding domain of mSTAT3<sup>R609K</sup>-ER could interfere with the DNA binding. The region of mSTAT3 aa 404-414 is described to be a nuclear export signaling element (NES) <sup>80</sup> and the point mutation of R414A did result in inhibition of DNA binding due to absence of nuclear translocation, although the STAT3 could be Y705 phosphorylated as normal <sup>42</sup>. In contrast, another point mutation in this region (L411A) did not have influence on nuclear translocation or DNA binding at all. Of course a lot of residues in the DNA binding domain interact with the DNA and although L413 is not described to be one of the essential residues in the process of DNA binding, the point mutation into a proline might lead to conformational change inhibiting other residues to bind DNA <sup>28</sup>. However this does not explain why the SH2 domain mutant could not be tyrosine phosphorylated. Jak1 was phosphorylated by IL-

---

6 stimulation, in MEFs expressing this mutant, so it might be that additional introduced mutations in the mSTAT3R609K-ER fusion protein, induce such a conformation of the protein that the tyrosine residue is not accessible anymore for kinases, induced by either IL-6 signaling or 4-HT.

Moreover we can not explain why the mSTAT3S727A-ER fusion protein could not be Y705 phosphorylated. No additional point mutation was discovered in the STAT sequence. A mSTAT3S727A mutant was reported to be Y705 phosphorylated and able to bind DNA<sup>85, 86, 292</sup>. Moreover it was shown to not have influence on DNA binding in both STAT1 and STAT3. It was suggested that the enhancement of transcription by the presence of the phosphorylated serine 727 residue occurs after DNA binding<sup>86</sup>.

New construction of the mutant fusion proteins or repair of these construct would be necessary to elucidate the mechanism behind the 4-HT-induced dimerization of mSTAT3-ER fusion proteins or/and the effect of the absence of serine phosphorylation.

## **mSTAT1-ER fusion proteins**

### *Cloning and mutagenesis procedures*

The mSTAT1<sub>wt</sub>-ER construct was cloned by the ligation of full length mSTAT1 cDNA with the modified ER LBD in a pcDNA3 vector, as described in the material and method section. Mutagenesis of pcDNA<sub>3</sub>mSTAT1<sub>wt</sub>-ER was performed according to the QuikChange™ XL Site-directed mutagenesis kit protocol as described in the materials and methods section, using the mutagenic primers designed forward and reverse complementary to opposite strands of pcDNA<sub>3</sub>mSTAT1<sub>wt</sub>-ER.

Because of the incompatibility of the selection marker in pcDNA3 with the STAT1Δ/Δ MEFs, mSTAT1-ER wild-type and mutant constructs were amplified by PCR from the pcDNA<sub>3</sub>mSTAT1-ER plasmids and transferred to the pEFzeo vector, which contains a Zeocin selection gene, designated pEFmSTAT1<sub>wt</sub>-ER, pEFmSTAT1R602K-ER, pEFmSTAT3Y701F-ER and pEFmSTAT1S727A-ER. These constructs were sequenced using forward and reverse primers at every 400 base pairs. In this way the sequencing results were confirmed by at least two primer readings. Sequencing results were compared to the NCBI GenBank. This revealed already many mutations in the STAT1 cDNA, which was used to clone mSTAT1-ER. In addition even more mutations have been introduced in the wild-type and mutant mSTAT1-ER fusion proteins compared to the original mSTAT1 cDNA, by the amplifying and mutagenesis procedures. These are summarized in Table 2.

**Table 2. Summary of sequence analysis of the mSTAT1 cDNA and mSTAT1-ER constructs.** Amino acid substitutions revealed by sequencing of the pEFmSTAT1-ER constructs. Confirmed aa mutations were summarized according to their location. Domains are labeled as in Figure 1. Presented in bold script are the intentionally introduced mutations, in grey the mutations already present in mSTAT1 cDNA and in normal script, the mutations introduced due to the amplifying and mutagenesis procedures.



	N	C-C	DNA	LD	SH2	P	T	ER LBD
mSTAT1		T261S	S345L, S354L, L356Y L357N, T358L, C362V, H363S, L404F	N567K, D568H	K592N			
mSTAT1wt-ER	T133I	T261S	S345L, S354L, L356Y L357N, T358L, C362V, H363S, L404F	L498P, N567K, D568H	K592N			<b>G1005R</b>
mSTAT1R602K-ER	T133I	K240R, T261S	S345L, S354L, L356Y L357N, T358L, C362V, H363S, L404F	L498P, N567K, D568H	A589T, K592N, <b>R602K</b>			M810T, <b>G1005R</b>
mSTAT1Y701F-ER	T133I	T261S	S345L, S354L, L356Y L357N, T358L, C362V, H363S, L404F	L498P, F506L, N567K, D568H	K592N	<b>Y701F</b>		<b>G1005R</b>
mSTAT1S727A-ER	S69G, T133I	T261S	S345L, S354L, L356Y L357N, T358L, C362V, H363S, L404F	L498P, N567K, D568H	K592N		<b>S727A</b>	<b>G1005R</b>

#### *Expression of pEFmSTAT1-ER constructs in STAT1-deficient MEFs*

The pEFmSTAT1-ER wild-type and mutant plasmids were introduced into STAT1 $\Delta/\Delta$  MEFs according to normal transfection procedures and stable transfectants were established. The expression level of the different pEFmSTAT1-ER wild type and mutant clones in STAT1-deficient MEFs is shown in Figure 6. The calculated size of mSTAT1-ER is 119.8 kDa. Clones with an expression level comparable to STAT1 expression in STAT3 $\Delta/\Delta$  MEFs were chosen to use in functional assays; i.e. nr.13 for mSTAT1wt-ER, nr.3 for mSTAT1R602K-ER, nr.5 for mSTAT1Y701F-ER and nr.32 for mSTAT1S727A-ER.

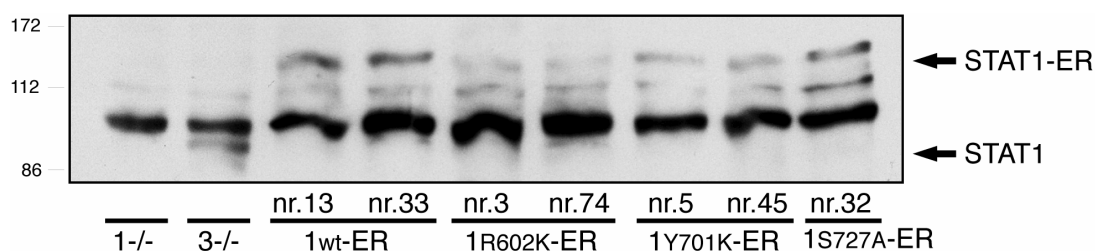


**Figure 6. Expression of the different pEFmSTAT1-ER clones in STAT1-deficient MEFs.** Expression levels were analyzed by Western blotting using a polyclonal antibody binding to the STAT1 C-terminal. Whole cell lysates were prepared from untreated MEFs either transfected or left untransfected. Arrows indicate the positions of the STAT1 and STAT1-ER proteins. Lanes are labeled as follows: 1-/- = untransfected STAT1 $\Delta/\Delta$  MEFs, 3-/- = untransfected STAT3 $\Delta/\Delta$  MEFs, 1wt-ER = STAT3  $\Delta/\Delta$  MEFs transfected with pEFmSTAT1wt-ER ect.

*mSTAT1<sup>wt</sup>-ER and mutant fusion proteins could not be activated*

In contrast to the results obtained with the mSTAT3<sup>wt</sup>-ER fusion protein, we could not activate the mSTAT1-ER wild-type by either 4-HT, mIFN $\alpha$  or mIFN $\gamma$ . As well the mutant mSTAT1-ER fusion proteins could not be activated upon stimulation. Also after longer periods of stimulation (up to 4 hours) and/or with higher concentrations of 4-HT (up to 10  $\mu$ M) tyrosine/serine phosphorylation and DNA binding of the fusion proteins could not be shown.

*Discussion*

The mSTAT1-ER constructs, even the wild-type, have been proven to be inactive, when expressed in STAT1-deficient MEFs. The sequence analysis data showed that already the mSTAT1 cDNA, received from Dr. Levy, did contain many additional mutations, when compared to the Genbank sequence. To exclude that the starting material was already infunfunctional due to the many mutations, we transiently transfected the pcDNA3-mSTAT1 plasmid, containing the full length mSTAT1 cDNA, in STAT1-deficient MEFs. Cells were stimulated with mIFN $\gamma$ , nuclear extracts were analyzed by EMSA and corresponding cytoplasmic extracts by Western blot. Figure 7 shows that transfected STAT1 is activated by mIFN $\gamma$  and can bind to DNA. The cytoplasmic extracts demonstrate the expression of mSTAT1 compared to non-transfected cells and STAT1 expressed by STAT3-deficient MEFs. Figure 7 summarizes results from two independent transfection experiments.

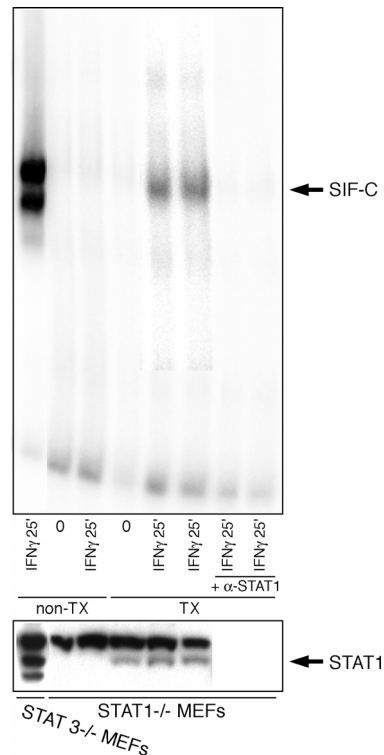


**Figure 7. Transient transfection of pcDNA3-mSTAT1 in STAT1  $\Delta/\Delta$  MEFs.** STAT1  $\Delta/\Delta$  MEFs were transfected (TX) with 2  $\mu$ g of plasmid DNA. After 24 hours the cells were either left untreated or stimulated for 25 min with 1000 U/ml mIFN $\gamma$ . Nuclear and cytoplasmic extracts were prepared and analyzed in respectively EMSA, using the M67 oligonucleotide and Western blotting using a polyclonal antibody against STAT1 (sc-346).

---

The position of SIF-C (i.e. STAT1:STAT1 homodimer) is indicated. Samples of IFN $\gamma$ -stimulated mSTAT1 could be shifted by either 1  $\mu$ l of polyclonal antibody against STAT1 (sc-592).

So the mutations in pcDNA3-mSTAT1 do not seem to interfere with the activation and DNA binding of the STAT1 protein. It is likely, that the infunctionality of the mSTAT1<sub>wt</sub>-ER fusion protein is caused by the T133I or L498P substitutions introduced during amplification of the mSTAT1 sequence by PCR, from the pcDNA3-mSTAT1 plasmid. Especially the L to P mutation could induce conformational changes (see discussion mSTAT3-ER) which might interfere with DNA binding. It might be that the combination of the mutations in the starting cDNA together with new mutations in the wild-type fusion protein results in conformational changes incompatible with STAT phosphorylation and DNA binding. Other possibility is the fusion of the modified ER LBD to the C-terminal of STAT1 is interfering with STAT activation. Second structure analyses of the mSTAT1<sub>wt</sub>-ER sequence did reveal a different structural organization in the region between phosphorylation domain and ER domain compared to the same region in the mSTAT3<sub>wt</sub>-ER fusion protein. However these predictions are difficult to interpret and moreover, a functional conditional active mSTAT1<sub>wt</sub>-ER fusion protein has been reported by Milocco et al. although they used an unmodified ligand binding domain of the ER <sup>287</sup>.

New mSTAT1-ER fusion proteins would have to be constructed to continue studies that could lead to the generation of a STAT1 gain-of-function model.

### **Acknowledgments**

We would like to thank Prof. Takashi Yokota for the pCAGGS-mSTAT3-ER and -mSTAT5a-rER constructs, Dr. Thomas Decker for the STAT1  $\Delta/\Delta$  MEFs and pEFzeo vector, Prof. Valeria Poli for the STAT3 $\Delta/\Delta$  MEFs, Dr. David Levy for the mSTAT1 cDNA and Philipp Ernst for helpful technical discussions. Sabina Hernandez Penna contributed to the generation of the sequence data.



**Generation of *in vivo* conditional gain-of-function models to study the role of STAT3 and STAT5a signaling in liver**

Simone T.D. Stutvoet,\* Emilio Casanova,<sup>†</sup> Sabina Hernandez Penna,\* and Markus H. Heim\*

\*Department of Research, University Hospital Basel, CH-4031 Basel, Switzerland

<sup>†</sup>Institute of Physiology, University of Basel, CH-4056 Basel, Switzerland

---

## Abstract

To obtain conditional and liver-specific gain-of-function models for STAT3 and STAT5a signaling, we generated transgenic mice that express the mSTAT3<sub>wt</sub>-ER and mSTAT5aR618K-rER fusion proteins under control of the liver-specific albumin promoter. In order to circumvent interference with the genomic organization of the mouse albumin gene, and acquire stable transgene expression patterns, the mSTAT3<sub>wt</sub>-ER and mSTAT5aR618K-rER coding sequences were inserted in the first exon of the albumin gene. Here, we describe the multistep cloning approach, involving site-specific homologous recombination with a P1-derived artificial chromosome (PAC), to prepare the fusion protein constructs for mouse oocyte injection. The PAC contained 185 kb of mouse chromosome 5 including the entire albumin gene.

The transgene animals, designated *albm*STAT3<sub>wt</sub>-ER and *albm*STAT5aR618K-rER, appeared to be healthy and show a normal phenotype. Several transgenic founders have been identified, as well as a transgenic F1 off spring. Presently the transgenic mice are being characterized and transgenic lines are being established. In the future we plan to use these transgenic mice to investigate involvement of STAT3 and STAT5a signaling in liver pathogenesis and repair.

## Introduction

We generated conditional gain-of-function mouse models to analyze the role of STAT3 and STAT5a signaling in liver. To obtain inducible activated STAT3 and STAT5a proteins, a wild-type fusion protein has been used between full length mSTAT3 and the modified ligand binding domain (LBD) of the estrogen receptor (ER) (i.e. mSTAT3<sup>wt</sup>-ER), and a SH2 domain mutant fusion protein of full length mSTAT5a and the modified LBD of the ER (i.e. mSTAT5aR618K-rER), to be expressed in mice. Activity of the fusion proteins can be regulated by administration of the synthetic steroid 4-Hydroxytamoxifen (4-HT), a metabolite of tamoxifen. The effects and pharmacology of 4-Hydroxytamoxifen have been well characterized through its use in animal and human trials and its not likely that its inhibiting effects on breast cell <sup>293</sup> and endometrium proliferation, lipid peroxidation <sup>294</sup> and formation of tumor promoted-induced hydrogen peroxide in human neutrophils <sup>295</sup>, will influence the experiments in the liver, especially because the concentration used in the described experiments is much lower then the concentrations required to give rise to 4-HT's other biological effects <sup>282</sup>.

Until now the only transgenic mouse expressing ubiquitously a fusion protein between a STAT protein and the ER LBD has been generated by Matsuda et al.. However, for unknown reasons, activation of their mSTAT3-ER fusion protein in an adult animal has not yet been shown <sup>284, 285</sup>. There are several other transgenic mice that expressing fusions of other proteins than STATs with the modified LBD of the ER. In these mice, the fusion proteins could be activated *in vivo* by 4-HT at doses that had no apparent toxicity. In a transgenic mouse expressing a Myc-ER fusion protein under control of the CD2 locus control region, Myc dimerization could be induced in thymocytes by 4-HT administration, causing myc mediate proliferation of thymocytes <sup>296</sup>. Another mouse, expressing a fusion protein between Cre and the ER (Cre-ER), allowed 4-HT inducible Cre-mediated recombination in diverse tissues of the mouse at embryonic and adult stages <sup>297</sup>. Leone et al. generated functional tamoxifen-inducible glia-specific Cre mice <sup>298</sup>.

To allow liver-specific expressing, the mSTAT3/5a-ER fusion proteins were expressed in mice under a liver specific promoter. Expression systems that have been used in the past to generate liver-specific expression *in vivo* include cosmids containing the human  $\alpha$ 1-antitrypsin gene <sup>220, 299, 300</sup>, expression vectors containing transthyretin (TTR) regulatory sequences and part of the coding sequence as well as additional poly A sequences <sup>301</sup> and expression vectors containing albumin enhancer/promoter fragments <sup>302, 303</sup> or albumin enhancer/promoter fragments in combination with alpha-fetoprotein enhancers <sup>304</sup>. The disadvantage of most of these approaches is that due to the disrupted genomic organisation/unnatural configuration of the albumin promoter, the transgene expression pattern can be highly variable <sup>305</sup>.

To circumvent this problem, we chose to embed the transgene in the first exon of the albumin 1 gene. Serum albumin is accounting for more then 10% of total protein synthesis by the liver <sup>306</sup>. The albumin gene is located upstream from the alpha-fetoprotein (AFP) gene and its expression is controlled by the AFP enhancers located between both genes as well as by other distant enhancer located 10 kb upstream of the albumin promoter <sup>307, 308</sup>. Extensive studies of

---

this region have suggested that interactions between enhancer and enhancer, as well as between promoter and enhancer are part of this regions organization. An important part of these interactions is mediate through the nuclear factor Y site in the albumin promoter <sup>309</sup>. So the genomic organization of the albumin-AFP locus is very complex. Therefore we decided to use an approach in which we cloned a continuous DNA stretch of approximately 185 kb from mouse chromosome 5, harbouring the entire albumin 1 gene, AFP gene, afamin gene, a gene coding a protein showing similarities to a hypothetical zink finger protein and a gene coding a protein showing similarities to AFP. This will allow us to express the transgenes in a natural context of native promoters, enhancers and introns that can affect expression and regulation. We used a P1 derived artificial chromosome (PAC), which is a cloning vector that can carry large inserts.

PACs are vectors that combine the features of two other vectors that can carry large DNA inserts, i.e. the bacteriophage P1 system and the F-factor based bacterial artificial chromosomes (BACs). The bacteriophage P1 system makes use of a vector which contains a P1 packaging site to package vector and cloned DNA into phage particles, two P1 loxP recombination sites to cyclize the packaged DNA once it has been injected into *E.coli* containing the P1 Cre recombinase, as well as a selection gene and a P1 plasmid replicon. It can hold DNA fragments up to only 100 kb and the use of a two-step in vitro bacteriophage T4 packaging reaction makes it more difficult to work with <sup>310, 311</sup>. BACs are bacterial artificial chromosomes, derived from the F-factor plasmid, a natural occurring plasmid of *E.coli*. The F plasmid in *E.coli* carries genes that give rise to male *E.coli*, its replication is strictly controlled and is maintained in low copy numbers. The F-factor not only codes for genes that are essential to regulate its own replication but also its copy number. The regulatory genes include *oriS*, *repE*, *paraA* and *parB*. The *oriS* and *repE* genes mediate the unidirectional replication of the F-factor while *paraA* and *parB* maintain copy number at a level of one or two per *E.coli* genome. The BAC incorporates these genes as well as a resistancy selection marker and a cloning segment. The BACs are introduced in bacteria by electroporation and exist as supercoiled circular plasmids in bacteria, which permit easy isolation <sup>312</sup>. BACs allow cloning of DNA fragments up to 350 kb (average insert 120kb), while PACs inserts are typical between 130 and 200 kb.

PAC vectors are derived from the bacteriophage P1, but can like BACs, be introduced to bacteria using electroporation. Like the bacteriophage P1, PACs are maintained in low copy number (one or two per cell) because of the integrated P1 phage based replicon, thus reducing the potential for at random recombination between DNA fragments carried by the plasmids <sup>313</sup>.

For the functional studies we have planned, it was necessary to insert the mSTAT3<sub>wt</sub>-ER and mSTAT5aR618K-rER transgenes in the albumin gene precisely at the desired site, i.e. in frame with the ATG of the albumin gene. Conventional cloning methods that rely on the occurrence of suitable restriction sites are impractical for this purpose because of the size of the PAC plus inserted mouse chromosomal DNA <sup>314, 315</sup>. Therefore, the transgenes were inserted in the albumin gene with a strategy allowing site specific or homologous recombination in *E.coli*. Homologous recombination allows exchange of genetic information between two DNA molecules in a precise,



specific and faithful manner. It occurs through homology regions, which are stretches of DNA shared by the two molecules that recombine genes<sup>316, 317</sup>. In our approach, albumin homologous arms of 150-200 bp were cloned to flank the target constructs. The used recombination strategy is mediated through the recombination genes *exo*, *beta* and *gam* from the defective  $\lambda$  prophage in *E.coli*<sup>318</sup>. The recombination genes are under the control of a temperature-sensitive  $\lambda$  repressor, which can be switched off at 42 °C and is switched on at 32 °C. When the recombination genes are switched on (at 42 °C) the cells become more recombinogenic and take up linear DNA without destruction. *Gam* inhibits the *E.coli* RecBCD exonuclease from attacking linear DNA, and *exo* and *beta* generate recombination activity for the in the cells introduced DNA<sup>318</sup>. The prophage system modified for the use in BAC/PAC recombinogenic engineering was developed by Lee et al. The system was transferred to DH10B *E.coli* cells, a BAC host strain, generating the strain EL250 among others<sup>319</sup>.

This system has several advantages over earlier published recET cloning system, in which *red $\alpha$* , *red $\beta$*  (=recombinases) and *gam* genes are expressed under an arabinose dependent promoter<sup>316</sup>. Most important, plasmid expression systems can be leaky. Uncontrolled presence of *gam* causes a RecBCD exonuclease defect, resulting in plasmid instability and loss of cell viability. *Gam* and *reds* can also cause BAC/PAC instability<sup>319</sup>.

Homologous recombination in this strategy is performed with the linearized target gene constructs flanked by homology arms, including as well a selectable marker gene (AmpR gene) in between site specific recombination target sites (FRT sites). Selection is necessary to identify the cells that carry the recombinant, because homologous recombination is a rare event. After recombination and selection, the recombined construct is exposed to EL250 integrated arabinose dependent expressed Flpe recombinases which delete the selectable cassette at the FRT sites, leaving behind a single FRT<sup>314, 316, 317 319</sup>.

We describe here the method that enabled us to generate two transgenic mice, *albmSTAT3<sup>wt</sup>-ER* and *albmSTAT5aR618K-rER*.

---

## Methods and Materials

### Cloning of the fusion protein constructs suited for homologous recombination

mSTAT3<sub>wt</sub>-ER and mSTAT5aR618K-rER constructs were cloned between flanking albumin homologous regions (albHR) to allow site specific recombination with the first exon of the albumin gene. The 5' albHR is an approximately 200 bp long sequence derived from the 3' end of the albumin promoter up to the ATG. The 5' albHR sequence correspond to nt 14478427 – 14478584 of C57Bl6 mouse chromosome 5 (NCBI MGI:87991 /NT:039307.1) The 3' albHR is an approximately 150 bp long sequence derived from first coding albumin exon plus connected intron and correspond to nt 14478603 – 14478751 of C57Bl6 mouse chromosome 5 (NCBI MGI:87991 /NT:039307.1).

#### *I. Cloning of mSTAT3<sub>wt</sub>-ER construct to allow homologous recombination*

A schematic overview of the cloning procedure for mSTAT3<sub>wt</sub>-ER is depicted in Figure 1. The 5' albHR was fused in front of the mSTAT3<sub>wt</sub>-ER sequence by 3 overlapping PCR reactions in order to replace the ATG of the albumin gene for the ATG of mSTAT3<sub>wt</sub>-ER.

**1)** The 5' albHR was amplified and at the 3' end elongated with 24bp of 5' end mSTAT3<sub>wt</sub>-ER sequence by PCR using as template p5' albHR (gift from Dr. Emilio Casanova, DKFZ, Heidelberg, Germany) and forwardEcoRV-NheI introducing **(primer 3A)** (5'-TTTTTTCGATATCCAAAGATGCTAGCATTTT GTAATGGGGTAGG-3'; EcoRV and NheI sites underlined) and reverse mSTAT3<sub>wt</sub>-ER overlapping **(primer 3B)** (5'-CTGCAGCTGGTTCCA CTGAGCCATTTTGCCAGAGGCTAGTGGGGT-3'; ATG boldface, STAT3<sub>wt</sub>-ER sequence underlined) primers.

**2)** A 5' mSTAT3<sub>wt</sub>-ER fragment of 986 bp up to a SphI restriction site was amplified and at the 5' end elongated with 21 bp of 3' end 5' albHR sequence by PCR using as template pCAGGS-mSTAT3<sub>wt</sub>-ER<sup>284</sup> and forward 5' albHR overlapping **(primer 3C)** (5'-ACCCCACTAGCCTCTGGCAAATGGCTCAGT GGAACCAGCTGCAG-3'; ATG boldface, 5' HRalbumin sequence underlined) and reverse SphI including **(primer 3D)** (5'-GGGCCGGTCCGGGTGCATG GGCATGCAGGGCTGCCGCTCCACC-3'; SphI site underlined) primers.

**3)** The products of these two reactions were mixed to serve as template, from which an overlapping 5' albHR-mSTAT3<sub>wt</sub>-ER-SphI product was amplified by PCR using forward primer 3A and reverse primer 3D.

The overlapping 5' albHR-mSTAT3<sub>wt</sub>-ER-SphI PCR product was digested EcoRV-SphI and ligated SphI-EcoRV in pSL1180 (Pharmacia, Amersham Biosciences Europe, CH), generating pSL5' albHR-mSTAT3<sub>wt</sub>-ER-SphI.

The remaining part of mSTAT3<sub>wt</sub>-ER was digested SphI-SacI from pCAGGS-mSTAT3-ER and ligated SacI-SphI in frame with the 5' albHR-mSTAT3<sub>wt</sub>-ER-SphI fragment in pSL5' albHR-mSTAT3<sub>wt</sub>-ER-SphI, generating pSL5' albHR-mSTAT3<sub>wt</sub>-ER. Thus, the 5' albHR-mSTAT3<sub>wt</sub>-ER sequence is inserted reverse and complement in pSL1180.

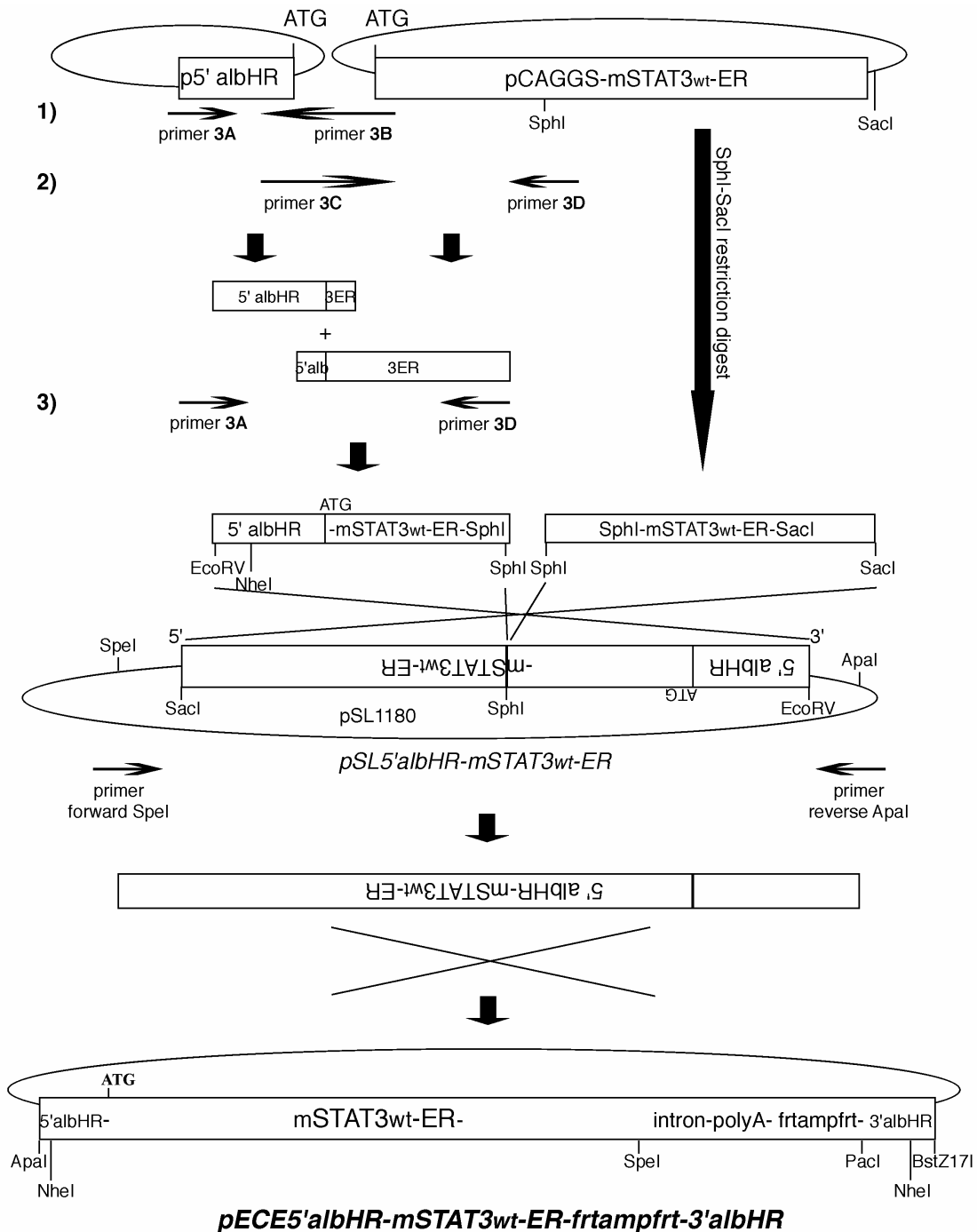


**Figure 1. Schematic overview of the cloning procedure for mSTAT3wt-ER.** Overlapping PCR (reaction 1-3 indicated in boldface script in the text) was performed using pCAGGS-mSTAT3wt-ER and p5'albHR as templates, and primers 3A-3D designed specific for mSTAT3wt-ER as described in boldface script in the text. The cloning procedure of the constructs into pSL1180 and into the pECE plasmid is described in the text.

The 5'albHR-mSTAT3wt-ER construct was amplified from *pSL5'albHR-mSTAT3wt-ER* using forwardSpeI (5'-ACGGCCCACGTGGCCACTAGTACTTCTCGAG-3'; SpeI site underlined) and reverseApaI (5'-TGAGGTAATTATAA CCGGGCCCTATATATGG-3'; ApaI site underlined) including primers. SpeI

---

and ApaI restriction sites were present upstream and downstream, respectively, of the construct inserted in pSL1180. This PCR product was digested and ligated ApaI-SpeI in the plasmid called: pECE-intron-polyA-frtampfrtnoIres, generating *pECE5'albHR-mSTAT3wt-ER-frtampfrt*. The 3' albHR sequence was excised PacI-BstZ17I from pGFP3' albHR (gift from Dr. E. Casanova) and ligated in *pECE5'albHR-mSTAT3wt-ER-frtampfrt*, creating *pECE5'albHR-mSTAT3wt-ER-frtampfrt-3' albHR*.

## II. Cloning of mSTAT5aR618K-rER construct to allow homologous recombination

A schematic overview of the cloning procedure for mSTAT5aR618K-rER is depicted in Figure 2. The 5' albHR was fused in front of the mSTAT5aR618K-rER sequence by 3 overlapping PCR reactions in order to replace the ATG of the albumin gene for the ATG of mSTAT5aR618K-rER.

**1)** The 5' albHR was amplified and at the 3' end elongated with 24bp of 5' end mSTAT5aR618K-rER sequence by PCR using as template p5' albHR and forwardApaI-NheI introducing (**primer 5A**) (5'-TTTTTTGGGCCCGCAAAGATGCTAGCATTGTAATGGGGTAGG-3'; ApaI and NheI sites underlined) and reverse mSTAT5aR618K-rER overlapping (**primer 5B**) (5'-CTGGGCTGAATCCAGCCCGCCATTTTGCCAGAGGCTAGTGGGGT-3'; ATG boldface, mSTAT5aR618K-rER sequence underlined) primers.

**2)** A 5' mSTAT5aR618K-rER fragment of 545 bp up to a BamHI restriction site was amplified and at the 5' end elongated with 21 bp of 3' end 5' albHR sequence by PCR using as template pCAGGS-mSTAT5aR618K-rER (construction is described in materials and method section of Chapter 4) and forward 5' albHR overlapping (**primer 5C**) (5'-ACCCACTAGCCTCTGGCAAATGGCGGGCTGGATTGAGCCAG-3'; ATG boldface, 5' albHR sequence underlined) and reverse BamHI including (**primer 5D**) (5'-GGGCAACTGAGCTTGGATCCGCAGGCTCTCTGGT-3'; BamHI site underlined) primers.

**3)** The products of these two reactions were mixed to serve as template, from which overlapping 5' albHR-mSTAT5aR618K-rER-BamHI product was amplified by PCR using forward primer 5A and reverse primer 5D.

The overlapping 5' albHR-mSTAT5aR618K-rER-BamHI PCR product was digested and ligated ApaI-BamHI in pECE-intron-polyA-frtampfrtnoIres.

The remaining part of mSTAT5aR618K-rER was amplified from its plasmid pCAGGS using forward BamHI including (5'-ACCAGGAGAGCCTGCGGATCCAAGCTCAGTTTGCCC-3', BamHI site underlined) and reverse SpeI introducing (5'-AGGGATTTCGAGAACTAGTGGGGAGCCTGGGAGT-3', SpeI site underlined) primers. The PCR product was digested and cloned BamHI-SpeI downstream of 5' albHR-mSTAT5aR618K-rER-BamHI in pECE-intron-polyA-frtampfrtnoIres, generating *pECE5'albHR-mSTAT5aR618K-rER-frtampfrt*.

The 3' albHR sequence was excised PacI-BstZ17I from pGFP3' albHR and ligated in *pECE5'albHR-mSTAT5aR618K-rER-frtampfrt*, creating *pECE5'albHR-mSTAT5aR618K-rER-frtampfrt-3' albHR*.

All sequences were confirmed using the DYEnamic Direct Cycle Sequencing system (Amersham Biosciences) or a ABI Prism™ DNA 3730 sequencer (Perkin Elmer, MA, USA).

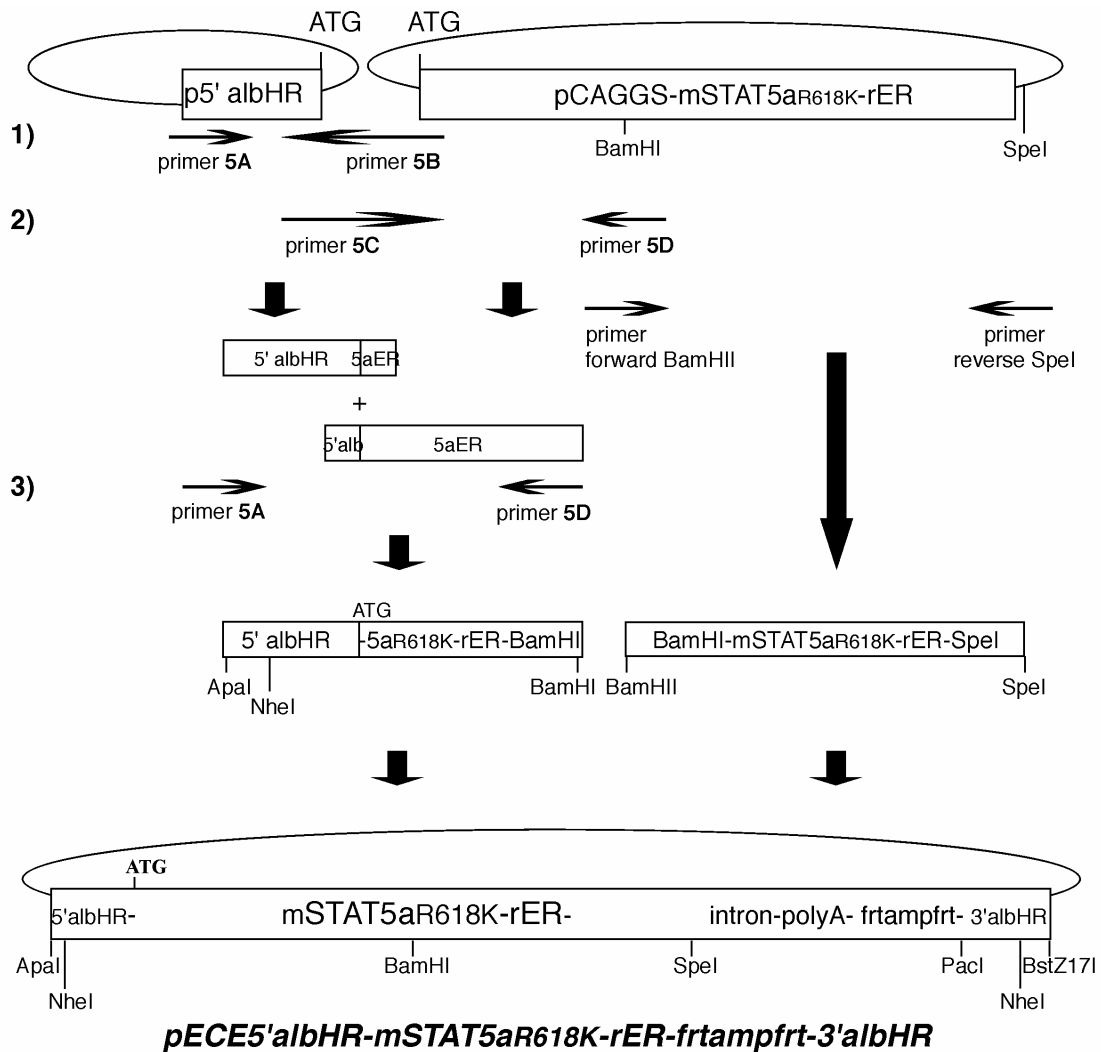


**Figure 2. Schematic overview of the cloning procedure for mSTAT5aR618K-rER.** Overlapping PCR (reaction 1-3 indicated in boldface script in the text) was performed using pCAGGS-mSTAT5aR618K-rER and p5'albHR as templates, and primers 5A-5D designed specific for mSTAT5aR618K-rER as described in boldface script in the text. The cloning procedure of the constructs into the pECE plasmid is described in the text.

### Homologous recombination procedure

An on scale overview of the integration of the 5'albHR-mSTAT-ER-3'albHR constructs into the first exon of the albumin gene is depicted in Figure 3.

A PAC (designated pPAC4, kanamycin resistant) harbouring 185 kb of the mouse chromosome 5 including the albumin gene (pPAC4-albumin), was isolated from the RPCI-21 mouse genomic library (RZPD library nr. 711, Germany. MM strain 129/SvevTACfBr<sup>320</sup>). pPAC4-albumin was grown in DH10B bacterial cells, extracted and electroporated into EL250 (genotype DH10B [ $\lambda$ cl857 (*cro-bioA*) substituted with *araC-P<sub>BAD</sub>flpe*]<sup>319</sup> *E.coli*, which contain the machinery to allow homologous recombination.

The pECE5'albHR-mSTAT3<sup>wt</sup>-ER-frtampfrrt-3'albHR and pECE5'albHR-mSTAT5aR618K-rER-frtampfrrt-3'albHR constructs were excised from their

---

plasmids at the NheI restriction sites, which were introduced at the 5' albHR and present at the 3' end of the 3' albHR.

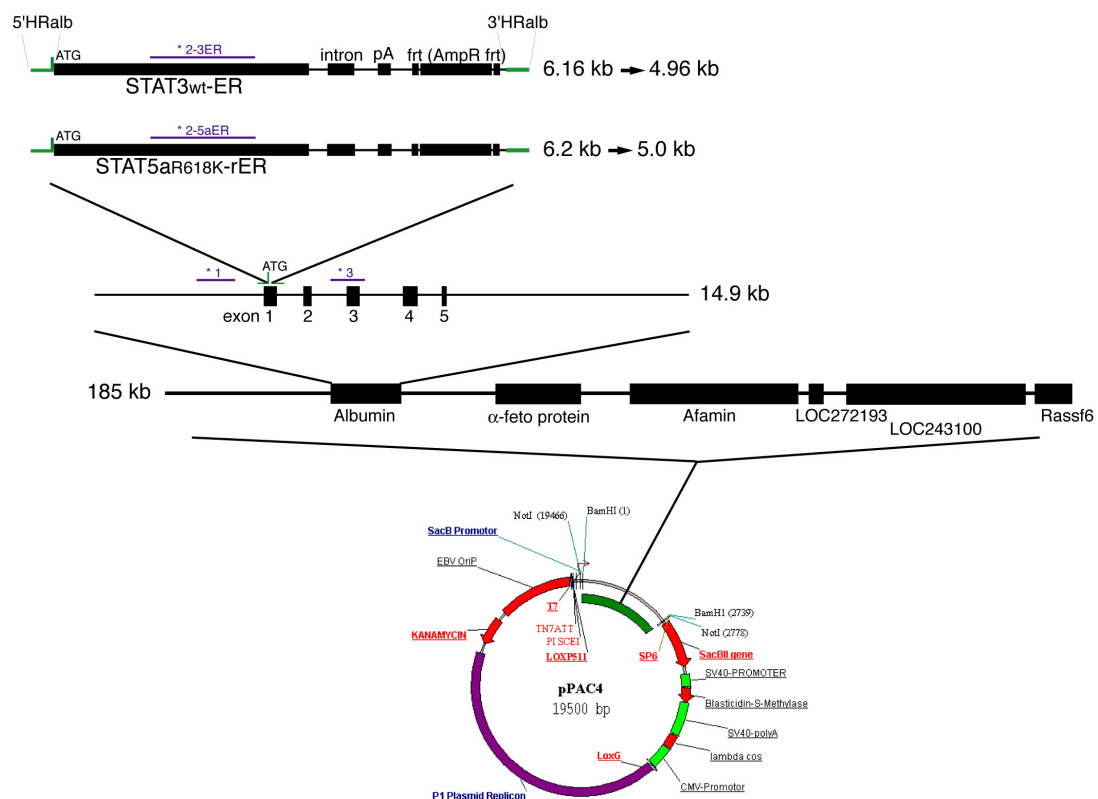
A 50 ml culture of EL250 pPAC4-albumin containing *E.coli* was grown at 32 °C until OD<sub>600</sub>=0.5-0.7. The culture was divided in 5 portions of 10 ml and grown at 42 °C for 15 min to induce the recombination machinery, i.e. induce *exo*, *beta* and *gam* expression. Each 10 ml culture of induced bacteria was centrifuged at 7000 rpm for 8 min at 1°C. The pellet was resuspended in 1 ml of ice cold water and transferred to an eppendorf tube. Subsequently the cells were washed three times in 1 ml of ice-cold water (2 min 7000 rpm 1 °C). The final pellet was resuspended in 100 µl of ice-cold water. 50µl of these electrocompetent prepared EL250 pPAC4-albumin containing *E.coli*, were electroporated with 150 or 300 ng of linearized construct. Electroporation was performed with a Biorad Gene Pulser at 1.8 kV and 25 µF. The cells were grown for an additional 2 hours at 32 °C, collected and plated. Recombinant pPAC4-albumin-mSTAT3<sub>wt</sub>-ER-*frtamp*-*frt* or pPAC4-albumin-mSTAT5aR618K-rER-*frtamp*-*frt* colonies were identified by double selection for ampicillin (50 µg/ml) and kanamycin (25 µg/ml). Positive colonies were identified by restriction site analysis /pulsed-field gel electrophoresis (PFGE) (CHEF DR-II system, BioRad Laboratories) and Southern blot. For the Southern blot analysis, probes were generated by PCR, designed to hybridize to the albumin promoter region (probe 1), to the mSTAT3<sub>wt</sub>-ER (probe 2-3ER) or mSTAT5aR618K-ER (probe 2-5aER) sequence or to a region containing part of intron 2, exon3 and intron 3 of the albumin gene (probes are indicated in purple in Figure 3). Probes were labeled by random-priming with α-<sup>32</sup>PdCTP. Restriction enzymes were purchased from either Promega, Catalys AG, CH or New England Biolabs, Bioconcept, CH.

To remove the ampicillin cassette, overnight recombinant cultures from single kan/amp<sup>R</sup> colonies were diluted 50-fold and grown at 32 °C till OD<sub>600</sub>=0.5. Transiently expression of Flpe recombinase from the EL250 *E.coli* was induced by incubating the cultures with 0.1% final concentration of L(+) arabinose for 1 h. Induced cultures were 10-fold, grown for another hour at 32 °C, collected and plated. Colonies growing with kanamycin but not with ampicillin, were selected, these bacteria contain pPAC4-albumin-mSTAT3<sub>wt</sub>-ER-*frt* or pPAC4-albumin-mSTAT5aR618K-rER-*frt* recombinants. The isolation of the correct ampicillin lacking recombinants was confirmed by restriction digest and by PCR.

**Figure 3. Integration of 5' albHR-mSTAT3<sub>wt</sub>-ER-3' albHR and 5' albHR-mSTAT5aR618K-rER-3' albHR transgenes, by site specific recombination into exon 1 of the albumin gene, present in the pPAC4.** Scheme of the DNA constructs used for transgenesis. Total length of the recombined pPAC4 inserts is 190 kb. The recombined pPAC4-albumin has approximately 34kb of genomic sequence upstream of the ATG and 156 kb of downstream sequence, included the mSTAT-ER fusion protein. The relative position of other genes present in the PAC, exons 1-5 of the albumin gene and Southern blot probes (\* 1, 2, 3) are presented on scale.

Location of the Southern blot probes are indicated in purple. The probe 1 (0.99 kb) hybridizes to a fragment of the albumin promoter, probe 3 (0.9 kb) to intron2-exon3-intron3 of the albumin gene. Probe 2-3ER (1.4 kb) hybridizes to a fragment including the c-terminal of STAT3 to the half-way down the ER domain in the mSTAT3<sub>wt</sub>-ER, Probe 2-5aER (1.47 kb)

hybridizes to a fragment including the c-terminal of STAT5a to the half-way down the ER domain in the mSTAT5aR618K-rER.



### Generation of the *albmSTAT-ER* mice

The pPAC4-albumin-mSTAT-ERfrt recombinants were isolated from EL250 *E. coli* by standard alkaline/SDS lysis procedure. Due to the fact that PACs replicate at low copy number in *E. coli* (one or two copies), the yield of DNA is limited and therefore large culture volumes are required to obtain sufficient PAC DNA (200ml  $\cong$  2 ng/ $\mu$ l DNA). Prior to lysis, the cells were once washed with 0.5 M NaCl to remove polysaccharides. The PAC DNA is not purified over columns, since this reduced the yield enormously. The DNA is filtered from the bacterial cell debris and precipitated with isopropanol. The DNA pellet was washed several times with 70% ethanol to remove salts and dissolved in 200  $\mu$ l 5mM Tris. 40  $\mu$ l of the prep DNA was digested overnight in a total volume of 100  $\mu$ l with 100 U of NotI at 37  $^{\circ}$ C, to release the inserts of 190 kb (185 kb chromosome 5 + 5 kb fusion protein sequence) from the 16.7 kb pPAC4. The digested fractions of the modified pPAC4-albumin separated through a 5 ml Sepharose 4B-CL (Pharmacia) column (methods according to <sup>321</sup>) in microinjection buffer (5 mM Tris pH 7.5, 0.1 mM EDTA pH 8.0, 100mM NaCl). Fractions of 0.5 ml were collected, from which 20  $\mu$ l was analyzed by PFGE. A typical PFGE gel showing the fractionated DNA in the collected fractions is shown in Figure 4.

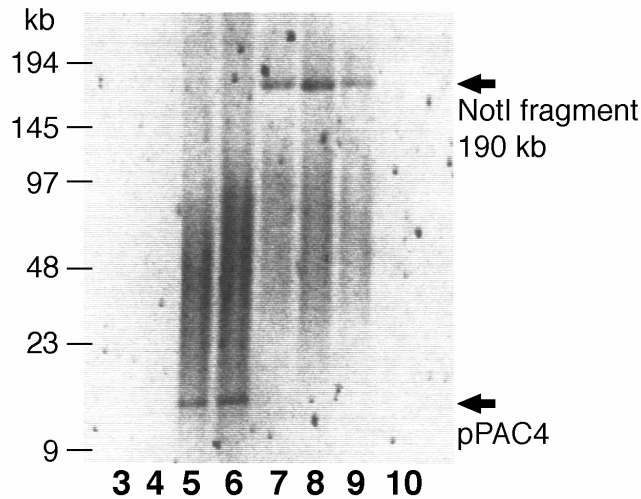


**Figure 4. NotI digested pPAC4-albumin-mSTAT-ERfrt fractions.** pPAC4-albumin-mSTAT-ERfrt recombinants were digested with NotI, applied to a Sepharose 4B-CL column and 0.5 ml fractions were collected. Fractions 3 to 10 were analyzed by PFGE. The fractions 7-9 contain the 190 kb pPAC4 recombinant insert and are devoid of vector, which is present in fraction 5 and 6.

Fractions containing the approx. 190 kb fragment were selected, and concentrated to 10ng/ $\mu$ l and purified in ultra clean microinjection buffer through Microcons<sup>®</sup> (YM-100, Amicon, Millipore AG, Switzerland). The DNA was throughout the whole procedure neither exposed to phenol, ethidium bromide or UV light, nor was it frozen, as well as it handled with extreme care to avoid shearing of the linearized constructs, or induce toxicity to the oocytes or unintentional mutagenesis in the mouse.

The linearized 190 kb inserts were microinjected at a concentration of 3  $\mu$ g/ml into the pronucleus of approx. 300 fertilized oocytes/per construct of B6D2/F1Crl mice, isolated from crosses between C57Bl6 females and DBA2 males using standard methods<sup>322</sup>. Approximately 86% of the oocytes survived the injection and were reimplanted in pseudopregnant mice. Microinjection was performed at the Transgene laboratory of the Zentrum für Molekulare Biologie of the University of Heidelberg (ZMBH), Germany. Mice were bred in a specific pathogen free environment under standard conditions.

### Genotyping of the transgenic offspring

DNA was prepared from mouse tail by overnight lysis at 56 °C in 200  $\mu$ l of tail buffer (10 mM EDTA pH8, 100 mM Tris pH8, 100 mM NaCl, 0.2% SDS and 0.25 mg/ml proteinase K). The next day the proteinase K was inactivated for 30 min at 70 °C and 700  $\mu$ l of autoclaved water was added. From this solution was 1  $\mu$ l used to identify the presence of the transgene by PCR. A mixture of three primers was used to obtain product amplified from the endogenous albumin gene, to serve as internal control and in case of a transgenic animal, a product amplified from the transgene. Primer1forward; 5'-TGCTCTGGCTTCTTCTCAGTTCAC-3', primer2reverse; 5'-ACTCTTACGTGCTTCTCGGCG-3',



mSTAT3<sub>wt</sub>-ER specific primer reverse; 5'-CTCCACCACCTTCATTTTC-3', and mSTAT5aR618K-rER specific primer reverse; 5'-GGGCAAAGCTGAGCTTGGATCCGCAGGCTCTCCTGGT-3'. The PCR strategy is schematically depicted in figure 8A.

## Results

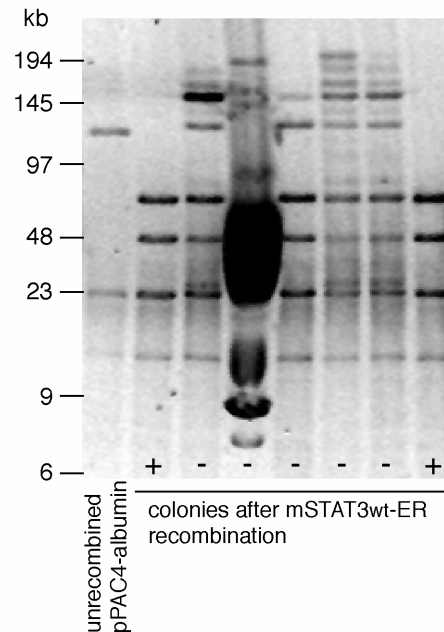
The pCAGGS-mSTAT3<sub>wt</sub>-ER and pCAGGS-mSTAT5a<sub>wt</sub>-rER plasmids, as described in Chapter 4 were used for the cloning of two transgenic mice expressing mSTAT3<sub>wt</sub>-ER or mSTAT5aR618K-rER fusion proteins under the control of the liver specific albumin promoter in a natural genomic configuration.

### ***alb*mSTAT3<sub>wt</sub>-ER mice**

A part of mSTAT3<sub>wt</sub>-ER construct was amplified from pCAGGS-mSTAT3<sub>wt</sub>-ER plasmid and fused to the 5' albHR by overlapping PCR. Together with the remaining part of the mSTAT3<sub>wt</sub>-ER sequence, the 5' albHR-mSTAT3<sub>wt</sub>-ER fragment was inserted into pSL1180. The 5' albHR-mSTAT3<sub>wt</sub>-ER fragment was subcloned in pSL1180 due to lack of suitable restriction sites in the pECE-intron-polyA-frtampfrtnoIres plasmid containing other expression enhancing elements and a selection (ampicillin) marker gene flanked by FRT sites. The extra intron and polyA were included to be assured of a stable mRNA product. Suitable restriction sites present in the multiple cloning site upstream and downstream of the inserted 5' albHR-mSTAT3<sub>wt</sub>-ER fragment, were used to excise and ligate the fragment into the pECE-intron-polyA-frtampfrtnoIres plasmid. The 3' albHR was excised from its vector and ligated downstream of the frtampfrt in pECE5' albHR-mSTAT3<sub>wt</sub>-ER-frtampfrt, creating *pECE5' albHR-mSTAT3<sub>wt</sub>-ER-frtampfrt-3' albHR*.

The fusion protein-intron-polyA-frtampfr construct flanked by the albHRs was excised from its plasmid and electroporated into EL250 containing the pPAC4-albumin E.coli, induced to allow homologous recombination of the construct at the ATG into the first exon of the albumin gene. Colonies were analysed for the desired recombination event and the orientation of the modified pPAC4-albumin by restriction enzyme analysis (NotI, SalI, EagI, and RsrII) and by Southern blot analysis. Restriction patterns were compared with unrecombined pPAC4-albumin by PFGE. An example is shown in Figure 5. Seven out of 18 analyzed colonies gave the expected pattern of recombination.

**Figure 5. Representative PFGE gel results of Sall digested PAC DNA from colonies obtained after homologous recombination of fusion protein-intron-polyA-frtampfr into pPAC4-albumin.** Lanes marked with (+) represent recombinant colonies, showing two Sall fragments of 88 and 51 kb instead of the one of 139 kb shown for the unrecombined pPAC4-albumin.



For the Southern blot analysis, recombinants for pPAC4-albumin-mSTAT3wt-ER-frtampfrt were digested with BamHI and hybridized to probe1, 2-3ER or 3 (probes are indicated in Figure 3). An example is shown in Figure 6.

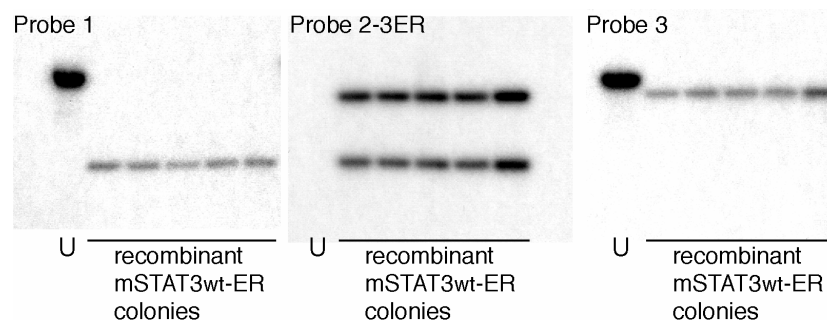
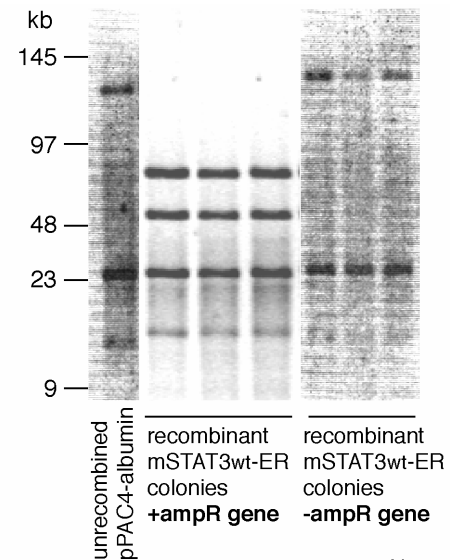


**Figure 6. Southern blot analysis of BamHI digested modified pPAC4-albumin.** BamHI cuts upstream from the probe 1 hybridization site (see Figure 3), in the probe 2-3ER hybridization site (so in the fusion protein sequence) and downstream of the hybridization site of probe 3. This results in the binding of probe 1 to a 17.2 kb fragment in the unrecombined pPAC4-albumin (U in the figure) and a fragment of 7.9 kb in the recombinant pPAC4-albumin. Probe 2-3ER can not bind the unrecombined, but binds two fragments of 7.9 and 15.1 kb obtained from recombinant colonies. Probe 3 binds a fragment of 17.2 kb (unrecombined) or 15.1 kb (recombinant DNA).

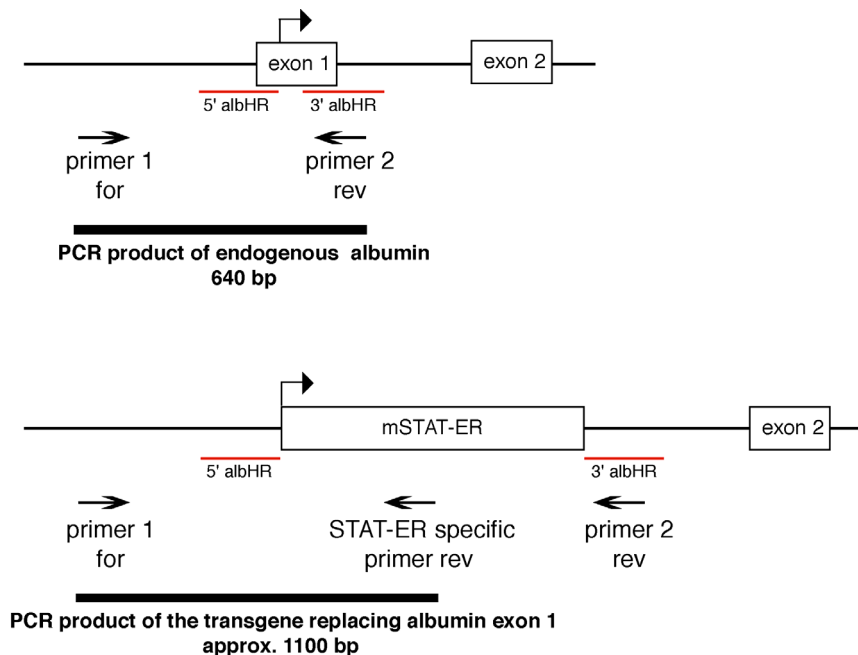
After removal of the ampicillin selection cassette, recombinants sensitive to ampicillin were confirmed by restriction digest with Sall, which cuts in the ampicillin cassette, and should be lost after Flpe recombination. The cassette was removed in all of the analyzed colonies. An example of the comparison of restriction digest patterns before and after removal of the ampicillin cassette is shown in Figure 7.

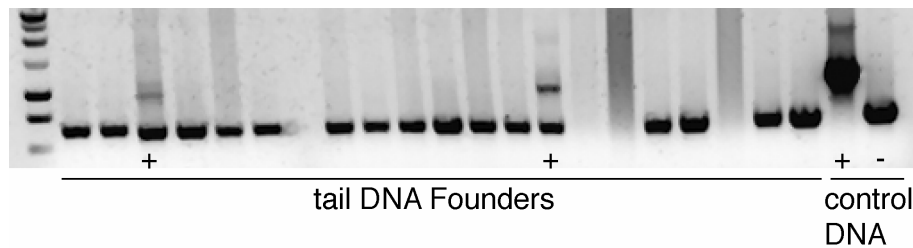
**Figure 7. Restoration of the *S*alI-digested restriction pattern of the modified pPAC4-albumin.** PFGE gel comparison of the restriction digest patterns of the modified pPAC4-albumin before and after the removal of the ampicillin selection cassette by Flpe recombination.



The injection of the linearized 190 kb chromosomal-mSTAT3<sup>wt</sup>-ER transgene integrated DNA into fertilized oocytes gave rise a total of 6 (out of 63 living analyzed animals) female pups carrying the *albm*STAT3<sup>wt</sup>-ER transgene. The transgenic offspring was identified by PCR amplification of tail DNA using three primers in one reaction, amplifying a fragment of transgene and an endogenous albumin fragment, to serve as internal control. Schematic overview (A) and results (B) of the genotyping of the founders is shown in Figure 8.

**A**



**B**

**Figure 8. Genotyping of mSTAT3<sup>wt</sup>-ER fusion protein expressing transgenic founder animals.** **A)** A PCR strategy was developed to amplify in one PCR reaction a fragment of endogenous albumin and when transgenic, a fragment of the fusion protein sequence. In case of the presence of the transgene is the product amplified by primer1for and primer2rev not amplified from the transgene sequence due to the size of the product. Instead is a product amplified by the primer1for and the mSTAT3<sup>wt</sup>-ER specific primer rev. **B)** Agarose gel electrophoresis of PCR products amplified from tail DNA of the founders animals, born from oocytes injected with the *alb*mSTAT3<sup>wt</sup>-ER transgene. Animals expressing the transgene are indicated by a (+).

F1 transgenic offspring was identified using the same PCR strategy. Figure 9 shows the results of the F1, proving that the *alb*mSTAT3<sup>wt</sup>-ER transgene is integrated in germline DNA. The transgenic mice appeared to have a normal phenotype and are healthy.

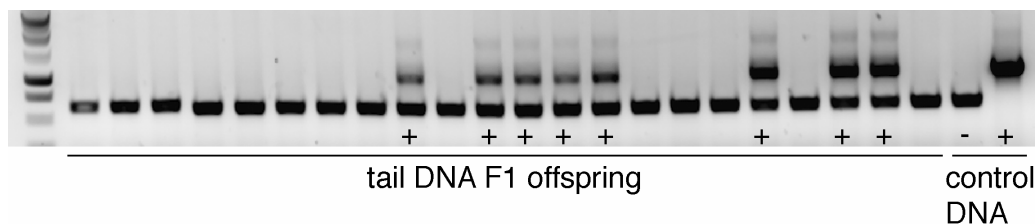


**Figure 9. Germline transmission of the *alb*mSTAT3<sup>wt</sup>-ER transgene.** Agarose gel electrophoresis of PCR products amplified from tail DNA of the F1 generation, born from founder animals carrying the *alb*mSTAT3<sup>wt</sup>-ER transgene crossed to C57Bl6 mice. Animals expressing the transgene are indicated by a (+).

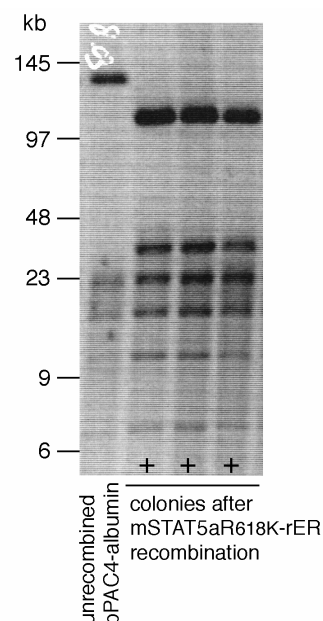
### ***alb*mSTAT5aR618K-rER mice**

Although we did not know whether a SH2 domain mutant of a STAT-ER fusion protein could be activated by 4-HT, we decided out of time saving motives, to take the risk and use the construct to generate a transgenic mouse. A part of mSTAT5aR618K-rER construct was amplified from pCAGGS-mSTAT5aR618K-rER plasmid and fused to the 5' *alb*HR by overlapping PCR. Together with the remaining part of the mSTAT5aR618K-rER sequence, the 5' *alb*HR-mSTAT5aR618K-rER fragment was inserted into the pECE-intron-polyA-frtampfrtnoIres plasmid. The 3' *alb*HR sequence was also inserted in this plasmid, creating *pECE5' albHR-mSTAT5aR618K-rER-frtampfrt-3' albHR*.

The fusion protein-intron-polyA-frtampfr construct flanked by the *alb*HRs was excised from its plasmid and electroporated into EL250 containing the

pPAC4-albumin *E. coli*, induced to allow homologous recombination of the construct in the first exon of the albumin gene. Colonies were analysed for the desired recombination event and the orientation of the modified pPAC4-albumin by restriction enzyme analysis (NotI, SalI, SacII, EagI, and RsrII) and by Southern blot analysis. Restriction patterns were compared with unrecombined pPAC4-albumin by pulsed-field gel electrophoresis. 16 out of 17 analyzed colonies gave the expected pattern of recombination (Figure 10).

**Figure 10. Representative PFGE gel results of SacII digested PAC DNA from colonies obtained after homologous recombination of fusion protein-intron-polyA-frtampfr into pPAC4-albumin.** Lanes marked with (+) represent recombinant colonies, showing two SalI fragments of 110 and 30 kb instead of the one of 140 kb shown for the unrecombined pPAC4-albumin



For the Southern blot analysis, recombinants for pPAC4-albumin-mSTAT5aR618K-rER-frtampfr were digested with BsaBI, PmlI or EcoRI and hybridized to probe1, 2-5aER or 3 (probes are indicated in Figure 3). An example is shown in Figure 11.

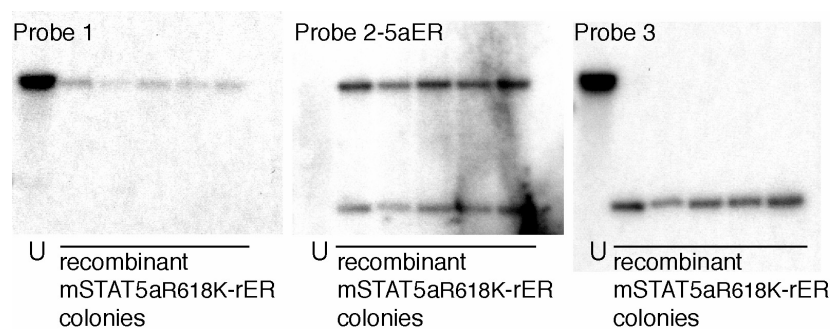


**Figure 11. Southern blot analysis of BsaBI digested modified pPAC4-albumin.** BsaBI cuts upstream from the probe 1 hybridization site (see Figure 3), in the probe 2-5aER hybridization site (so in the fusion protein sequence) and downstream of the hybridization site of probe 3. This results in the binding of probe 1 to a 13.9 kb fragment in the unrecombined pPAC4-albumin (U in the figure) and a fragment of 13.2 kb in the recombinant pPAC4-albumin. Probe 2-5aER can not bind the unrecombined, but binds two fragments of

13.2 and 6.5 kb obtained from recombinant colonies. Probe 3 binds a fragment of 13.9 kb (unrecombined) or 6.5 kb (recombinant DNA).

After removal of the ampicillin selection cassette, recombinants sensitive to ampicillin were confirmed by restriction digest with SalI. The cassette was removed in 100% of the analyzed colonies, like for the mSTAT3<sup>wt</sup>-ER modified pPAC4-albumin.

The injection of the linearized 190 kb chromosomal-mSTAT5<sup>aR618K</sup>-rER transgene integrated DNA into fertilized oocytes gave rise a total of 9 (out of 79 living analyzed animals) pups (8 female and 1 male) carrying the *albm*STAT5<sup>aR618K</sup>-rER transgene. The transgenic offspring was identified by PCR amplification of tail DNA as described for *albm*STAT3<sup>wt</sup>-ER transgene. The result of the PCR analysis of the founders is shown in Figure 12.

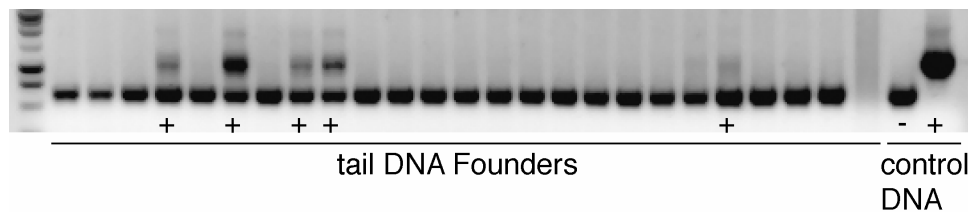


**Figure 12. Genotyping of mSTAT5<sup>aR618K</sup>-rER fusion protein expressing transgenic founder animals.** Agarose gel electrophoresis of PCR products amplified from tail DNA of the founders animals, born from oocytes injected with the *albm*STAT5<sup>aR618K</sup>-rER transgene. Animals expressing the transgene are indicated by a (+). PCR approach is as described under Figure 8A, instead of mSTAT3<sup>wt</sup>-ER specific primer rev, the mSTAT5<sup>aR618K</sup>-rER specific primer rev was used.

F1 transgenic offspring was identified using the same PCR strategy. Figure 13 shows the results of the F1, proving that the *albm*STAT5<sup>aR618K</sup>-rER transgene is integrated in germline DNA. The transgenic mice appeared to have a normal phenotype and are healthy.

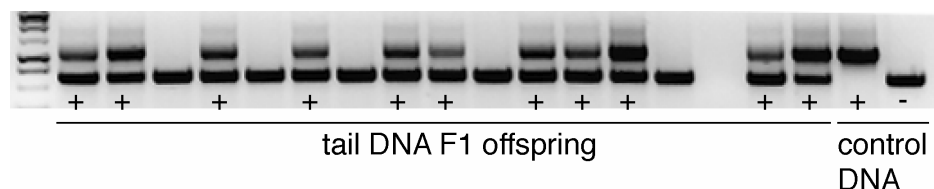


**Figure 13. Germline transmission of the *albm*STAT5<sup>aR618K</sup>-rER transgene.** Agarose gel electrophoresis of PCR products amplified from tail DNA of the F1 generation, born from crossed founder animals carrying the *albm*STAT5<sup>aR618K</sup>-rER transgene. Animals expressing the transgene are indicated by a (+).

---

## Ongoing work to characterize the transgenic mice

We have established a new approach to generate inducible and liver-specific STAT3 and STAT5a gain-of-function mouse models. We have showed germline transmission of the described transgenes. The transgenic mice will be tested on copy number of the integrated transgenes in the genome and on expression patterns of the fusion proteins in liver. Transgene copy number will be determined by Southern blot analysis and/or RT-PCR. Expression and levels of expression of the fusion protein will be investigated by Western blot using antibodies against STAT3, STAT5a or the ER $\alpha$ . Furthermore could expression levels of the mSTAT3<sub>wt</sub>-ER and mSTAT5a<sub>R618K</sub>-rER fusion proteins be compared to respectively endogenous STAT3 or STAT5a and examine whether the protein expression levels are dependent on copy number of the transgene. Also could the total integration of the transgene (190 kb pPAC4 insert) in the genome of the founder, F1 and F2 mice be examined by PAC end PCR amplification.

Parallel to the ongoing work on the characterization of the mice, the activation of the fusion protein induced by i.p. and p.o. administration of different amounts of 4-HT. Liver samples will be analyzed by phospho-STAT Western blots, EMSAs and upregulation of STAT3 or STAT5a target genes (cell cycle mediators c-myc, junB, c-fos, cyclins D1, D2, D3 and A, SOCS3, coagulation factor/acute phase proteins fibrinogen, haptoglobin and SAP and proteinase inhibitor  $\alpha$ 2-macroglobulin) using Western blotting and RNase protection assays.

Possible applications and future plans for the use of the mice will be discussed in chapter 6.

## Acknowledgments

We are grateful to Professor Dr. Günther Schütz and Dr. Emilio Casanova for the pPAC4-albumin plasmid and other plasmids as described, and especially to Emilio for all his technical assistance and helpful discussions. We thank Dr. Neal G. Copeland for providing the EL250 bacteria, Dr. Saulius Zuklys and Dr. Tibor Schomber for helpful technical suggestions and use of equipment. Sabina Hernandez Penna performed the genotyping of the transgenic offspring (data in Figures 8B, 9, 12 and 13).





Chapter 6

**Outlook on the use of the conditional  
*alb*mSTAT3<sup>wt-ER</sup> and *alb*mSTAT5a  
R618K-rER gain-of-function mice  
models**

---

The inducible liver-specific gain-of-function mouse models for STAT3 and STAT5a, as described in Chapter 4 and 5, will be a powerful tool to analyze involvement of STAT3 and STAT5a signaling in many different physiological and pathophysiological conditions in liver. Future possible applications of transgenic mice will be discussed here.

### **The *albmSTAT3wt-ER* transgenic mouse to study effects of STAT3 signaling**

We plan to perform partial hepatectomy in these mice to examine liver cell regeneration in presence and absence of mSTAT3wt-ER activation by 4-HT.

We hope to elucidate the importance of STAT3 signaling in liver cell regeneration. Is liver cell regeneration hampered by the lack of SHP2/MAPK signaling? Would continuous activation of mSTAT3wt-ER for a certain period induce the liver cells to regenerate faster after two-third hepatectomy? Could continuous STAT3 signaling disturb the process that stops hepatocytes proliferating once the original size of the liver has been restored?

In our experiments with STAT3-deficient MEFs stably transfected with mSTAT3wt-ER we found that only 4-HT but not IL-6 stimulation resulted in the upregulation of STAT3 target genes. *In vivo* the results might be different. If the mSTAT3wt-ER fusion protein can indeed be activated by IL-6 *in vivo*, we plan to cross the *albmSTAT3wt-ER* transgenic mice with IL-6 KO mice. In this model, the role of STAT3 signaling in liver regeneration could be investigated independent from other intracellular signals generated by IL-6 stimulation of liver cells.

Due to the importance of STAT3 signaling in promoting mitogenesis and inhibiting apoptosis, the transgenic mice could be well used in studying STAT3 mediated cellular transformation.

STAT3 was shown to be upregulated (together with SOCS3 and cyclin D1) in HCC compared to normal liver tissue <sup>323</sup>. Also in chemically induced rat HCC a high activity of STAT3 was observed using EMSA. Dexamethasone treatment resulted in downregulation of the STAT3 activation and reduction of cell proliferation in the tumors, thus STAT activity might be required for HCC growth <sup>324</sup>. Furthermore, it has been shown that a constitutive active form of STAT3 can be an oncogene <sup>150</sup>. STAT3 seems to promote cell cycle G1 to S phase transition by upregulating cyclins D1, 2, 3 and A, *cdc25A* and downregulating *p21* and *p27* <sup>325</sup>. A recent study showed that constitutive active STAT3 induced cellular transformation of fibroblasts through upregulation of *c-fos* expression <sup>326</sup>. Through the upregulation of *Bcl-X<sub>L</sub>* and *Mcl-1*, STAT3 protects against apoptosis <sup>151</sup>. STAT3 is also involved in tumorigenesis through the activation of VEGF to promote angiogenesis <sup>155</sup>.

Long-term administration of 4-HT would constitutive activate STAT3 signaling through mSTAT3wt-ER fusion protein. Periodic examination of the livers on development of tumors and analysis of induction of STAT3 target genes, like the ones described here, could contribute to clarify the role of STAT3 in oncogenesis. It could also be examined whether chemically induced carcinogenesis could be accelerated by activated mSTAT3wt-ER.

In addition, the use of the *albmSTAT3wt-ER* transgenic could be interesting in some other liver pathology research areas, which involve STAT3 signaling.

Absence of STAT3 leads to an impaired acute phase response, which is commonly induced by bacterial infection. This was shown in LPS-induced acute phase response in mice displaying an interferon-induced deletion of STAT3. These mice were generated by crossing of a conditional Cre-mediated STAT3 deficient mice to a Mx-Cre transgenic mouse, in which the expression of Cre recombinase can be induced by IFN type I <sup>25, 72</sup>. *AlbmSTAT3wt-ER* mice could be used to investigate the function of STAT3 in the protection or defense against bacterial infection. *AlbmSTAT3wt-ER* mice could be challenged with a bacterial infection, and the effect of 4-HT induced mSTAT3wt-ER activation could be analyzed.

Otherwise it might be worthwhile to examine the function of STAT3 in regulation of hepatic gluconeogenic genes and carbohydrate metabolism in the context of diabetes mellitus. Mice with a liver specific deficiency in STAT3 are insulin resistant, probably caused by an increased expression of G6PC and PCK-1. Restoration of hepatic STAT3 expression normalized insulin levels and expression of gluconeogenic genes. Overexpression of STAT3 reduced expression of these genes, as well as blood glucose and plasma insulin levels in leptin receptor KO diabetic mice <sup>111</sup>. Inducing diabetes in our *albmSTAT3wt-ER* mice could provide a model to reveal STAT3 function further and examine STAT3 down stream targets involved. This could provide insights for development of new therapeutic targets for diabetes mellitus.

### **The *albmSTAT5aR618K-rER* transgenic mouse to study effects of STAT5a signaling**

STAT5a is a promoter of cell proliferation, cellular transformation and inhibitor of apoptosis. Activated STAT5a is critical in GH, prolactin, GM-CSF and IL-2 signaling. STAT5a KO mice showed normal body growth or serum IGF-1 (mediator of the somatic effects of GH) levels <sup>122</sup>. Still, in liver STAT5a and 5b are the most prominent mediators activated by GH <sup>123</sup>. The *albmSTAT5aR618K-rER* transgenic mouse could be used to examine STAT5a contribution to liver growth or liver cell proliferation during liver regeneration after partial hepatectomy.

Constitutively activated mutants of STAT5 have been found to transform Ba/F3 cells <sup>327</sup> and STAT5a was found to be constitutively activated in several leukemias <sup>5, 328</sup>, showing STAT5a involvement in oncogenesis. Constitutive activation of STAT5a/b was shown to deregulate the cyclin complexes D/CDK4-6, which controls progression from the G1 to the S-phase of the cell cycle, deregulate c-Myc dependent cell growth, and activate antiapoptotic signals and therefore induce cell survival <sup>149, 151</sup>.

The antiapoptotic properties of STAT5a could be investigated in the context of ischemia injuries induced by partial hepatectomy and its consequences for the progress of liver regeneration. The protection of hepatocytes against apoptosis could be examined in *albmSTAT5aR618K-rER* transgenic mouse during liver regeneration after partial hepatectomy or in sham surgery induced apoptosis, in presence and absence of activated mSTAT5aR618K-ER by 4-HT.

Furthermore one could, like for the *albmSTAT3wt-ER* transgenics, activate mSTAT5aR618K-rER over longer periods by 4-HT and check for development of hyperplasia or tumors, and involvement of specific STAT5a target genes in the process of oncogenesis. Another possibility would be to cross both

---

transgenic mice and activate both fusion proteins over a longer period of time by 4-HT. It might be that in parallel activated STAT3 and STAT5a signaling enhances each others cell transformational and antiapoptotic effects. This would be interesting in the context of many tumors in which both STAT3 and STAT5a are constitutively activated. Maybe regulatory mechanisms from one signaling pathway to the other could be revealed when oncogenesis would be studied in double fusion protein expressing transgenic mice compared to the single fusion protein expressing transgenic mice.



---

## References

1. Darnell JE, Jr. STATs and gene regulation. *Science* 1997;277:1630-5.
2. Schindler C, Shuai K, Prezioso VR, Darnell JE, Jr. Interferon-dependent tyrosine phosphorylation of a latent cytoplasmic transcription factor. *Science* 1992;257:809-13.
3. Shuai K, Schindler C, Prezioso VR, Darnell JE, Jr. Activation of transcription by IFN-gamma: tyrosine phosphorylation of a 91-kD DNA binding protein. *Science* 1992;258:1808-12.
4. Heim MH. The Jak-STAT pathway: specific signal transduction from the cell membrane to the nucleus. *Eur J Clin Invest* 1996;26:1-12.
5. Calo V, Migliavacca M, Bazan V, Macaluso M, Buscemi M, Gebbia N, Russo A. STAT proteins: from normal control of cellular events to tumorigenesis. *J Cell Physiol* 2003;197:157-68.
6. Rawlings JS, Rosler KM, Harrison DA. The JAK/STAT signaling pathway. *J Cell Sci* 2004;117:1281-3.
7. Fu XY, Zhang JJ. Transcription factor p91 interacts with the epidermal growth factor receptor and mediates activation of the c-fos gene promoter. *Cell* 1993;74:1135-45.
8. Choudhury GG, Ghosh-Choudhury N, Abboud HE. Association and direct activation of signal transducer and activator of transcription1alpha by platelet-derived growth factor receptor. *J Clin Invest* 1998;101:2751-60.
9. Heim MH. The Jak-STAT pathway: cytokine signalling from the receptor to the nucleus. *J Recept Signal Transduct Res* 1999;19:75-120.
10. Bazan JF. Structural design and molecular evolution of a cytokine receptor superfamily. *Proc Natl Acad Sci U S A* 1990;87:6934-8.
11. Taga T, Kishimoto T. Gp130 and the interleukin-6 family of cytokines. *Annu Rev Immunol* 1997;15:797-819.
12. Heinrich PC, Behrmann I, Muller-Newen G, Schaper F, Graeve L. Interleukin-6-type cytokine signalling through the gp130/Jak/STAT pathway. *Biochem J* 1998;334:297-314.
13. Kisseleva T, Bhattacharya S, Braunstein J, Schindler CW. Signaling through the JAK/STAT pathway, recent advances and future challenges. *Gene* 2002;285:1-24.
14. Novick D, Cohen B, Rubinstein M. The human interferon alpha/beta receptor: characterization and molecular cloning. *Cell* 1994;77:391-400.
15. Oritani K, Kincade PW, Zhang C, Tomiyama Y, Matsuzawa Y. Type I interferons and limitin: a comparison of structures, receptors, and functions. *Cytokine Growth Factor Rev* 2001;12:337-48.
16. Russell-Harde D, Wagner TC, Rani MR, Vogel D, Colamonici O, Ransohoff RM, Majchrzak B, Fish E, Perez HD, Croze E. Role of the intracellular domain of the human type I interferon receptor 2 chain (IFNAR2c) in interferon signaling. Expression of IFNAR2c truncation mutants in U5A cells. *J Biol Chem* 2000;275:23981-5.
17. Taniguchi T, Takaoka A. A weak signal for strong responses: interferon-alpha/beta revisited. *Nat Rev Mol Cell Biol* 2001;2:378-86.
18. Darnell JE, Jr., Kerr IM, Stark GR. Jak-STAT pathways and transcriptional activation in response to IFNs and other extracellular signaling proteins. *Science* 1994;264:1415-21.
19. Marrero MB, Schieffer B, Paxton WG, Heerdt L, Berk BC, Delafontaine P, Bernstein KE. Direct stimulation of Jak/STAT pathway by the angiotensin II AT1 receptor. *Nature* 1995;375:247-50.
20. Leonard WJ, O'Shea JJ. Jaks and STATs: biological implications. *Annu Rev Immunol* 1998;16:293-322.
21. Hubbard SR, Till JH. Protein tyrosine kinase structure and function. *Annu Rev Biochem* 2000;69:373-98.
22. Luo H, Rose P, Barber D, Hanratty WP, Lee S, Roberts TM, D'Andrea AD, Dearolf CR. Mutation in the Jak kinase JH2 domain hyperactivates Drosophila and mammalian Jak-Stat pathways. *Mol Cell Biol* 1997;17:1562-71.
23. O'Shea JJ, Gadina M, Schreiber RD. Cytokine signaling in 2002: new surprises in the Jak/Stat pathway. *Cell* 2002;109:S121-31.

24. Rodig SJ, Meraz MA, White JM, Lampe PA, Riley JK, Arthur CD, King KL, Sheehan KC, Yin L, Pennica D, Johnson EM, Jr., Schreiber RD. Disruption of the Jak1 gene demonstrates obligatory and nonredundant roles of the Jaks in cytokine-induced biologic responses. *Cell* 1998;93:373-83.
25. Levy DE, Darnell JE, Jr. Stats: transcriptional control and biological impact. *Nat Rev Mol Cell Biol* 2002;3:651-62.
26. Schindler C, Darnell JE, Jr. Transcriptional responses to polypeptide ligands: the JAK-STAT pathway. *Annu Rev Biochem* 1995;64:621-51.
27. Copeland NG, Gilbert DJ, Schindler C, Zhong Z, Wen Z, Darnell JE, Jr., Mui AL, Miyajima A, Quelle FW, Ihle JN, et al. Distribution of the mammalian Stat gene family in mouse chromosomes. *Genomics* 1995;29:225-8.
28. Becker S, Groner B, Muller CW. Three-dimensional structure of the Stat3beta homodimer bound to DNA. *Nature* 1998;394:145-51.
29. Chen X, Vinkemeier U, Zhao Y, Jeruzalmi D, Darnell JE, Jr., Kuriyan J. Crystal structure of a tyrosine phosphorylated STAT-1 dimer bound to DNA. *Cell* 1998;93:827-39.
30. Vinkemeier U, Cohen SL, Moarefi I, Chait BT, Kuriyan J, Darnell JE, Jr. DNA binding of in vitro activated Stat1 alpha, Stat1 beta and truncated Stat1: interaction between NH2-terminal domains stabilizes binding of two dimers to tandem DNA sites. *Embo J* 1996;15:5616-26.
31. John S, Vinkemeier U, Soldaini E, Darnell JE, Jr., Leonard WJ. The significance of tetramerization in promoter recruitment by Stat5. *Mol Cell Biol* 1999;19:1910-8.
32. Vinkemeier U, Moarefi I, Darnell JE, Jr., Kuriyan J. Structure of the amino-terminal protein interaction domain of STAT-4. *Science* 1998;279:1048-52.
33. Chen X, Bhandari R, Vinkemeier U, Van Den Akker F, Darnell JE, Jr., Kuriyan J. A reinterpretation of the dimerization interface of the N-terminal domains of STATs. *Protein Sci* 2003;12:361-5.
34. Zhang JJ, Vinkemeier U, Gu W, Chakravarti D, Horvath CM, Darnell JE, Jr. Two contact regions between Stat1 and CBP/p300 in interferon gamma signaling. *Proc Natl Acad Sci U S A* 1996;93:15092-6.
35. Mowen KA, Tang J, Zhu W, Schurter BT, Shuai K, Herschman HR, David M. Arginine methylation of STAT1 modulates IFNalpha/beta-induced transcription. *Cell* 2001;104:731-41.
36. Shuai K, Liao J, Song MM. Enhancement of antiproliferative activity of gamma interferon by the specific inhibition of tyrosine dephosphorylation of Stat1. *Mol Cell Biol* 1996;16:4932-41.
37. Zhang T, Kee WH, Seow KT, Fung W, Cao X. The coiled-coil domain of Stat3 is essential for its SH2 domain-mediated receptor binding and subsequent activation induced by epidermal growth factor and interleukin-6. *Mol Cell Biol* 2000;20:7132-9.
38. Strehlow I, Schindler C. Amino-terminal signal transducer and activator of transcription (STAT) domains regulate nuclear translocation and STAT deactivation. *J Biol Chem* 1998;273:28049-56.
39. Horvath CM, Stark GR, Kerr IM, Darnell JE, Jr. Interactions between STAT and non-STAT proteins in the interferon-stimulated gene factor 3 transcription complex. *Mol Cell Biol* 1996;16:6957-64.
40. Zhang X, Wrzeszczynska MH, Horvath CM, Darnell JE, Jr. Interacting regions in Stat3 and c-Jun that participate in cooperative transcriptional activation. *Mol Cell Biol* 1999;19:7138-46.
41. Nakajima H, Brindle PK, Handa M, Ihle JN. Functional interaction of STAT5 and nuclear receptor co-repressor SMRT: implications in negative regulation of STAT5-dependent transcription. *Embo J* 2001;20:6836-44.
42. Ma J, Zhang T, Novotny-Diermayr V, Tan AL, Cao X. A novel sequence in the coiled-coil domain of Stat3 essential for its nuclear translocation. *J Biol Chem* 2003;278:29252-60. Epub 2003 May 13.
43. Yang E, Wen Z, Haspel RL, Zhang JJ, Darnell JE, Jr. The linker domain of Stat1 is required for gamma interferon-driven transcription. *Mol Cell Biol* 1999;19:5106-12.
44. Yang E, Henriksen MA, Schaefer O, Zakharova N, Darnell JE, Jr. Dissociation time from DNA determines transcriptional function in a STAT1 linker mutant. *J Biol Chem* 2002;277:13455-62. Epub 2002 Feb 7.
45. Shuai K. The STAT family of proteins in cytokine signaling. *Prog Biophys Mol Biol* 1999;71:405-22.

- 
46. Heim MH, Kerr IM, Stark GR, Darnell JE, Jr. Contribution of STAT SH2 groups to specific interferon signaling by the Jak-STAT pathway. *Science* 1995;267:1347-9.
  47. Shuai K, Horvath CM, Huang LH, Qureshi SA, Cowburn D, Darnell JE, Jr. Interferon activation of the transcription factor Stat91 involves dimerization through SH2-phosphotyrosyl peptide interactions. *Cell* 1994;76:821-8.
  48. Shuai K, Stark GR, Kerr IM, Darnell JE, Jr. A single phosphotyrosine residue of Stat91 required for gene activation by interferon-gamma. *Science* 1993;261:1744-6.
  49. Heim MH. The STAT protein family. In: Sehgal P.B. LDE HT, ed. *Signal Transducers and activators of transcription (STATs)*. Amsterdam: Kluwer Academic Publishers, 2003:11-26.
  50. Wen Z, Zhong Z.,Darnell Jr. J.E. Maximal activation of transcription by STAT1 and STAT3 requires both tyrosine and serine phosphorylation. *Cell* 1995;82:241-250.
  51. Horvath CM, Darnell JE, Jr. The antiviral state induced by alpha interferon and gamma interferon requires transcriptionally active Stat1 protein. *J Virol* 1996;70:647-50.
  52. Shen Y, Schlessinger K, Zhu X, Meffre E, Quimby F, Levy DE, Darnell JE, Jr. Essential role of STAT3 in postnatal survival and growth revealed by mice lacking STAT3 serine 727 phosphorylation. *Mol Cell Biol* 2004;24:407-19.
  53. Caldenhoven E, van Dijk TB, Solari R, Armstrong J, Raaijmakers JA, Lammers JW, Koenderman L, de Groot RP. STAT3beta, a splice variant of transcription factor STAT3, is a dominant negative regulator of transcription. *J Biol Chem* 1996;271:13221-7.
  54. Sen GC, Lengyel P. The interferon system. A bird's eye view of its biochemistry. *J Biol Chem* 1992;267:5017-20.
  55. Boehm U, Klamp T, Groot M, Howard JC. Cellular responses to interferon-gamma. *Annu Rev Immunol* 1997;15:749-95.
  56. van den Broek MF, Muller U, Huang S, Zinkernagel RM, Aguet M. Immune defence in mice lacking type I and/or type II interferon receptors. *Immunol Rev* 1995;148:5-18.
  57. Sato M, Taniguchi T, Tanaka N. The interferon system and interferon regulatory factor transcription factors -- studies from gene knockout mice. *Cytokine Growth Factor Rev* 2001;12:133-42.
  58. Heim MH. A new survival trick of hepatitis C virus: blocking the activation of interferon regulatory factor-3. *Hepatology* 2003;38:1582-4.
  59. Kalvakolanu DV. Alternate interferon signaling pathways. *Pharmacol Ther* 2003;100:1-29.
  60. Samuel CE. Antiviral actions of interferons. *Clin Microbiol Rev* 2001;14:778-809, table of contents.
  61. Muller U, Steinhoff U, Reis LF, Hemmi S, Pavlovic J, Zinkernagel RM, Aguet M. Functional role of type I and type II interferons in antiviral defense. *Science* 1994;264:1918-21.
  62. Huang S, Hendriks W, Althage A, Hemmi S, Bluethmann H, Kamijo R, Vilcek J, Zinkernagel RM, Aguet M. Immune response in mice that lack the interferon-gamma receptor. *Science* 1993;259:1742-5.
  63. Der SD, Zhou A, Williams BR, Silverman RH. Identification of genes differentially regulated by interferon alpha, beta, or gamma using oligonucleotide arrays. *Proc Natl Acad Sci U S A* 1998;95:15623-8.
  64. Leaman DW, Chawla-Sarkar M, Jacobs B, Vyas K, Sun Y, Ozdemir A, Yi T, Williams BR, Borden EC. Novel growth and death related interferon-stimulated genes (ISGs) in melanoma: greater potency of IFN-beta compared with IFN-alpha2. *J Interferon Cytokine Res* 2003;23:745-56.
  65. Heim MH. Intracellular signalling and antiviral effects of interferons. *Dig Liver Dis* 2000;32:257-63.
  66. Ahmed ST, Ivashkiv LB. Inhibition of IL-6 and IL-10 signaling and Stat activation by inflammatory and stress pathways. *J Immunol* 2000;165:5227-37.
  67. Streetz KL, Luedde T, Manns MP, Trautwein C. Interleukin 6 and liver regeneration. *Gut* 2000;47:309-12.
  68. Mangnall D, Bird NC, Majeed AW. The molecular physiology of liver regeneration following partial hepatectomy. *Liver Int* 2003;23:124-38.
  69. Maione D, Di Carlo E, Li W, Musiani P, Modesti A, Peters M, Rose-John S, Della Rocca C, Tripodi M, Lazzaro D, Taub R, Savino R, Ciliberto G. Coexpression of IL-6



- and soluble IL-6R causes nodular regenerative hyperplasia and adenomas of the liver. *Embo J* 1998;17:5588-97.
70. Heinrich PC, Behrmann I, Haan S, Hermanns HM, Muller-Newen G, Schaper F. Principles of interleukin (IL)-6-type cytokine signalling and its regulation. *Biochem J* 2003;374:1-20.
  71. Carbia-Nagashima A, Arzt E. Intracellular proteins and mechanisms involved in the control of gp130/JAK/STAT cytokine signaling. *IUBMB Life* 2004;56:83-8.
  72. Alonzi T, Maritano D, Gorgoni B, Rizzuto G, Libert C, Poli V. Essential role of STAT3 in the control of the acute-phase response as revealed by inducible gene inactivation [correction of activation] in the liver. *Mol Cell Biol* 2001;21:1621-32.
  73. Kim H, Baumann H. Dual signaling role of the protein tyrosine phosphatase SHP-2 in regulating expression of acute-phase plasma proteins by interleukin-6 cytokine receptors in hepatic cells. *Mol Cell Biol* 1999;19:5326-38.
  74. Lehmann U, Schmitz J, Weissenbach M, Sobota RM, Hortner M, Friederichs K, Behrmann I, Tsiaris W, Sasaki A, Schneider-Mergener J, Yoshimura A, Neel BG, Heinrich PC, Schaper F. SHP2 and SOCS3 contribute to Tyr-759-dependent attenuation of interleukin-6 signaling through gp130. *J Biol Chem* 2003;278:661-71. Epub 2002 Oct 27.
  75. Kopf M, Baumann H, Freer G, Freudenberg M, Lamers M, Kishimoto T, Zinkernagel R, Bluethmann H, Kohler G. Impaired immune and acute-phase responses in interleukin-6-deficient mice. *Nature* 1994;368:339-42.
  76. Fattori E, Cappelletti M, Costa P, Sellitto C, Cantoni L, Carelli M, Faggioni R, Fantuzzi G, Ghezzi P, Poli V. Defective inflammatory response in interleukin 6-deficient mice. *J Exp Med* 1994;180:1243-50.
  77. Kopf M, Ramsay A, Brombacher F, Baumann H, Freer G, Galanos C, Gutierrez-Ramos JC, Kohler G. Pleiotropic defects of IL-6-deficient mice including early hematopoiesis, T and B cell function, and acute phase responses. *Ann N Y Acad Sci* 1995;762:308-18.
  78. Melen K, Kinnunen L, Julkunen I. Arginine/lysine-rich structural element is involved in interferon-induced nuclear import of STATs. *J Biol Chem* 2001;276:16447-55. Epub 2001 Jan 9.
  79. McBride KM, Banninger G, McDonald C, Reich NC. Regulated nuclear import of the STAT1 transcription factor by direct binding of importin-alpha. *Embo J* 2002;21:1754-63.
  80. Bhattacharya S, Schindler C. Regulation of Stat3 nuclear export. *J Clin Invest* 2003;111:553-9.
  81. McBride KM, Reich NC. The ins and outs of STAT1 nuclear transport. *Sci STKE* 2003;2003:RE13.
  82. Ehret GB, Reichenbach P, Schindler U, Horvath CM, Fritz S, Nabholz M, Bucher P. DNA binding specificity of different STAT proteins. Comparison of in vitro specificity with natural target sites. *J Biol Chem* 2001;276:6675-88. Epub 2000 Oct 26.
  83. Horvath CM. STAT proteins and transcriptional responses to extracellular signals. *Trends Biochem Sci* 2000;25:496-502.
  84. Zakharova N, Lymar ES, Yang E, Malik S, Zhang JJ, Roeder RG, Darnell JE, Jr. Distinct transcriptional activation functions of STAT1alpha and STAT1beta on DNA and chromatin templates. *J Biol Chem* 2003;278:43067-73. Epub 2003 Aug 25.
  85. Zhu X, Wen Z, Xu LZ, Darnell JE, Jr. Stat1 serine phosphorylation occurs independently of tyrosine phosphorylation and requires an activated Jak2 kinase. *Mol Cell Biol* 1997;17:6618-23.
  86. Wen Z, Darnell JE, Jr. Mapping of Stat3 serine phosphorylation to a single residue (727) and evidence that serine phosphorylation has no influence on DNA binding of Stat1 and Stat3. *Nucleic Acids Res* 1997;25:2062-7.
  87. Goh KC, Haque SJ, Williams BR. p38 MAP kinase is required for STAT1 serine phosphorylation and transcriptional activation induced by interferons. *Embo J* 1999;18:5601-8.
  88. Aaronson DS, Horvath CM. A road map for those who don't know JAK-STAT. *Science* 2002;296:1653-5.
  89. Starr R, Hilton DJ. Negative regulation of the JAK/STAT pathway. *Bioessays* 1999;21:47-52.
  90. Liao J, Fu Y, Shuai K. Distinct roles of the NH2- and COOH-terminal domains of the protein inhibitor of activated signal transducer and activator of transcription (STAT)

- 
- 1 (PIAS1) in cytokine-induced PIAS1-Stat1 interaction. *Proc Natl Acad Sci U S A* 2000;97:5267-72.
91. Zhu W, Mustelin T, David M. Arginine methylation of STAT1 regulates its dephosphorylation by T cell protein tyrosine phosphatase. *J Biol Chem* 2002;277:35787-90. Epub 2002 Aug 8.
  92. Liu B, Mink S, Wong KA, Stein N, Getman C, Dempsey PW, Wu H, Shuai K. PIAS1 selectively inhibits interferon-inducible genes and is important in innate immunity. *Nat Immunol* 2004;15:15.
  93. Jackson PK. A new RING for SUMO: wrestling transcriptional responses into nuclear bodies with PIAS family E3 SUMO ligases. *Genes Dev* 2001;15:3053-8.
  94. Ali S, Nouhi Z, Chughtai N. SHP-2 regulates SOCS-1-mediated Janus kinase-2 ubiquitination/degradation downstream of the prolactin receptor. *J Biol Chem* 2003;278:52021-31. Epub 2003 Oct 1.
  95. Simoncic PD, Lee-Loy A, Barber DL, Tremblay ML, McGlade CJ. The T cell protein tyrosine phosphatase is a negative regulator of janus family kinases 1 and 3. *Curr Biol* 2002;12:446-53.
  96. ten Hoeve J, de Jesus Ibarra-Sanchez M, Fu Y, Zhu W, Tremblay M, David M, Shuai K. Identification of a nuclear Stat1 protein tyrosine phosphatase. *Mol Cell Biol* 2002;22:5662-8.
  97. Ishihara K, Hirano T. Molecular basis of the cell specificity of cytokine action. *Biochim Biophys Acta* 2002;1592:281-96.
  98. Stahl N, Farruggella TJ, Boulton TG, Zhong Z, Darnell JE, Jr., Yancopoulos GD. Choice of STATs and other substrates specified by modular tyrosine-based motifs in cytokine receptors. *Science* 1995;267:1349-53.
  99. Wiederkehr-Adam M, Ernst P, Muller K, Bieck E, Gombert FO, Ottl J, Graff P, Grossmuller F, Heim MH. Characterization of phosphopeptide motifs specific for the Src homology 2 domains of signal transducer and activator of transcription 1 (STAT1) and STAT3. *J Biol Chem* 2003;278:16117-28. Epub 2003 Feb 18.
  100. Horvath CM, Wen Z, Darnell JE, Jr. A STAT protein domain that determines DNA sequence recognition suggests a novel DNA-binding domain. *Genes Dev* 1995;9:984-94.
  101. Soldaini E, John S, Moro S, Bollenbacher J, Schindler U, Leonard WJ. DNA binding site selection of dimeric and tetrameric Stat5 proteins reveals a large repertoire of divergent tetrameric Stat5a binding sites. *Mol Cell Biol* 2000;20:389-401.
  102. Durbin JE, Hackenmiller R, Simon MC, Levy DE. Targeted disruption of the mouse Stat1 gene results in compromised innate immunity to viral disease. *Cell* 1996;84:443-50.
  103. Chin YE, Kitagawa M, Kuida K, Flavell RA, Fu XY. Activation of the STAT signaling pathway can cause expression of caspase 1 and apoptosis. *Mol Cell Biol* 1997;17:5328-37.
  104. Shankaran V, Ikeda H, Bruce AT, White JM, Swanson PE, Old LJ, Schreiber RD. IFN $\gamma$  and lymphocytes prevent primary tumour development and shape tumour immunogenicity. *Nature* 2001;410:1107-11.
  105. Townsend PA, Scarabelli TM, Davidson SM, Knight RA, Latchman DS, Stephanou A. STAT-1 interacts with p53 to enhance DNA damage-induced apoptosis. *J Biol Chem* 2004;279:5811-20. Epub 2003 Nov 5.
  106. Park C, Li S, Cha E, Schindler C. Immune response in Stat2 knockout mice. *Immunity* 2000;13:795-804.
  107. Takeda K, Akira S. Multi-functional roles of Stat3 revealed by conditional gene targeting. *Arch Immunol Ther Exp (Warsz)* 2001;49:279-83.
  108. Sano S, Itami S, Takeda K, Tarutani M, Yamaguchi Y, Miura H, Yoshikawa K, Akira S, Takeda J. Keratinocyte-specific ablation of Stat3 exhibits impaired skin remodeling, but does not affect skin morphogenesis. *Embo J* 1999;18:4657-68.
  109. Takeda K, Kaisho T, Yoshida N, Takeda J, Kishimoto T, Akira S. Stat3 activation is responsible for IL-6-dependent T cell proliferation through preventing apoptosis: generation and characterization of T cell-specific Stat3-deficient mice. *J Immunol* 1998;161:4652-60.
  110. Akaishi H, Takeda K, Kaisho T, Shineha R, Satomi S, Takeda J, Akira S. Defective IL-2-mediated IL-2 receptor alpha chain expression in Stat3-deficient T lymphocytes. *Int Immunol* 1998;10:1747-51.

111. Inoue H, Ogawa W, Ozaki M, Haga S, Matsumoto M, Furukawa K, Hashimoto N, Kido Y, Mori T, Sakaue H, Teshigawara K, Jin S, Iguchi H, Hiramatsu R, LeRoith D, Takeda K, Akira S, Kasuga M. Role of STAT-3 in regulation of hepatic gluconeogenic genes and carbohydrate metabolism in vivo. *Nat Med* 2004;10:168-74. Epub 2004 Jan 11.
112. Li W, Liang X, Kellendonk C, Poli V, Taub R. STAT3 contributes to the mitogenic response of hepatocytes during liver regeneration. *J Biol Chem* 2002;277:28411-7. Epub 2002 May 24.
113. Sano S, Takahama Y, Sugawara T, Kosaka H, Itami S, Yoshikawa K, Miyazaki J, van Ewijk W, Takeda J. Stat3 in thymic epithelial cells is essential for postnatal maintenance of thymic architecture and thymocyte survival. *Immunity* 2001;15:261-73.
114. Takeda K, Clausen BE, Kaisho T, Tsujimura T, Terada N, Forster I, Akira S. Enhanced Th1 activity and development of chronic enterocolitis in mice devoid of Stat3 in macrophages and neutrophils. *Immunity* 1999;10:39-49.
115. Chapman RS, Lourenco PC, Tonner E, Flint DJ, Selbert S, Takeda K, Akira S, Clarke AR, Watson CJ. Suppression of epithelial apoptosis and delayed mammary gland involution in mice with a conditional knockout of Stat3. *Genes Dev* 1999;13:2604-16.
116. Yoo JY, Huso DL, Nathans D, Desiderio S. Specific ablation of Stat3beta distorts the pattern of Stat3-responsive gene expression and impairs recovery from endotoxic shock. *Cell* 2002;108:331-44.
117. Maritano D, Sugrue ML, Tininini S, Dewilde S, Strobl B, Fu X, Murray-Tait V, Chiarle R, Poli V. The STAT3 isoforms alpha and beta have unique and specific functions. *Nat Immunol* 2004;5:401-9. Epub 2004 Mar 14.
118. Wurster AL, Tanaka T, Grusby MJ. The biology of Stat4 and Stat6. *Oncogene* 2000;19:2577-84.
119. Chitnis T, Najafian N, Benou C, Salama AD, Grusby MJ, Sayegh MH, Khoury SJ. Effect of targeted disruption of STAT4 and STAT6 on the induction of experimental autoimmune encephalomyelitis. *J Clin Invest* 2001;108:739-47.
120. Liu X, Robinson GW, Wagner KU, Garrett L, Wynshaw-Boris A, Hennighausen L. Stat5a is mandatory for adult mammary gland development and lactogenesis. *Genes Dev* 1997;11:179-86.
121. Udy GB, Towers RP, Snell RG, Wilkins RJ, Park SH, Ram PA, Waxman DJ, Davey HW. Requirement of STAT5b for sexual dimorphism of body growth rates and liver gene expression. *Proc Natl Acad Sci U S A* 1997;94:7239-44.
122. Teglund S, McKay C, Schuetz E, van Deursen JM, Stravopodis D, Wang D, Brown M, Bodner S, Grosveld G, Ihle JN. Stat5a and Stat5b proteins have essential and nonessential, or redundant, roles in cytokine responses. *Cell* 1998;93:841-50.
123. Zhu T, Goh EL, Graichen R, Ling L, Lobie PE. Signal transduction via the growth hormone receptor. *Cell Signal* 2001;13:599-616.
124. Park SH, Liu X, Hennighausen L, Davey HW, Waxman DJ. Distinctive roles of STAT5a and STAT5b in sexual dimorphism of hepatic P450 gene expression. Impact of STAT5a gene disruption. *J Biol Chem* 1999;274:7421-30.
125. Woelfle J, Chia DJ, Rotwein P. Mechanisms of growth hormone (GH) action. Identification of conserved Stat5 binding sites that mediate GH-induced insulin-like growth factor-I gene activation. *J Biol Chem* 2003;278:51261-6. Epub 2003 Oct 7.
126. Takeda K, Tanaka T, Shi W, Matsumoto M, Minami M, Kashiwamura S, Nakanishi K, Yoshida N, Kishimoto T, Akira S. Essential role of Stat6 in IL-4 signalling. *Nature* 1996;380:627-30.
127. Takeda K, Kishimoto T, Akira S. STAT6: its role in interleukin 4-mediated biological functions. *J Mol Med* 1997;75:317-26.
128. Terabe M, Park JM, Berzofsky JA. Role of IL-13 in regulation of anti-tumor immunity and tumor growth. *Cancer Immunol Immunother* 2004;53:79-85. Epub 2003 Nov 11.
129. Blindenbacher A, Duong FH, Hunziker L, Stutvoet ST, Wang X, Terracciano L, Moradpour D, Blum HE, Alonzi T, Tripodi M, La Monica N, Heim MH. Expression of hepatitis c virus proteins inhibits interferon alpha signaling in the liver of transgenic mice. *Gastroenterology* 2003;124:1465-75.
130. Duong FH, Filipowicz M, Tripodi M, La Monica N, Heim MH. Hepatitis C virus inhibits interferon signaling through up-regulation of protein phosphatase 2A. *Gastroenterology* 2004;126:263-77.

- 
131. Didcock L, Young DF, Goodbourn S, Randall RE. The V protein of simian virus 5 inhibits interferon signalling by targeting STAT1 for proteasome-mediated degradation. *J Virol* 1999;73:9928-33.
  132. Yokota S, Yokosawa N, Kubota T, Suzutani T, Yoshida I, Miura S, Jimbow K, Fujii N. Herpes simplex virus type 1 suppresses the interferon signaling pathway by inhibiting phosphorylation of STATs and janus kinases during an early infection stage. *Virology* 2001;286:119-24.
  133. Foster GR, Ackrill AM, Goldin RD, Kerr IM, Thomas HC, Stark GR. Expression of the terminal protein region of hepatitis B virus inhibits cellular responses to interferons alpha and gamma and double-stranded RNA. *Proc Natl Acad Sci U S A* 1991;88:2888-92.
  134. Garcin D, Marq JB, Strahle L, le Mercier P, Kolakofsky D. All four Sendai Virus C proteins bind Stat1, but only the larger forms also induce its mono-ubiquitination and degradation. *Virology* 2002;295:256-65.
  135. Parisien JP, Lau JF, Rodriguez JJ, Sullivan BM, Moscona A, Parks GD, Lamb RA, Horvath CM. The V protein of human parainfluenza virus 2 antagonizes type I interferon responses by destabilizing signal transducer and activator of transcription 2. *Virology* 2001;283:230-9.
  136. Leonard GT, Sen GC. Restoration of interferon responses of adenovirus E1A-expressing HT1080 cell lines by overexpression of p48 protein. *J Virol* 1997;71:5095-101.
  137. Look DC, Roswit WT, Frick AG, Gris-Alevy Y, Dickhaus DM, Walter MJ, Holtzman MJ. Direct suppression of Stat1 function during adenoviral infection. *Immunity* 1998;9:871-80.
  138. Barnard P, McMillan NA. The human papillomavirus E7 oncoprotein abrogates signaling mediated by interferon-alpha. *Virology* 1999;259:305-13.
  139. Chang YE, Laimins LA. Microarray analysis identifies interferon-inducible genes and Stat-1 as major transcriptional targets of human papillomavirus type 31. *J Virol* 2000;74:4174-82.
  140. Cebulla CM, Miller DM, Sedmak DD. Viral inhibition of interferon signal transduction. *Intervirology* 1999;42:325-30.
  141. Miller DM, Zhang Y, Rahill BM, Waldman WJ, Sedmak DD. Human cytomegalovirus inhibits IFN-alpha-stimulated antiviral and immunoregulatory responses by blocking multiple levels of IFN-alpha signal transduction. *J Immunol* 1999;162:6107-13.
  142. Yokosawa N, Kubota T, Fujii N. Poor induction of interferon-induced 2',5'-oligoadenylate synthetase (2-5 AS) in cells persistently infected with mumps virus is caused by decrease of STAT-1 alpha. *Arch Virol* 1998;143:1985-92.
  143. Kubota T, Yokosawa N, Yokota S, Fujii N. Association of mumps virus V protein with RACK1 results in dissociation of STAT-1 from the alpha interferon receptor complex. *J Virol* 2002;76:12676-82.
  144. Palosaari H, Parisien JP, Rodriguez JJ, Ulane CM, Horvath CM. STAT protein interference and suppression of cytokine signal transduction by measles virus V protein. *J Virol* 2003;77:7635-44.
  145. Horvath CM. Silencing STATs: lessons from paramyxovirus interferon evasion. *Cytokine Growth Factor Rev* 2004;15:117-27.
  146. Notarangelo LD, Mella P, Jones A, de Saint Basile G, Savoldi G, Cranston T, Vihinen M, Schumacher RF. Mutations in severe combined immune deficiency (SCID) due to JAK3 deficiency. *Hum Mutat* 2001;18:255-63.
  147. Welte T, Zhang SS, Wang T, Zhang Z, Hesslein DG, Yin Z, Kano A, Iwamoto Y, Li E, Craft JE, Bothwell AL, Fikrig E, Koni PA, Flavell RA, Fu XY. STAT3 deletion during hematopoiesis causes Crohn's disease-like pathogenesis and lethality: a critical role of STAT3 in innate immunity. *Proc Natl Acad Sci U S A* 2003;100:1879-84. Epub 2003 Feb 5.
  148. Lovato P, Brender C, Agnholt J, Kelsen J, Kaltoft K, Svejgaard A, Eriksen KW, Woetmann A, Odum N. Constitutive STAT3 activation in intestinal T cells from patients with Crohn's disease. *J Biol Chem* 2003;278:16777-81. Epub 2003 Mar 3.
  149. Bowman T, Garcia R, Turkson J, Jove R. STATs in oncogenesis. *Oncogene* 2000;19:2474-88.
  150. Bromberg JF, Wrzeszczynska MH, Devgan G, Zhao Y, Pestell RG, Albanese C, Darnell JE, Jr. Stat3 as an oncogene. *Cell* 1999;98:295-303.

151. Buettner R, Mora LB, Jove R. Activated STAT signaling in human tumors provides novel molecular targets for therapeutic intervention. *Clin Cancer Res* 2002;8:945-54.
152. Sommer VH, Clemmensen OJ, Nielsen O, Wasik M, Lovato P, Brender C, Eriksen KW, Woetmann A, Kaestel CG, Nissen MH, Ropke C, Skov S, Odum N. In vivo activation of STAT3 in cutaneous T-cell lymphoma. Evidence for an antiapoptotic function of STAT3. *Leukemia* 2004;18:1288-95.
153. Sinibaldi D, Wharton W, Turkson J, Bowman T, Pledger WJ, Jove R. Induction of p21WAF1/CIP1 and cyclin D1 expression by the Src oncoprotein in mouse fibroblasts: role of activated STAT3 signaling. *Oncogene* 2000;19:5419-27.
154. Amin HM, McDonnell TJ, Ma Y, Lin Q, Fujio Y, Kunisada K, Leventaki V, Das P, Rassidakis GZ, Cutler C, Medeiros LJ, Lai R. Selective inhibition of STAT3 induces apoptosis and G(1) cell cycle arrest in ALK-positive anaplastic large cell lymphoma. *Oncogene* 2004;23:5426-34.
155. Niu G, Wright KL, Huang M, Song L, Haura E, Turkson J, Zhang S, Wang T, Sinibaldi D, Coppola D, Heller R, Ellis LM, Karras J, Bromberg J, Pardoll D, Jove R, Yu H. Constitutive Stat3 activity up-regulates VEGF expression and tumor angiogenesis. *Oncogene* 2002;21:2000-8.
156. Teoh NC, Farrell GC. Management of chronic hepatitis C virus infection: a new era of disease control. *Intern Med J* 2004;34:324-37.
157. Pawlotsky JM. Pathophysiology of hepatitis C virus infection and related liver disease. *Trends Microbiol* 2004;12:96-102.
158. Gao B, Hong F, Radaeva S. Host factors and failure of interferon-alpha treatment in hepatitis C virus. *Hepatology* 2004;39:880-90.
159. NIH Consensus Development Conference Statement. Management of Hepatitis C: 2002. *Hepatology* 2002;36:S3-20.
160. Chisari FV. Cytotoxic T cells and viral hepatitis. *J Clin Invest* 1997;99:1472-7.
161. Thomson M, Nascimbeni M, Havert MB, Major M, Gonzales S, Alter H, Feinstone SM, Murthy KK, Rehmann B, Liang TJ. The clearance of hepatitis C virus infection in chimpanzees may not necessarily correlate with the appearance of acquired immunity. *J Virol* 2003;77:862-70.
162. Logvinoff C, Major ME, Oldach D, Heyward S, Talal A, Balfe P, Feinstone SM, Alter H, Rice CM, McKeating JA. Neutralizing antibody response during acute and chronic hepatitis C virus infection. *Proc Natl Acad Sci U S A* 2004;101:10149-54. Epub 2004 Jun 25.
163. Takamizawa A, Mori C, Fuke I, Manabe S, Murakami S, Fujita J, Onishi E, Andoh T, Yoshida I, Okayama H. Structure and organization of the hepatitis C virus genome isolated from human carriers. *J Virol* 1991;65:1105-13.
164. Grakoui A, Wychowski C, Lin C, Feinstone SM, Rice CM. Expression and identification of hepatitis C virus polyprotein cleavage products. *J Virol* 1993;67:1385-95.
165. Eisen-Vandervelde AL, Yao ZQ, Hahn YS. The molecular basis of HCV-mediated immune dysregulation. *Clin Immunol* 2004;111:16-21.
166. Lohmann V, Koch JO, Bartenschlager R. Processing pathways of the hepatitis C virus proteins. *J Hepatol* 1996;24:11-9.
167. Penin F, Dubuisson J, Rey FA, Moradpour D, Pawlotsky JM. Structural biology of hepatitis C virus. *Hepatology* 2004;39:5-19.
168. Griffin SD, Beales LP, Clarke DS, Worsfold O, Evans SD, Jaeger J, Harris MP, Rowlands DJ. The p7 protein of hepatitis C virus forms an ion channel that is blocked by the antiviral drug, Amantadine. *FEBS Lett* 2003;535:34-8.
169. Hugle T, Fehrmann F, Bieck E, Kohara M, Krausslich HG, Rice CM, Blum HE, Moradpour D. The hepatitis C virus nonstructural protein 4B is an integral endoplasmic reticulum membrane protein. *Virology* 2001;284:70-81.
170. Penin F, Brass V, Appel N, Ramboarina S, Montserret R, Ficheux D, Blum HE, Bartenschlager R, Moradpour D. Structure and function of the membrane anchor domain of hepatitis C virus nonstructural protein 5A. *J Biol Chem* 2004;7:7.
171. Ivashkina N, Wolk B, Lohmann V, Bartenschlager R, Blum HE, Penin F, Moradpour D. The hepatitis C virus RNA-dependent RNA polymerase membrane insertion sequence is a transmembrane segment. *J Virol* 2002;76:13088-93.
172. Agnello V, Abel G, Elfahal M, Knight GB, Zhang QX. Hepatitis C virus and other flaviviridae viruses enter cells via low density lipoprotein receptor. *Proc Natl Acad Sci U S A* 1999;96:12766-71.

- 
173. Friebe P, Lohmann V, Krieger N, Bartenschlager R. Sequences in the 5' nontranslated region of hepatitis C virus required for RNA replication. *J Virol* 2001;75:12047-57.
  174. Major ME, Feinstone SM. The molecular virology of hepatitis C. *Hepatology* 1997;25:1527-38.
  175. Wolk B, Sansonno D, Krausslich HG, Dammacco F, Rice CM, Blum HE, Moradpour D. Subcellular localization, stability, and trans-cleavage competence of the hepatitis C virus NS3-NS4A complex expressed in tetracycline-regulated cell lines. *J Virol* 2000;74:2293-304.
  176. Egger D, Wolk B, Gosert R, Bianchi L, Blum HE, Moradpour D, Bienz K. Expression of hepatitis C virus proteins induces distinct membrane alterations including a candidate viral replication complex. *J Virol* 2002;76:5974-84.
  177. Gosert R, Egger D, Lohmann V, Bartenschlager R, Blum HE, Bienz K, Moradpour D. Identification of the hepatitis C virus RNA replication complex in Huh-7 cells harboring subgenomic replicons. *J Virol* 2003;77:5487-92.
  178. Kohara M. Hepatitis C virus replication and pathogenesis. *J Dermatol Sci* 2000;22:161-8.
  179. Thimme R, Oldach D, Chang KM, Steiger C, Ray SC, Chisari FV. Determinants of viral clearance and persistence during acute hepatitis C virus infection. *J Exp Med* 2001;194:1395-406.
  180. Lanford RE, Bigger C. Advances in model systems for hepatitis C virus research. *Virology* 2002;293:1-9.
  181. Moradpour D, Kary P, Rice CM, Blum HE. Continuous human cell lines inducibly expressing hepatitis C virus structural and nonstructural proteins. *Hepatology* 1998;28:192-201.
  182. Lohmann V, Korner F, Koch J, Herian U, Theilmann L, Bartenschlager R. Replication of subgenomic hepatitis C virus RNAs in a hepatoma cell line. *Science* 1999;285:110-3.
  183. Lanford RE, Bigger C, Bassett S, Klimpel G. The chimpanzee model of hepatitis C virus infections. *Ilar J* 2001;42:117-26.
  184. Moriya K, Fujie H, Shintani Y, Yotsuyanagi H, Tsutsumi T, Ishibashi K, Matsuura Y, Kimura S, Miyamura T, Koike K. The core protein of hepatitis C virus induces hepatocellular carcinoma in transgenic mice. *Nat Med* 1998;4:1065-7.
  185. Majumder M, Steele R, Ghosh AK, Zhou XY, Thornburg L, Ray R, Phillips NJ, Ray RB. Expression of hepatitis C virus non-structural 5A protein in the liver of transgenic mice. *FEBS Lett* 2003;555:528-32.
  186. Kawamura T, Furusaka A, Koziel MJ, Chung RT, Wang TC, Schmidt EV, Liang TJ. Transgenic expression of hepatitis C virus structural proteins in the mouse. *Hepatology* 1997;25:1014-21.
  187. Honda A, Arai Y, Hirota N, Sato T, Ikegaki J, Koizumi T, Hatano M, Kohara M, Moriyama T, Imawari M, Shimotohno K, Tokuhisa T. Hepatitis C virus structural proteins induce liver cell injury in transgenic mice. *J Med Virol* 1999;59:281-9.
  188. Mercer DF, Schiller DE, Elliott JF, Douglas DN, Hao C, Rinfret A, Addison WR, Fischer KP, Churchill TA, Lakey JR, Tyrrell DL, Kneteman NM. Hepatitis C virus replication in mice with chimeric human livers. *Nat Med* 2001;7:927-33.
  189. Borgia G. Specific immunoglobulin against HCV: new perspectives. *IDrugs* 2004;7:570-4.
  190. Duenas-Carrera S. DNA vaccination against hepatitis C. *Curr Opin Mol Ther* 2004;6:146-50.
  191. Dasgupta A, Das S, Izumi R, Venkatesan A, Barat B. Targeting internal ribosome entry site (IRES)-mediated translation to block hepatitis C and other RNA viruses. *FEMS Microbiol Lett* 2004;234:189-99.
  192. Fausto N. Liver regeneration. *J Hepatol* 2000;32:19-31.
  193. Koniaris LG, McKillop IH, Schwartz SI, Zimmers TA. Liver regeneration. *J Am Coll Surg* 2003;197:634-59.
  194. Higgins G.M ARM. Experimental pathology of the liver. I. Restoration of the liver of the white rat following partial surgical removal. *Arch Pathol* 1931;12:186-202.
  195. Bucher NLR. Liver Regeneration Then and Now. Liver regeneration and carcinogenesis: Academic press Inc., 1995:1-25.
  196. Costa RH, Kalinichenko VV, Holterman AX, Wang X. Transcription factors in liver development, differentiation, and regeneration. *Hepatology* 2003;38:1331-47.

197. Cressman DE, Greenbaum LE, DeAngelis RA, Ciliberto G, Furth EE, Poli V, Taub R. Liver failure and defective hepatocyte regeneration in interleukin-6-deficient mice. *Science* 1996;274:1379-83.
198. Zimmers TA, McKillop IH, Pierce RH, Yoo JY, Koniaris LG. Massive liver growth in mice induced by systemic interleukin 6 administration. *Hepatology* 2003;38:326-34.
199. Blindenbacher A, Wang X, Langer I, Savino R, Terracciano L, Heim MH. Interleukin 6 is important for survival after partial hepatectomy in mice. *Hepatology* 2003;38:674-82.
200. Baumann H, Gauldie J. The acute phase response. *Immunol Today* 1994;15:74-80.
201. Fausto N. Liver regeneration and repair: hepatocytes, progenitor cells, and stem cells. *Hepatology* 2004;39:1477-87.
202. Fujii H, Hirose T, Oe S, Yasuchika K, Azuma H, Fujikawa T, Nagao M, Yamaoka Y. Contribution of bone marrow cells to liver regeneration after partial hepatectomy in mice. *J Hepatol* 2002;36:653-9.
203. Dahlke MH, Popp FC, Bahlmann FH, Aselmann H, Jager MD, Neipp M, Piso P, Klempnauer J, Schlitt HJ. Liver regeneration in a retrorsine/CCL4-induced acute liver failure model: do bone marrow-derived cells contribute? *J Hepatol* 2003;39:365-73.
204. Kanazawa Y, Verma IM. Little evidence of bone marrow-derived hepatocytes in the replacement of injured liver. *Proc Natl Acad Sci U S A* 2003;100:11850-3. Epub 2003 Aug 14.
205. Jiang Y, Vaessen B, Lenvik T, Blackstad M, Reyes M, Verfaillie CM. Multipotent progenitor cells can be isolated from postnatal murine bone marrow, muscle, and brain. *Exp Hematol* 2002;30:896-904.
206. Jiang Y, Jahagirdar BN, Reinhardt RL, Schwartz RE, Keene CD, Ortiz-Gonzalez XR, Reyes M, Lenvik T, Lund T, Blackstad M, Du J, Aldrich S, Lisberg A, Low WC, Largaespada DA, Verfaillie CM. Pluripotency of mesenchymal stem cells derived from adult marrow. *Nature* 2002;418:41-9.
207. Austin TW, Lagasse E. Hepatic regeneration from hematopoietic stem cells. *Mech Dev* 2003;120:131-5.
208. EASL International Consensus Conference on Hepatitis C. Paris, 26-28, February 1999, Consensus Statement. European Association for the Study of the Liver. *J Hepatol* 1999;30:956-61.
209. Alter MJ, Margolis HS, Krawczynski K, Judson FN, Mares A, Alexander WJ, Hu PY, Miller JK, Gerber MA, Sampliner RE, et al. The natural history of community-acquired hepatitis C in the United States. The Sentinel Counties Chronic non-A, non-B Hepatitis Study Team. *N Engl J Med* 1992;327:1899-905.
210. El-Serag HB, Mason AC. Risk factors for the rising rates of primary liver cancer in the United States. *Arch Intern Med* 2000;160:3227-30.
211. Cerny A, Chisari FV. Pathogenesis of chronic hepatitis C: immunological features of hepatic injury and viral persistence. *Hepatology* 1999;30:595-601.
212. Guidotti LG, Borrow P, Brown A, McClary H, Koch R, Chisari FV. Noncytopathic clearance of lymphocytic choriomeningitis virus from the hepatocyte. *J Exp Med* 1999;189:1555-64.
213. Guidotti LG, Rochford R, Chung J, Shapiro M, Purcell R, Chisari FV. Viral clearance without destruction of infected cells during acute HBV infection. *Science* 1999;284:825-9.
214. Silvennoinen O, Schindler C, Schlessinger J, Levy DE. Ras-independent growth factor signaling by transcription factor tyrosine phosphorylation. *Science* 1993;261:1736-9.
215. Meraz MA, White JM, Sheehan KC, Bach EA, Rodig SJ, Dighe AS, Kaplan DH, Riley JK, Greenlund AC, Campbell D, Carver-Moore K, DuBois RN, Clark R, Aguet M, Schreiber RD. Targeted disruption of the Stat1 gene in mice reveals unexpected physiologic specificity in the JAK-STAT signaling pathway. *Cell* 1996;84:431-42.
216. Miller DM, Rahill BM, Boss JM, Lairmore MD, Durbin JE, Waldman JW, Sedmak DD. Human cytomegalovirus inhibits major histocompatibility complex class II expression by disruption of the Jak/Stat pathway. *J Exp Med* 1998;187:675-83.
217. Heim MH, Moradpour D, Blum HE. Expression of hepatitis C virus proteins inhibits signal transduction through the Jak-STAT pathway. *J Virol* 1999;73:8469-75.
218. Tomei L, Failla C, Santolini E, De Francesco R, La Monica N. NS3 is a serine protease required for processing of hepatitis C virus polyprotein. *J Virol* 1993;67:4017-26.

- 
219. Tripodi M, Perfumo S, Ali R, Amicone L, Abbott C, Cortese R. Generation of small mutation in large genomic fragments by homologous recombination: description of the technique and examples of its use. *Nucleic Acids Res* 1990;18:6247-51.
  220. Amicone L, Galimi MA, Spagnoli FM, Tommasini C, De Luca V, Tripodi M. Temporal and tissue-specific expression of the MET ORF driven by the complete transcriptional unit of human A1AT gene in transgenic mice. *Gene* 1995;162:323-8.
  221. Hogan B BR, Costantini F, Lacy E. Manipulating the mouse embryo. A laboratory manual. CSHL Press, 1994.
  222. Moradpour D, Englert C, Wakita T, Wands JR. Characterization of cell lines allowing tightly regulated expression of hepatitis C virus core protein. *Virology* 1996;222:51-63.
  223. Heim MH, Gamboni G, Beglinger C, Gyr K. Specific activation of AP-1 but not Stat3 in regenerating liver in mice. *Eur J Clin Invest* 1997;27:948-55.
  224. Battegay M, Cooper S, Althage A, Banziger J, Hengartner H, Zinkernagel RM. Quantification of lymphocytic choriomeningitis virus with an immunological focus assay in 24- or 96-well plates [published errata appears in *J Virol Methods* 1991 Nov;35(1):115 and 1992 Aug;38(2):263]. *J Virol Methods* 1991;33:191-8.
  225. Barba G, Harper F, Harada T, Kohara M, Goulinet S, Matsuura Y, Eder G, Schaff Z, Chapman MJ, Miyamura T, Brechot C. Hepatitis C virus core protein shows a cytoplasmic localization and associates to cellular lipid storage droplets. *Proc Natl Acad Sci U S A* 1997;94:1200-5.
  226. Yasui K, Wakita T, Tsukiyama-Kohara K, Funahashi SI, Ichikawa M, Kajita T, Moradpour D, Wands JR, Kohara M. The native form and maturation process of hepatitis C virus core protein. *J Virol* 1998;72:6048-55.
  227. Wang Q, Miyakawa Y, Fox N, Kaushansky K. Interferon-alpha directly represses megakaryopoiesis by inhibiting thrombopoietin-induced signaling through induction of SOCS-1. *Blood* 2000;96:2093-9.
  228. Zinkernagel RM, Haenseler E, Leist T, Cerny A, Hengartner H, Althage A. T cell-mediated hepatitis in mice infected with lymphocytic choriomeningitis virus. Liver cell destruction by H-2 class I-restricted virus-specific cytotoxic T cells as a physiological correlate of the 51Cr-release assay? *J Exp Med* 1986;164:1075-92.
  229. Lohler J, Gossmann J, Kratzberg T, Lehmann-Grube F. Murine hepatitis caused by lymphocytic choriomeningitis virus. I. The hepatic lesions. *Lab Invest* 1994;70:263-78.
  230. Gale MJ, Jr., Korth MJ, Tang NM, Tan SL, Hopkins DA, Dever TE, Polyak SJ, Gretch DR, Katze MG. Evidence that hepatitis C virus resistance to interferon is mediated through repression of the PKR protein kinase by the nonstructural 5A protein. *Virology* 1997;230:217-27.
  231. Polyak SJ, Paschal DM, McArdle S, Gale MJ, Jr., Moradpour D, Gretch DR. Characterization of the effects of hepatitis C virus nonstructural 5A protein expression in human cell lines and on interferon-sensitive virus replication. *Hepatology* 1999;29:1262-71.
  232. Taylor DR, Shi ST, Romano PR, Barber GN, Lai MM. Inhibition of the interferon-inducible protein kinase PKR by HCV E2 protein. *Science* 1999;285:107-10.
  233. Liu ZX, Nishida H, He JW, Lai MM, Feng N, Dennert G. Hepatitis C virus genotype 1b core protein does not exert immunomodulatory effects on virus-induced cellular immunity. *J Virol* 2002;76:990-7.
  234. Sun J, Bodola F, Fan X, Irshad H, Soong L, Lemon SM, Chan TS. Hepatitis C virus core and envelope proteins do not suppress the host's ability to clear a hepatic viral infection. *J Virol* 2001;75:11992-8.
  235. Lau JY, Krawczynski K, Negro F, Gonzalez-Peralta RP. In situ detection of hepatitis C virus--a critical appraisal. *J Hepatol* 1996;24:43-51.
  236. Poynard T, Leroy V, Cohard M, Thevenot T, Mathurin P, Opolon P, Zarski JP. Meta-analysis of interferon randomized trials in the treatment of viral hepatitis C: effects of dose and duration. *Hepatology* 1996;24:778-89.
  237. Moradpour D, Cerny A, Heim MH, Blum HE. Hepatitis C: an update. *Swiss Med Wkly* 2001;131:291-8.
  238. Manns MP, McHutchison JG, Gordon SC, Rustgi VK, Shiffman M, Reindollar R, Goodman ZD, Koury K, Ling M, Albrecht JK. Peginterferon alfa-2b plus ribavirin compared with interferon alfa-2b plus ribavirin for initial treatment of chronic hepatitis C: a randomised trial. *Lancet* 2001;358:958-65.



239. Pawlotsky JM. Hepatitis C virus resistance to antiviral therapy. *Hepatology* 2000;32:889-96.
240. Rehmann B. Interaction between the hepatitis C virus and the immune system. *Semin Liver Dis* 2000;20:127-41.
241. Goodbourn S, Didcock L, Randall RE. Interferons: cell signalling, immune modulation, antiviral response and virus countermeasures. *J Gen Virol* 2000;81:2341-64.
242. Levy DE, Garcia-Sastre A. The virus battles: IFN induction of the antiviral state and mechanisms of viral evasion. *Cytokine Growth Factor Rev* 2001;12:143-56.
243. Francois C, Duverlie G, Rebouillat D, Khorsi H, Castelain S, Blum HE, Gatignol A, Wychowski C, Moradpour D, Meurs EF. Expression of hepatitis C virus proteins interferes with the antiviral action of interferon independently of PKR-mediated control of protein synthesis. *J Virol* 2000;74:5587-96.
244. Kolykhalov AA, Agapov EV, Blight KJ, Mihalik K, Feinstone SM, Rice CM. Transmission of hepatitis C by intrahepatic inoculation with transcribed RNA. *Science* 1997;277:570-4.
245. Gossen M, Bujard H. Tight control of gene expression in mammalian cells by tetracycline-responsive promoters. *Proc Natl Acad Sci U S A* 1992;89:5547-51.
246. Moradpour D, Wakita T, Wands JR, Blum HE. Tightly regulated expression of the entire hepatitis C virus structural region in continuous human cell lines. *Biochem Biophys Res Commun* 1998;246:920-4.
247. Wakita T, Wands JR. Specific inhibition of hepatitis C virus expression by antisense oligodeoxynucleotides. In vitro model for selection of target sequence. *J Biol Chem* 1994;269:14205-10.
248. Schmidt-Mende J, Bieck E, Hogle T, Penin F, Rice CM, Blum HE, Moradpour D. Determinants for membrane association of the hepatitis C virus RNA-dependent RNA polymerase. *J Biol Chem* 2001;276:44052-63.
249. Brass V, Bieck E, Montserret R, Wolk B, Hellings JA, Blum HE, Penin F, Moradpour D. An amino-terminal amphipathic alpha-helix mediates membrane association of the hepatitis C virus nonstructural protein 5A. *J Biol Chem* 2002;277:8130-9.
250. Englert C, Hou X, Maheswaran S, Bennett P, Ngwu C, Re GG, Garvin AJ, Rosner MR, Haber DA. WT1 suppresses synthesis of the epidermal growth factor receptor and induces apoptosis. *Embo J* 1995;14:4662-75.
251. Chen C, Okayama H. High-efficiency transformation of mammalian cells by plasmid DNA. *Mol Cell Biol* 1987;7:2745-52.
252. Morgenstern JP, Land H. Advanced mammalian gene transfer: high titre retroviral vectors with multiple drug selection markers and a complementary helper-free packaging cell line. *Nucleic Acids Res* 1990;18:3587-96.
253. DW SJaR. *Molecular cloning: a laboratory manual*. Cold Spring Harbor Laboratory Press, 2001.
254. Erickson AL, Kimura Y, Igarashi S, Eichelberger J, Houghton M, Sidney J, McKinney D, Sette A, Hughes AL, Walker CM. The outcome of hepatitis C virus infection is predicted by escape mutations in epitopes targeted by cytotoxic T lymphocytes. *Immunity* 2001;15:883-95.
255. Seifert U, Liermann H, Racanelli V, Halenius A, Wiese M, Wedemeyer H, Ruppert T, Rispeter K, Henklein P, Sijts A, Hengel H, Kloetzel PM, Rehmann B. Hepatitis C virus mutation affects proteasomal epitope processing. *J Clin Invest* 2004;114:250-9.
256. Moradpour D, Grabscheid B, Kammer AR, Schmidtke G, Groettrup M, Blum HE, Cerny A. Expression of hepatitis C virus proteins does not interfere with major histocompatibility complex class I processing and presentation in vitro. *Hepatology* 2001;33:1282-7.
257. Moradpour D, HM, Cerny A, Rice CM, Blum HE. Cell lines that allow regulated expression of HCV proteins: principles and applications. In: R.F. Schinazi CMR, J.-P. Sommadossi, ed. *Frontiers in viral Hepatitis*. Amsterdam: Elsevier Science, 2002.
258. Frese M, Pietschmann T, Moradpour D, Haller O, Bartenschlager R. Interferon-alpha inhibits hepatitis C virus subgenomic RNA replication by an MxA-independent pathway. *J Gen Virol* 2001;82:723-33.
259. Mihm S, Frese M, Meier V, Wietzke-Braun P, Scharf JG, Bartenschlager R, Ramadori G. Interferon type I gene expression in chronic hepatitis C. *Lab Invest* 2004;84:1148-59.

- 
260. Patzwahl R, Meier V, Ramadori G, Mihm S. Enhanced expression of interferon-regulated genes in the liver of patients with chronic hepatitis C virus infection: detection by suppression-subtractive hybridization. *J Virol* 2001;75:1332-8.
261. Thimme R, Bukh J, Spangenberg HC, Wieland S, Pemberton J, Steiger C, Govindarajan S, Purcell RH, Chisari FV. Viral and immunological determinants of hepatitis C virus clearance, persistence, and disease. *Proc Natl Acad Sci U S A* 2002;99:15661-8. Epub 2002 Nov 19.
262. Bigger CB, Brasky KM, Lanford RE. DNA microarray analysis of chimpanzee liver during acute resolving hepatitis C virus infection. *J Virol* 2001;75:7059-66.
263. Su AI, Pezacki JP, Wodicka L, Brideau AD, Supekova L, Thimme R, Wieland S, Bukh J, Purcell RH, Schultz PG, Chisari FV. Genomic analysis of the host response to hepatitis C virus infection. *Proc Natl Acad Sci U S A* 2002;99:15669-74. Epub 2002 Nov 19.
264. Yu SH, Nagayama K, Enomoto N, Izumi N, Marumo F, Sato C. Intrahepatic mRNA expression of interferon-inducible antiviral genes in liver diseases: dsRNA-dependent protein kinase overexpression and RNase L inhibitor suppression in chronic hepatitis C. *Hepatology* 2000;32:1089-95.
265. MacQuillan GC, Mamotte C, Reed WD, Jeffrey GP, Allan JE. Upregulation of endogenous intrahepatic interferon stimulated genes during chronic hepatitis C virus infection. *J Med Virol* 2003;70:219-27.
266. Basu A, Meyer K, Ray RB, Ray R. Hepatitis C virus core protein modulates the interferon-induced transacting factors of Jak/Stat signaling pathway but does not affect the activation of downstream IRF-1 or 561 gene. *Virology* 2001;288:379-90.
267. Keskinen P, Melen K, Julkunen I. Expression of HCV structural proteins impairs IFN-mediated antiviral response. *Virology* 2002;299:164-71.
268. Gale M, Jr., Blakely CM, Kwieciszewski B, Tan SL, Dossett M, Tang NM, Korth MJ, Polyak SJ, Gretch DR, Katze MG. Control of PKR protein kinase by hepatitis C virus nonstructural 5A protein: molecular mechanisms of kinase regulation. *Mol Cell Biol* 1998;18:5208-18.
269. Pflugheber J, Fredericksen B, Sumpter R, Jr., Wang C, Ware F, Sodora DL, Gale M, Jr. Regulation of PKR and IRF-1 during hepatitis C virus RNA replication. *Proc Natl Acad Sci U S A* 2002;99:4650-5.
270. Polyak SJ, Khabar KS, Paschal DM, Ezelle HJ, Duverlie G, Barber GN, Levy DE, Mukaida N, Gretch DR. Hepatitis C virus nonstructural 5A protein induces interleukin-8, leading to partial inhibition of the interferon-induced antiviral response. *J Virol* 2001;75:6095-106.
271. Aizaki H, Saito S, Ogino T, Miyajima N, Harada T, Matsuura Y, Miyamura T, Kohase M. Suppression of interferon-induced antiviral activity in cells expressing hepatitis C virus proteins. *J Interferon Cytokine Res* 2000;20:1111-20.
272. Gale M, Jr., Kwieciszewski B, Dossett M, Nakao H, Katze MG. Antiapoptotic and oncogenic potentials of hepatitis C virus are linked to interferon resistance by viral repression of the PKR protein kinase. *J Virol* 1999;73:6506-16.
273. Paterson M, Laxton CD, Thomas HC, Ackrill AM, Foster GR. Hepatitis C virus NS5A protein inhibits interferon antiviral activity, but the effects do not correlate with clinical response. *Gastroenterology* 1999;117:1187-97.
274. Podevin P, Sabile A, Gajardo R, Delhem N, Abadie A, Lozach PY, Beretta L, Brechot C. Expression of hepatitis C virus NS5A natural mutants in a hepatocytic cell line inhibits the antiviral effect of interferon in a PKR-independent manner. *Hepatology* 2001;33:1503-11.
275. Song J, Fujii M, Wang F, Itoh M, Hotta H. The NS5A protein of hepatitis C virus partially inhibits the antiviral activity of interferon. *J Gen Virol* 1999;80:879-86.
276. Charleston B, Fray MD, Baigent S, Carr BV, Morrison WI. Establishment of persistent infection with non-cytopathic bovine viral diarrhoea virus in cattle is associated with a failure to induce type I interferon. *J Gen Virol* 2001;82:1893-7.
277. Schweizer M, Peterhans E. Noncytopathic bovine viral diarrhoea virus inhibits double-stranded RNA-induced apoptosis and interferon synthesis. *J Virol* 2001;75:4692-8.
278. Chin YE, Kitagawa M, Su WC, You ZH, Iwamoto Y, Fu XY. Cell growth arrest and induction of cyclin-dependent kinase inhibitor p21 WAF1/CIP1 mediated by STAT1. *Science* 1996;272:719-22.

279. Kaplan DH, Shankaran V, Dighe AS, Stockert E, Aguet M, Old LJ, Schreiber RD. Demonstration of an interferon gamma-dependent tumor surveillance system in immunocompetent mice. *Proc Natl Acad Sci U S A* 1998;95:7556-61.
280. Onishi M, Nosaka T, Misawa K, Mui AL, Gorman D, McMahon M, Miyajima A, Kitamura T. Identification and characterization of a constitutively active STAT5 mutant that promotes cell proliferation. *Mol Cell Biol* 1998;18:3871-9.
281. Danielian PS, White R, Hoare SA, Fawell SE, Parker MG. Identification of residues in the estrogen receptor that confer differential sensitivity to estrogen and hydroxytamoxifen. *Mol Endocrinol* 1993;7:232-40.
282. Littlewood TD, Hancock DC, Danielian PS, Parker MG, Evan GI. A modified oestrogen receptor ligand-binding domain as an improved switch for the regulation of heterologous proteins. *Nucleic Acids Res* 1995;23:1686-90.
283. Arnold SF, Notides AC. An antiestrogen: a phosphotyrosyl peptide that blocks dimerization of the human estrogen receptor. *Proc Natl Acad Sci U S A* 1995;92:7475-9.
284. Matsuda T, Nakamura T, Nakao K, Arai T, Katsuki M, Heike T, Yokota T. STAT3 activation is sufficient to maintain an undifferentiated state of mouse embryonic stem cells. *Embo J* 1999;18:4261-9.
285. Matsui T, Kinoshita T, Hirano T, Yokota T, Miyajima A. STAT3 down-regulates the expression of cyclin D during liver development. *J Biol Chem* 2002;277:36167-73. Epub 2002 Jul 29.
286. Kamogawa Y, Lee HJ, Johnston JA, McMahon M, O'Garra A, Arai N. A conditionally active form of STAT6 can mimic certain effects of IL-4. *J Immunol* 1998;161:1074-7.
287. Milocco LH, Haslam JA, Rosen J, Seidel HM. Design of conditionally active STATs: insights into STAT activation and gene regulatory function. *Mol Cell Biol* 1999;19:2913-20.
288. Kovarik P, Mangold M, Ramsauer K, Heidari H, Steinborn R, Zotter A, Levy DE, Muller M, Decker T. Specificity of signaling by STAT1 depends on SH2 and C-terminal domains that regulate Ser727 phosphorylation, differentially affecting specific target gene expression. *Embo J* 2001;20:91-100.
289. Costa-Pereira AP, Tininini S, Strobl B, Alonzi T, Schlaak JF, Is'harc H, Gesualdo I, Newman SJ, Kerr IM, Poli V. Mutational switch of an IL-6 response to an interferon-gamma-like response. *Proc Natl Acad Sci U S A* 2002;99:8043-7.
290. Arcone R, Pucci P, Zappacosta F, Fontaine V, Malorni A, Marino G, Ciliberto G. Single-step purification and structural characterization of human interleukin-6 produced in *Escherichia coli* from a T7 RNA polymerase expression vector. *Eur J Biochem* 1991;198:541-7.
291. Hirano T, Ishihara K, Hibi M. Roles of STAT3 in mediating the cell growth, differentiation and survival signals relayed through the IL-6 family of cytokine receptors. *Oncogene* 2000;19:2548-56.
292. Decker T, Kovarik P. Serine phosphorylation of STATs. *Oncogene* 2000;19:2628-37.
293. Malet C, Gompel A, Spritzer P, Bricout N, Yaneva H, Mowszowicz I, Kuttenn F, Mauvais-Jarvis P. Tamoxifen and hydroxytamoxifen isomers versus estradiol effects on normal human breast cells in culture. *Cancer Res* 1988;48:7193-9.
294. Custodio JB, Dinis TC, Almeida LM, Madeira VM. Tamoxifen and hydroxytamoxifen as intramembraneous inhibitors of lipid peroxidation. Evidence for peroxy radical scavenging activity. *Biochem Pharmacol* 1994;47:1989-98.
295. Lim JS, Frenkel K, Troll W. Tamoxifen suppresses tumor promoter-induced hydrogen peroxide formation by human neutrophils. *Cancer Res* 1992;52:4969-72.
296. Blyth K, Stewart M, Bell M, James C, Evan G, Neil JC, Cameron ER. Sensitivity to myc-induced apoptosis is retained in spontaneous and transplanted lymphomas of CD2-mycER mice. *Oncogene* 2000;19:773-82.
297. Hayashi S, McMahon AP. Efficient recombination in diverse tissues by a tamoxifen-inducible form of Cre: a tool for temporally regulated gene activation/inactivation in the mouse. *Dev Biol* 2002;244:305-18.
298. Leone DP, Genoud S, Atanasoski S, Grausenburger R, Berger P, Metzger D, Macklin WB, Chambon P, Suter U. Tamoxifen-inducible glia-specific Cre mice for somatic mutagenesis in oligodendrocytes and Schwann cells. *Mol Cell Neurosci* 2003;22:430-40.
299. Amicone L, Spagnoli FM, Spath G, Giordano S, Tommasini C, Bernardini S, De Luca V, Della Rocca C, Weiss MC, Comoglio PM, Tripodi M. Transgenic expression in the

- 
- liver of truncated Met blocks apoptosis and permits immortalization of hepatocytes. *Embo J* 1997;16:495-503.
300. Alonzi T, Agrati C, Costabile B, Cicchini C, Amicone L, Cavallari C, Rocca CD, Folgiori A, Fipaldini C, Poccia F, Monica NL, Tripodi M. Steatosis and intrahepatic lymphocyte recruitment in hepatitis C virus transgenic mice. *J Gen Virol* 2004;85:1509-20.
301. Tannour-Louet M, Porteu A, Vaulont S, Kahn A, Vasseur-Cognet M. A tamoxifen-inducible chimeric Cre recombinase specifically effective in the fetal and adult mouse liver. *Hepatology* 2002;35:1072-81.
302. Postic C, Shiota M, Niswender KD, Jetton TL, Chen Y, Moates JM, Shelton KD, Lindner J, Cherrington AD, Magnuson MA. Dual roles for glucokinase in glucose homeostasis as determined by liver and pancreatic beta cell-specific gene knock-outs using Cre recombinase. *J Biol Chem* 1999;274:305-15.
303. Yakar S, Liu JL, Stannard B, Butler A, Accili D, Sauer B, LeRoith D. Normal growth and development in the absence of hepatic insulin-like growth factor I. *Proc Natl Acad Sci U S A* 1999;96:7324-9.
304. Kellendonk C, Opherck C, Anlag K, Schutz G, Tronche F. Hepatocyte-specific expression of Cre recombinase. *Genesis* 2000;26:151-3.
305. Casanova E, Fehsenfeld S, Mantamadiotis T, Lemberger T, Greiner E, Stewart AF, Schutz G. A CamKIIalpha iCre BAC allows brain-specific gene inactivation. *Genesis* 2001;31:37-42.
306. Peavy DE, Taylor JM, Jefferson LS. Alterations in albumin secretion and total protein synthesis in livers of thyroidectomized rats. *Biochem J* 1981;198:289-99.
307. Wen P, Group ER, Buzard G, Crawford N, Locker J. Enhancer, repressor, and promoter specificities combine to regulate the rat alpha-fetoprotein gene. *DNA Cell Biol* 1991;10:525-36.
308. Pinkert CA, Ornitz DM, Brinster RL, Palmiter RD. An albumin enhancer located 10 kb upstream functions along with its promoter to direct efficient, liver-specific expression in transgenic mice. *Genes Dev* 1987;1:268-76.
309. Vorachek WR, Steppan CM, Lima M, Black H, Bhattacharya R, Wen P, Kajiyama Y, Locker J. Distant enhancers stimulate the albumin promoter through complex proximal binding sites. *J Biol Chem* 2000;275:29031-41.
310. Sternberg N. Bacteriophage P1 cloning system for the isolation, amplification, and recovery of DNA fragments as large as 100 kilobase pairs. *Proc Natl Acad Sci U S A* 1990;87:103-7.
311. Sternberg NL. Cloning high molecular weight DNA fragments by the bacteriophage P1 system. *Trends Genet* 1992;8:11-6.
312. Shizuya H, Birren B, Kim UJ, Mancino V, Slepak T, Tachiiri Y, Simon M. Cloning and stable maintenance of 300-kilobase-pair fragments of human DNA in *Escherichia coli* using an F-factor-based vector. *Proc Natl Acad Sci U S A* 1992;89:8794-7.
313. Ioannou PA, Amemiya CT, Garnes J, Kroisel PM, Shizuya H, Chen C, Batzer MA, de Jong PJ. A new bacteriophage P1-derived vector for the propagation of large human DNA fragments. *Nat Genet* 1994;6:84-9.
314. Zhang Y, Buchholz F, Muyrers JP, Stewart AF. A new logic for DNA engineering using recombination in *Escherichia coli*. *Nat Genet* 1998;20:123-8.
315. Muyrers JP, Zhang Y, Benes V, Testa G, Ansoerge W, Stewart AF. Point mutation of bacterial artificial chromosomes by ET recombination. *EMBO Rep* 2000;1:239-43.
316. Muyrers JP, Zhang Y, Testa G, Stewart AF. Rapid modification of bacterial artificial chromosomes by ET-recombination. *Nucleic Acids Res* 1999;27:1555-7.
317. Muyrers JP, Zhang Y, Stewart AF. Techniques: Recombinogenic engineering--new options for cloning and manipulating DNA. *Trends Biochem Sci* 2001;26:325-31.
318. Yu D, Ellis HM, Lee EC, Jenkins NA, Copeland NG, Court DL. An efficient recombination system for chromosome engineering in *Escherichia coli*. *Proc Natl Acad Sci U S A* 2000;97:5978-83.
319. Lee EC, Yu D, Martinez de Velasco J, Tessarollo L, Swing DA, Court DL, Jenkins NA, Copeland NG. A highly efficient *Escherichia coli*-based chromosome engineering system adapted for recombinogenic targeting and subcloning of BAC DNA. *Genomics* 2001;73:56-65.
320. Osoegawa K, Tateno M, Woon PY, Frengen E, Mammoser AG, Catanese JJ, Hayashizaki Y, de Jong PJ. Bacterial artificial chromosome libraries for mouse sequencing and functional analysis. *Genome Res* 2000;10:116-28.

- 
321. Yang XW, Model P, Heintz N. Homologous recombination based modification in *Escherichia coli* and germline transmission in transgenic mice of a bacterial artificial chromosome. *Nat Biotechnol* 1997;15:859-65.
  322. Hogan B, Beddington, R., Constantini, F., Lacy, E. *Manipulating the mouse embryo*. Cold Spring Harbor Laboratory Press, 1994.
  323. Tannapfel A, Anhalt K, Hausermann P, Sommerer F, Benicke M, Uhlmann D, Witzigmann H, Hauss J, Wittekind C. Identification of novel proteins associated with hepatocellular carcinomas using protein microarrays. *J Pathol* 2003;201:238-49.
  324. Sanchez A, Nagy P, Thorgeirsson SS. STAT-3 activity in chemically-induced hepatocellular carcinoma. *Eur J Cancer* 2003;39:2093-8.
  325. Fukada T, Ohtani T, Yoshida Y, Shirogane T, Nishida K, Nakajima K, Hibi M, Hirano T. STAT3 orchestrates contradictory signals in cytokine-induced G1 to S cell-cycle transition. *Embo J* 1998;17:6670-7.
  326. Joo A, Aburatani H, Morii E, Iba H, Yoshimura A. STAT3 and MITF cooperatively induce cellular transformation through upregulation of c-fos expression. *Oncogene* 2004;23:726-34.
  327. Ariyoshi K, Nosaka T, Yamada K, Onishi M, Oka Y, Miyajima A, Kitamura T. Constitutive activation of STAT5 by a point mutation in the SH2 domain. *J Biol Chem* 2000;275:24407-13.
  328. Lin TS, Mahajan S, Frank DA. STAT signaling in the pathogenesis and treatment of leukemias. *Oncogene* 2000;19:2496-504.

---

## Acknowledgments

I could not wait to write this part of the thesis, because it would mean that the tough, scientific part would be finished. So now the time has finally come. Following are words of acknowledgment in Dutch style. These last four and a half years have been an amazing time, not only because of the whole circus of going through a Ph.D. studentship, but also because of living and working in Switzerland. Switzerland, and especially Basel has become my home, more and more I felt like an outsider in the Netherlands. At this point I would like to thank the people who have contributed, in many different ways, to the accomplishment of this thesis.

Professor Dr. Heim, dear Markus, as head of our lab and supervisor of my project, I would like to thank you for the opportunity you have given me to come to Basel and work for you. You have given me space to work very independently, often so much that it was difficult for me to decide when to ask for help (most of the time too late), however it did teach me how to deal with my own research problems. Thank you for sharing your scientific ideas and intelligence, I have learned so much from you. Thank you for all the effort you put in the correction of this thesis. Thank you for all the meetings you let me attend, it was inspiring and encouraging from a scientific point of view and great fun from a social point of view.

Professor Dr. Hauri, thank you for acting as my doktorvater. It was encouraging that you showed occasionally interest in my work, I felt that if something had gone wrong, you would have helped.

Professor Dr. Meyer, thank you for acting as coreferent. From what I have heard, you are often involved in this procedure, so thank you for the interest you put in my work.

Dear colleagues from our Hepato-Gastroenterology Lab, we worked for such a long time in close connection because of the size of our lab. As many people as we have projects, but still an atmosphere of scientific exchange and growth. Francois, I was every time again amazed how you can get results out of apparently nothing, so many protocols you got to work, you must have magic hands or you are just a true scientist. Since Verena came to the lab, I realized you can talk the hind legs off a donkey, its killing. I will however never believe that you really can catch fish. Verena, apparently shy, but so full of fun, thanks for your company and above all thanks for the milk in the coffee you faithfully provided every single day. Good luck with your Ph.D. and with exploring the big unknown afterwards.

Dear Elke, you are a friend and not 'just' a colleague. You are so dear to me. I admire your abilities in research, you are definitely so good at what you do. But above all I admire your ability to keep people together and let them feel part of it all and accepted. I am glad for you that you moved to Lausanne with your Darius and start something new. I wish you a great future there and I will come and visit you often. Xueya, I admire your drive to reach your goals, it is amazing what you already have accomplished, and nevertheless you were never discouraged and always cheerful. I wish you lots of success for your Ph.D. Sabina, good luck with the mice! Dear Michael, enjoy your wonderful

youth as long as it lasts and good luck with your studies, Magda thanks for your giggles and cakes that you always brought round during the years you were in and out our lab and good luck with your Ph.D. Alex and Philipp, ex-colleagues and very much Swiss men, thanks for the relaxing cart playing lunch breaks. Philipp I think you were very brave to stop your Ph.D. after two years, I was never so brave at the too many frustrating moments, however now I am glad I did not.

Our ex-neighboring and clinically related Gastroenterology lab was always enjoyable for extra Christmas dinners or nice meetings (with dinners or apero's). Especially thanks to Professor Beglinger, for your interest in the ongoing work and encouraging words.

From the other labs in our Department of Research, thanks to several that made the workplace worth working: Dear Stephanie (I wish you lots of success to finish and to move back home as soon as possible), Michel (you are the only man I have known so far that can make me blush), and Anna (the English community in Basel is really cool), Jameel (thank you for your sound English and French!) and in the past, the German doctor-assistants Ueli, Jochen and Matthias. It made the evenings and weekends worth working knowing one of you would be there to have a little chat with.

Emilio, from the Pharmazentrum at the other side of the road, you have been of enormous help in generating the mice, although you drove me temporarily to the bottle when I discovered that you had provided me with the wrong plasmid. In the end everything became well. You still owe me a beer I hope.

A big thank you to the people from the collaborating lab in Freiburg for scientific exchange and many social outings. Coming along now and then with you was very refreshing and encouraging and made me remember the joyous challenge of medical research. Dear Professor Blum, thank you for the interest you always showed in the progress of my work; that was really encouraging and enjoyable. Dear Professor Moradpour, dear Darius; your scientific abilities are enormous. Thank you so much for all the efforts you put in to get our paper published, although it never was in the end. Wish you lots of success in Lausanne. The Limmat swimming excursion was a very interesting experience indeed. Orange fish go very well along with HCV.

My dear friends, probably I do not tell you often enough how important you are to me. In no specific order; here in Basel, dear Anne, you are so special and dear to me, the weekends away with you to the chalet were always wonderful. Rainer, I hope we can soon drink to your PD and wedding! Lieve Barbara en Annemarie, heerlijk om een paar nederlandse vriendinnen hier in Basel te hebben! Too many nice evenings, sport activities, weekends and other outings to report here. Bruno, I did make it! Martin and Liesbeth; it is always nice to have more Dutch in Basel. Madeleine and Renske, it has always been very 'gezellig' so far and we will see more of each other in the coming years!

My dear friends back in the 'NL', if it had not been for your friendship, I would be a different person. Dear Vivi, I admire your inner strength, but at the same time your vulnerability. You are great. Thanks for the encouraging emails during the last months; it was just what I often needed. Good luck in Boston; I will come soon to visit you. Wendy, thanks for the loving friendship through all the years and the exciting weekends together with Vivi, in Basel, there will be more to follow... Dear Marieke, nothing is ever too much for you, thank

---

you for all the hiking weekends and other so nice weekends together; there will be more to follow; and especially for the time that you came on Christmas day to bring me to my parents' home. Dear Ingrid, the weekend with you in Cambridge was so cool and a turning point for me in many ways, in the first place because of the fun we had. Dear Mascha, Saskia, Nienke and Elianne; thanks for the weekends away, encouraging words and loving friendship, already for so many years. Martijn, Gerrit, Michel; mannen! Feessie, whisky, sigaar?!! You are the best.

Jolanda, for so long we have been friends now, some things will never change. Bart, you know how much you meant to me, you'll keep a special spot. You made me grow in many ways. Just that you know, you are so much more academic in your way of thinking and reasoning than so many people I know; in spite of all the abbreviations in front of their names. So do not lose courage. Cari and Mark; thanks for the wonderful and relaxing skiing holidays.

Ernst, Harro and Robert, little-tall brothers of mine, I have seen with interest how you set out your paths in the world and I am sure also you Robert will find the force to get/keep yourself on your way. I am so proud of you three, you have become to be wonderful men, and I look forward of seeing much more of you in the coming years. Irina, it is great to finally have a sister, especially because it is you. You made Ernst the perfect wife. Ann-Katharine, sister-in-law to be, good to have you on board.

Dear mum and dad, you having given me the basis of what I have become today. Thank you for showing me how to live and work. Thank you for letting me become my own person, for teaching me always to aim for the highest and to not cover my 'light' with a vessel. Thank you for showing me the beauty and joy of living and for the love you have always surrounded and encouraged me with.

My dearest Alwin, a few weeks ago these acknowledgments would have ended here and very differently. We have met just in time. Since I met you, my life changed for the very best. With you I need nothing else, you are everything to me. Thank you so much for the way you supported me during the last weeks of writing, it made all the difference.

The future will be ours, here in Switzerland.

*Simone*

Basel, 7<sup>th</sup> September 2004





## Curriculum Vitae

Name: Simone Tjitske Dorothea Stutvoet

Date of birth: 10.07.1975

Nationality: Dutch

Address: Bruderholzweg 32, 4053 Basel

### Education and work experience

1987-1993: Grammar school (Gymnasium): Christelijk Lyceum Apeldoorn, Apeldoorn, the Netherlands

1993-1999: Medical Biology (Master of Science), Faculty of Medicine, University of Utrecht, NL

- 9-months term trainee: Department of Pathology, University hospital Utrecht (UMC), NL, under the supervision of Dr. R. de Weger. Subject: The T-cell receptor V $\beta$  family expression of T lymphocytes in human heart transplantation recipients.
- 12-months term trainee: Department of Transplantation, Pharmacokinetics / pharmacodynamics Laboratory, Novartis Pharma Basle, Switzerland, under the supervision of Dr. G. Weckbecker. Subject: Four-color flow cytometric analysis of activated B-cells as early pharmacodynamic readouts of transplantation drugs in mice.

01.09.1999-28.02.2000: Scientific associate at Cytomorphology / Serology Laboratory, Department of General Medical Immunology, UMC, NL

01.03.2000-30.09.2004: Phil.II Dissertantin at the Hepato-Gastroenterology Division, Department of Research, University Hospital Basel, Switzerland, under supervision of Professor Dr. M.H.Heim. Results accomplished during this period, are described in this thesis.

### Thesis committee

Prof. Dr. phil. H.P.Hauri (doktorvater)

Prof. Dr. med. M.H.Heim (supervisor)

Prof. Dr. med. U.A. Meyer (coreferent)

### Publications

S.T.D. Stutvoet, A. Blindenbacher, F. Duong, L. Hunziker, X. Wang, L. Terracciano, T. Alonzi, D. Moradpour, H. E. Blum, M. Tripodi, N. La Monica, M. H. Heim. *Expression of Hepatitis C virus proteins inhibits Interferon alpha signaling in the liver of transgenic mice.*

**Gastroenterology**, 124;1465-75 (2003).